



Norwegian University
of Life Sciences

Master's Thesis 2021 60 ECTS

Faculty of Chemistry, Biotechnology and Food Science

Characterization of the protein complex EloR-KhpA-MltG, which controls cell elongation in *Streptococcus pneumoniae*

Marie Leangen Herigstad
Biotechnology

Acknowledgements

This master thesis was completed as a part of the Master programme in Biotechnology at the Norwegian University of Life Sciences (NMBU), in the Molecular Microbiology (MolMik) research group at the Faculty of Chemistry, Biotechnology and Food Science (KBM), between August 2020 and June 2021.

First and foremost, I would like to thank my two supervisors, Dr. Daniel Straume and Dr. Anja Ruud Winther, for excellent guidance, both during the laboratory work and the writing process and for always taking time to answer my questions. I would also like to thank Dr. Morten Kjos for sharing his knowledge about Microbe J with me.

A special thanks to Anja for teaching me everything I know about EloR-MltG-KhpA, and for continuing the EloR-project. I also want to share my gratitude to MolMik for letting me have the opportunity to participate on the “EloR Interacts with the Lytic Transglycosylase MltG at Midcell in *Streptococcus pneumoniae* R6” paper.

Finally, I also want to give a huge thanks to everyone in the Molecular Microbiology research group for the support and guidance, and for the great work environment. Thanks to my fellow master students Henriette, Anna and Maria for making the days in the lab joyful and for the moral support during the master period.

Marie Leangen Herigstad

Ås, June 2021

Abstract

Streptococci are ovoid shaped Gram-positive bacteria which are typically arranged in pairs or chains. *Streptococcus pneumoniae* is recognized as a human pathogen which can cause disease that ranges from middle ear infections to invasive infections and is a major contributor to morbidity and mortality especially among children, elderly, and immune compromised individuals. Antibiotics have been an instrumental defence against these kinds of infections, but the worldwide increase in antibiotic resistant bacterial strains are of great concern and requires attention. To discover new potential drug targets, we need better understanding of different essential cellular processes, including cell-division.

The shape of *S. pneumoniae* is determined by the synchronised actions of the elongasome and the divisome, creating a protective layer of peptidoglycan (PG), that envelops the cell membrane. The divisome synthesizes the septal PG, that divides the cell into two new daughter cells, while the elongasome expands PG in the longitudinal direction, contributing to the elongated shape of the cell. PBP2b/RodA and PBP2x/FtsW are essential transpeptidase/transglycosylase pairs that incorporate new PG into the existing PG sacculus and are considered the cores of the elongasome and divisome, respectively. The actions of the two machineries must be coordinated throughout the cell cycle, but detailed knowledge of this is lacking. It was recently discovered that elongation is regulated by two RNA binding proteins, EloR and KhpA, which forms a complex that work closely with the Ser/Thr kinase StkP. StkP functions by phosphorylating its targets in PG synthesis to facilitate switching between septal and peripheral synthesis. StkP also regulates the activity of EloR through phosphorylation. Studies have found that EloR/KhpA localizes to midcell, and that the presence of KhpA at midcell is fully dependent upon EloR. It has also been published that the deletion of PBP2b creates suppressor mutations in the genes coding *eloR*, *khpA* and *mltG*, suggesting a functional connection between these. We have shown that EloR is dependent on its Jag domain to locate to midcell and interact with the essential lytic transglycosylase MltG, also known as a part of the elongasome. In this work, fluorescence microscopy and protein-protein interaction assays were employed to further explore the interaction between EloR and MltG in *S. pneumoniae*. Also, co-immunoprecipitation assays and gel filtration analysis was performed to verify the protein complex formation of MltG and EloR. Fluorescence microscopy demonstrated that the Jag domain of EloR is critical for midcell localization and its interaction with MltG, and co-immunoprecipitation confirmed the EloR-MltG interaction *in vivo*. The results suggest that MltG is responsible for the recruitment of the EloR/KhpA complex to the division zone.

Sammendrag

Streptokokker er en ovococci-formet Gram-positiv bakterie som vanligvis vokser i par eller i kjeder. *Streptococcus pneumoniae* er en kjent patogen hos mennesker og kan forårsake sykdom som variere mellom infeksjon i mellomøret til invasive infeksjoner og er en stor bidragsyter til sykdom og død blant barn, eldre og de med svakt immunforsvar. Antibiotika er et viktig forsvar mot slike sykdommer, men den verdensomspennende økningen av antibiotikaresistente bakterier er urovekkende og krever oppmerksomhet. For å kunne oppdage nye mål for antibiotika må vi få bedre kjennskap til ulike essensielle cellulære prosesser, inkludert celledeling.

Formen til *Streptococcus pneumoniae* bestemmes av de synkroniserte handlingene til elongasomet og divisomet, som danner et beskyttende lag av peptidoglycan (PG) som omslutter cellemembranen. Divisomet syntetiserer septal PG som fører til at cellen deler seg i to nye datterceller, mens elongasomet ekspanderer PG i lengderetning, noe som er med på å bidra til den elongerte celleformen. PBP2b/RodA og PBP2x/FtsW er essensielle transpeptidaser/transglycosylase-par som inkorporerer nytt PG inn til eksisterende PG og blir betegnet som kjernen av elongasomet og divisomet. Dette maskineriet må koordineres gjennom cellyklusen, men detaljert informasjon om dette mangler. Det har nylig blitt oppdaget at elongeringen er regulert av to RNA-bindende protein, EloR og KhpA, som danner et kompleks som jobber tett med Ser/Thr kinasen StkP. StkP fungerer ved å fosforylere dens mål under PG syntesen for å bytte mellom septal og perifer syntese. StkP regulerer også aktiviteten til EloR gjennom fosforylering. Studier har vist at EloR/KhpA lokaliseres til midten av cellen og at tilstedeværelsen av KhpA i denne delen av cellen er avhengig av EloR. Publikasjoner viser også at sletting av PBP2b danner suppressormutasjoner i genene *eloR*, *khpA* and *mltG*, som tyder på en funksjonell forbindelse mellom disse. Vi har vist at EloR er avhengig av Jag domenet sitt for å lokalisere til midten av cellen og interagerer med den essensielle transglykosylasen MltG, også kjent som en del av elongasomet. I dette arbeidet har fluorescensmikroskopering og protein-protein interaksjonsstudier blitt brukt til å utforske interaksjonen mellom EloR og MltG i *S. pneumoniae*. Også, co-immunoprecipitation studier og gelfiltreringsanalyser ble gjennomført for å verifisere proteinkompleksformasjonen av MltG og EloR. Fluorescensmikroskopi viste at Jag-domenet av EloR er kritisk for lokalisering til midten av cellen og dens interaksjon med MltG, og co-immunoprecipitation bekreftet EloR-MltG interaksjonen *in vivo*. Disse resultatene viser at MltG er ansvarlig for rekrutteringen av EloR/KhpA-komplekset til delingssonen.

Index

1. Introduction	1
1.1 The genus <i>Streptococcus</i>	1
1.1.1 <i>Streptococcus pneumoniae</i>	2
1.1.2 Pneumococcal virulence	3
1.2 The pneumococcal cell wall	4
1.2.1 Teichoic acids	5
1.2.2 Pneumococcal peptidoglycan synthesis in <i>S. pneumoniae</i>	6
1.2.3 Penicillin Binding Proteins in <i>S. pneumoniae</i>	7
1.3 Cell division in <i>S. pneumoniae</i>	9
1.3.1 Coordination of lateral and septal PG synthesis in <i>S. pneumoniae</i>	10
1.4 The EloR-KhpA-MltG complex	11
1.5 Aim of Study	14
2. Materials	15
2.1 Bacterial strains and plasmids	15
2.2 Primers	16
2.3 Kits	18
2.4 Antibiotics	18
2.5 Chemicals	19
2.6 Equipment	19
2.7 Growth mediums and buffers	19
2.7.1 Solutions for C-medium	19
2.7.2 Buffers and solutions for agarose gel electrophoresis	21
2.7.3 Buffers and solutions for SDS-PAGE	22
2.7.4 Buffers and solutions for Western blot and co- immunoprecipitation	23
2.7.5 Buffers for IMAC and Gel filtration	23
2.7.6 Other buffers and solutions	24
3. Methods	26
3.1 Growth and storage of bacteria	26
3.1.1 <i>Streptococcus pneumoniae</i>	26
3.1.2 <i>Escherichia coli</i>	26
3.2 Plasmid isolation	26
3.3 The Polymerase Chain Reaction	27
3.3.1 Primer design and preparation	28
3.3.2 PCR using Phusion high fidelity DNA polymerase	29
3.3.3 Screening of transformants using Red Taq® Ready Mix™	30

3.3.4	Overlap extension PCR	31
3.4	Gel electrophoresis	33
3.4.1	Agarose gel electrophoresis.....	33
3.4.2	PCR product clean up and extraction of DNA from agarose gels	34
3.5	DNA restriction cutting and ligation	35
3.6	DNA sequencing	37
3.7	SDS-PAGE.....	38
3.8	Co-immunoprecipitation (pulldown).....	39
3.9	Immunoblot analysis	40
3.10	Chemically competent <i>E. coli</i> cells	41
3.10.1	Transformation of chemically competent <i>E. coli</i>	41
3.11	Transformation of <i>S. pneumoniae</i>	41
3.12	The Janus cassette	42
3.13	Ectopic overexpression of genes using the ComRS system.....	43
3.14	BACTH: Bacterial Adenylate cyclase Two- Hybrid System	44
3.15	Microscopy analysis and construction of fluorescent fusion proteins.....	46
3.16	Gel filtration	46
3.16.1	Overexpression and protein purification	46
3.16.2	Gel filtration on purified proteins.....	48
4.	Results	50
4.1	Microscopy analysis suggesting the Jag domain exclusively directs EloR to the division zone.....	50
4.2	Exploring possible interaction partners of EloR.....	52
4.3	StkP is not critical for EloR localization	52
4.4	The Jag domain of EloR interacts with the DUF domain of MltG.....	54
4.5	Does MltG follow the same localization pattern as EloR in a $\Delta yidC2$ genetic background?	55
4.6	Amino acids in the conserved motif KKGFLG in Jag could be involved in protein-protein interactions	56
4.6.1	Testing the interaction between EloR and MltGcyt from other streptococci	57
4.6.2	Will point mutations in Jag reveal the amino acid important for interaction between Jag and MltG?.....	59
4.7	Co-immunoprecipitation of EloR and MltG.....	60
4.8	Over expression and purification of Jag-linker and MltGcyt	61
	64
5.	Discussion	66
5.1	Microscopy imaging revealing midcell localization	67
5.2	BACTH experiments to identify EloR and MltG interaction.....	69

5.3 Challenges with the essential MltG.....	70
5.4 Co-IP to verify interaction between EloR/Jag and MltG in vivo	71
5.5 Using gel filtration to detect EloR/MltG complex formation.....	72
6. Concluding remarks and further research	73
References	74
Appendix	80

1. Introduction

1.1 The genus *Streptococcus*

Streptococci are ovoid shaped Gram-positive bacteria, which are typically arranged in pairs or chains. Some of the main characteristics are that they are facultative anaerobe, catalase negative and have special nutritional requirements (Hardie and Whiley, 1997). They can be classified as either α -hemolytic, β -hemolytic or γ -hemolytic. α -hemolytic streptococci are identified by their ability to oxidize hemoglobin to the green coloured biliverdin. This is a result from hydrogen peroxide production by the bacteria and can be seen as a green zone surrounding the streptococci when grown on blood agar. β -hemolytic streptococci produce protein-based toxins called streptolysin-O and streptolysin-S. These completely lyse blood cells, which can be seen as a clearing zone around the colonies on blood agar. Finally, γ -hemolytic streptococci do not have any hemolytic effect (Lancefield, 1933, Hardie and Whiley, 1997, Facklam, 2002). Regardless of hemolytic properties, phylogenetic classification of the genus *Streptococcus* has been determined by comparing 16s rRNA sequences. Streptococci are divided into six phylogenetic groups: the pyogenic group, the anginosus group, the mitis group, the salivarius group, the bovis group and the mutans group (Figure 1)(Song et al., 2013). Although many streptococci are commensals being part of the natural microbiota in humans and animals, several species are also opportunistic pathogens e.g., causing mastitis in animals and meningitis and respiratory infections in humans (Song et al., 2013). One of the most important human pathogens is *Streptococcus pneumoniae*, belongs to the mitis group.

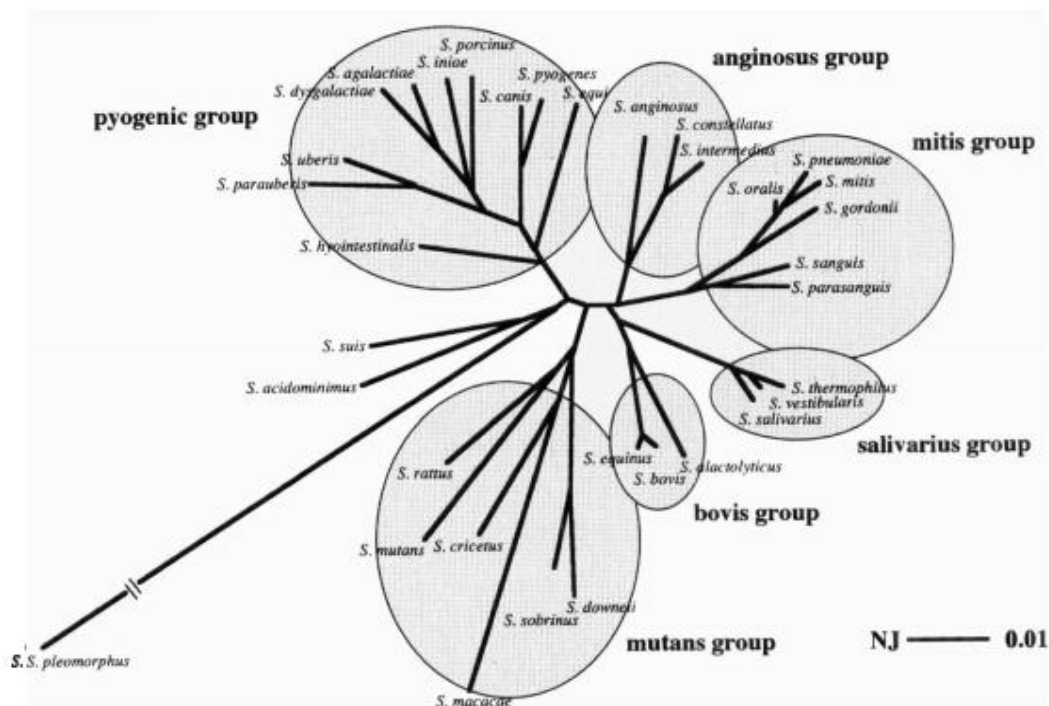


Figure 1 Phylogenetic relationships among the Streptococcus species where *S. pneumoniae* is found in the mitis group. Streptococci are divided into six main groups; the anginosus bovis, mitis, mutans salivarius and pyogenic group (Kawamura et al., 1995)

1.1.1 *Streptococcus pneumoniae*

S. pneumoniae, also called the pneumococcus, colonizes the nasopharynx and the upper respiratory tract in 5-10% of the adult population without causing disease. Under the right circumstances, however, it can cause invasive infections and is a major contributor to morbidity and mortality especially among children, elderly, and immune compromised individuals (Song et al., 2013, Henriques-Normark and Tuomanen, 2013). *S. pneumoniae* is mainly transmitted between individuals by direct contact with contaminated respiratory secretion. This bacterium can either survive having specific clones selected for an invasive pneumococcal disease phenotype, or as a persistent colonization phenotype. Non-invasive strains can be retained in human populations, but defects in the host immune systems can alter this host-pathogen interaction, allowing strains of low virulence to invade the immunocompromised host (van der Poll and Opal, 2009). The pneumococcus can cause infections such as otitis media and sinusitis and exacerbations of chronic bronchitis, to more severe and invasive infections such as pneumonia, meningitis and bacteremia (Song et al., 2013). The pneumococcal meningitis is frequent in young children and the elderly, where *S. pneumoniae* has become the most common cause of meningitis in the US. In developing countries, the same disease is associated with approximately 30% of acute cases of bacterial meningitis. Pneumococci can also cause acute

otitis media often in conjunction with a respiratory tract infection. Otitis media is associated with considerable morbidity and high health care costs due to high number of physician visits and extensive use of antibiotics. In the US, there are 7 to 12 million cases of this infection each year (Cartwright, 2002).

1.1.2 Pneumococcal virulence

The two most important virulence factors in pneumococci are a 53 kDa protein called pneumolysin and the polysaccharide capsule covering the bacterial cell wall (Walker et al., 1987). Pneumolysin is a pore-forming toxin produced in the cytoplasm of *S. pneumoniae*. It is released from dying bacteria attacked by the host immune system during infection. Pneumolysin molecules integrates into the cell membrane of host cells where it polymerizes into a pore leading to death of the host cell. The polysaccharide capsule is very important for *S. pneumoniae* in evading the host immune system. The composition of the capsule varies between pneumococcal strains giving rise to different serotypes of pneumococcal strains. To date, 100 different serotypes have been identified. Different serogroups of pneumococcal strains can be more prevalent in some countries than others based on distribution of geography, age and gender, but in general some serotypes have been seen to dominate among invasive pneumococci (Scott et al., 1996) (Hoskins et al., 2001, Cartwright, 2002). The pneumococcal conjugate vaccine used today is therefore based on the polysaccharide capsule, and it covers 23 of the most common serotypes associated with infections. The vaccine has proved highly efficient in reducing the mortality among children, but sadly in many parts of the world vaccination is absent or poorly distributed. In addition, infections by serotypes not included in the vaccine are observed in immunized populations. These cases require treatment with antibiotics. Penicillin (β -lactam antibiotics) have been the antibiotic of choice, however, the number of isolates resistant to penicillin and other antibiotics has increased rapidly in recent years, often rendering treatment regimens inefficient (Linares et al., 2010, Cherazard et al., 2017).

Pneumococci have the ability to become naturally competent for genetic transformation, which means that they can take up and incorporate exogenous DNA from the milieu or closely related species, in the same surroundings in a process called horizontal gene transfer. This is one of the main reasons why antibiotic resistant genes are quickly acquired and shared among pneumococcal strains (Straume et al., 2015), and is also driving pneumococcal serotype switching leading to vaccine escape. A study of otitis media over 15 years has shown that

pneumococcal strains become increasingly resistant to penicillin over time. Among the cultures with positive result, the prevalence of *S. pneumoniae* increased from 18 % to 44 %. No resistance was observed in cultures collected in 1989, but present in 97 % of cultures collected in 1996 in France. This could explain the increase in the incidence of persistent acute otitis media (Loundon et al., 1999). A combination of vaccination programmes and restrictive use of antibiotics will slow down the spread of resistant strains, but not eliminate it. To have effective treatment options in the future, new drugs and treatment strategies to combat resistant pathogens must be developed.

Considering the success of β -lactams, which target an essential process in bacterial cell wall synthesis, this conserved function in bacteria is regarded to hold high potential as target for future antibiotics (Blair et al., 2015). The differences between prokaryotic and eukaryotic cell composition are taken advantage of to find new drug targets involved in cell wall synthesis and bacterial cell division, that will not affect the mammalian host cells negatively. Among the antibacterial agents targeting the cell wall, is the β -lactam antibiotics (Epanand et al., 2016). β -lactams such as penicillin bind to Penicillin Binding Proteins (PBPs), which are instrumental in building the cell wall, making the bacterial cell wall of *S. pneumoniae* an important target for future antibiotics (Di Guilmi and Dessen, 2002).

1.2 The pneumococcal cell wall

Most bacteria have a cell wall that envelopes their cytoplasmic membrane. It represents the outermost boundary of the cell, providing maintenance of the cell shape and protection from lysis by turgor pressure. Gram-negative bacteria have a thin cell wall that is surrounded by an outer membrane, while Gram-positive bacteria, such as *S. pneumoniae*, lack the outer membrane but have a thicker cell wall instead (Pasquina-Lemonche et al., 2020, Seltmann and Holst, 2013, Straume et al., 2020). The main constituents making up the structure of the bacterial cell wall is a mesh like structure called peptidoglycan (PG). In addition, most Gram-positives have a polymer called teichoic acid (see section 1.2.1) covalently attached to the peptidoglycan (Bui et al., 2012). The PG layer is made up of linear glycan strands that are cross-linked by peptide bridges. The glycan chain consists of repeating units of a disaccharide containing *N*-acetylglucosamine (GlcNAc) and *N*-acetylmuramic acid (MurNAc). The glycan strand composition is similar in most bacteria but varies in length from species to species. In comparison to *E. coli* that has a relatively short glycan strand with length of around 5-10

disaccharide units, the glycan chains of *S. pneumoniae* consists of at least 25 disaccharide units (Höltje, 1998, Bui et al., 2012). The MurNAc residues have pentapeptides attached to them. The sequence of the pentapeptide varies between bacterial species. In *S. pneumoniae* it has the composition L- Alanine – Iso-D-Glutamine – L-Lysine – D-Alanine – D-Alanine. These so-called stem peptides are involved in crosslinking neighboring glycan chains (Bui et al., 2012, Vollmer et al., 2008). Cross-linking of the glycan strands happens either directly or via a dipeptide bridge (L-Ala – L-Ala or L-Ser – L-Ala) between the carboxy group of D-Ala at position 4, and the ϵ amino group of the L-Lys residue at position 3 (Figure 2) (Vollmer et al., 2008). In addition to cross-linking, the glycan chains are subjected to secondary modifications such as GlcNAc becoming deacetylated and GlcNAc residues becoming O-acetylated (Bui et al., 2012, Vollmer et al., 2008).

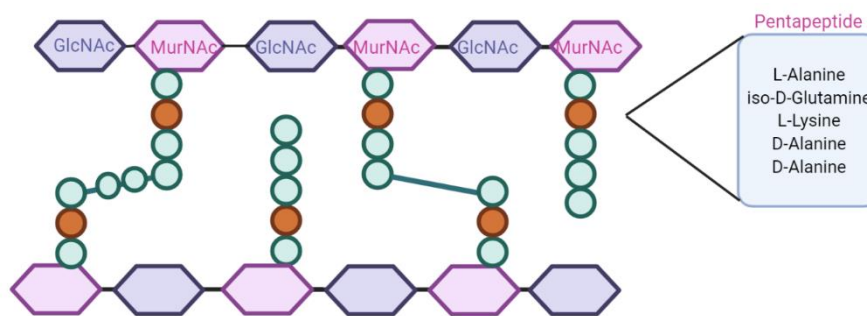


Figure 2: Illustration of peptidoglycan structure in *S. pneumoniae*. PG consists of long glycan chains, built up of alternating GlcNAc and MurNAc molecules, interconnected with via short stem peptides attached to MurNAc. The pentapeptide consists of five amino acids, L-Alanine-iso-D-Glutamine-L-lysine-D-Alanine-D-Alanine which make up pneumococcal PG with different cross-linking. Figure adapted from Biorender.com

1.2.1 Teichoic acids

As mentioned, the cell wall contains other components in addition to PG. The polymeric molecule called wall teichoic acid (WTA) is covalently attached to the MurNAc residue in peptidoglycan. In addition, most Gram-positive bacteria have lipoteichoic acid (LTA) anchored to the membrane, resulting in a thick and complex cell wall. The teichoic acids (TAs) bind cell surface proteins and are involved in other processes like cell wall hydrolyses, regulation of cell elongation and division. In most species, the structure of WTA is different from LTA and is synthesized by two different pathways. In the pneumococcal cell wall however, both WTA and the membrane-anchored LTA have identical repeating unit structures and length distribution, indicating that they are produced in the same biosynthetic pathway (Denapaitte et al., 2012). The pneumococcal TAs are made up of identical structures with two to eight repeating units

consisting of AATGal (2-acetamido-4-amino-2,4,6-trideoxygalactidose) (Behr et al., 1992). Also, the TAs contain phosphorylcholine which is very rare in bacteria. The phosphocholine serves as an anchor for the class of choline-binding proteins such as LytA, LytB and Cbpd (Denapaite et al., 2012).

1.2.2 Pneumococcal peptidoglycan synthesis in *S. pneumoniae*

PG synthesis can be divided into three main stages: (i) synthesis of PG precursors in the cytoplasm, (ii) translocation of the PG precursors across the cytoplasmic membrane and (iii) incorporation of new PG material into the existing cell wall outside the cell membrane (Figure 3). Synthesis of PG precursors in the cytoplasm involves the process of UDP-GlcNAc (undecaprenyl-linked N-acetyl glucosamine) being synthesized from fructose-6-phosphate by Glm enzymes. UDP-GlcNAc is then used as template to synthesize UDP-MurNAc linked to the pentapeptide (UDP-*N*-acetylmuramyl-pentapeptide) by the sequential actions of the MurABCDEF enzymes (Lovering et al., 2012, Lloyd et al., 2008). UDP-MurNAc-pentapeptide is transferred to a transport lipid, lipid I by the membrane embedded *MraY* enzyme. Then, GlcNAc is attached to MurNAc on lipid I by *MurG* to form Lipid II (Typas et al., 2012). Also, the D-Glu amino acid, in position 2 is transformed to a D-isoglutamine (iGln) by *GatD/MurT*. The addition of the di-peptide bridges (L-ala/L-Ser) to the ϵ -amino group on L-Lys is performed at the Lipid II-level, by the *MurM* and *MurN* ligases (Vollmer et al., 2008, Filipe et al., 2001, Lloyd et al., 2008).

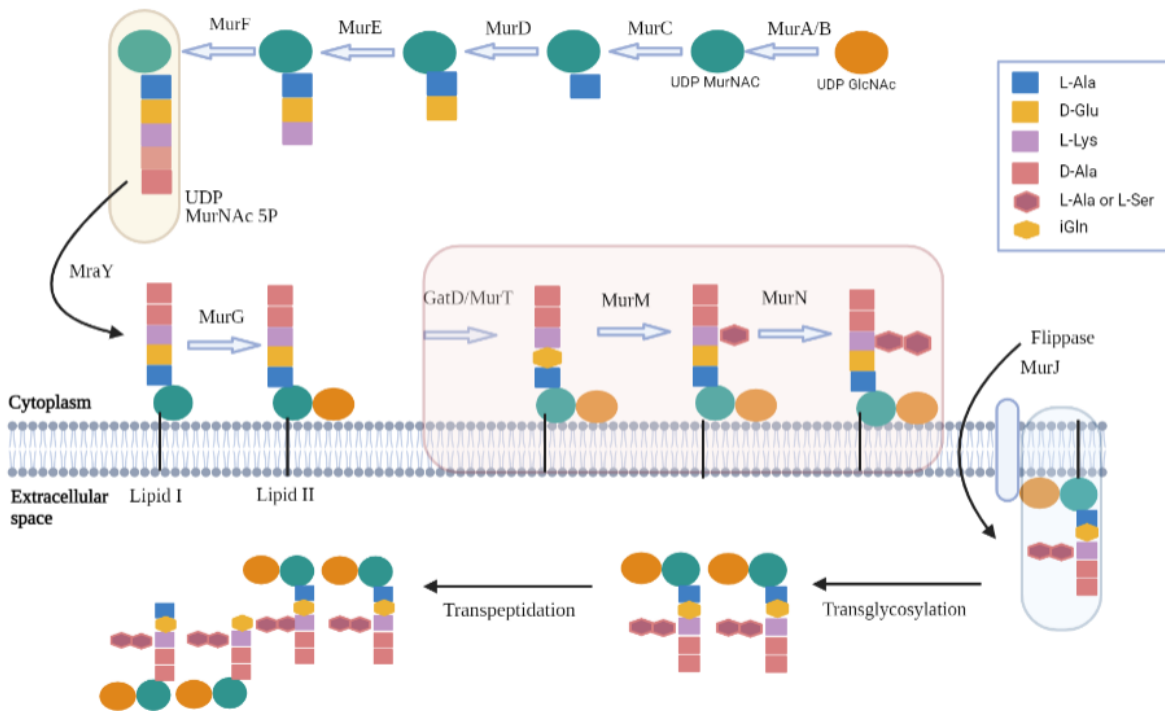


Figure 3 Peptidoglycan synthesis in *S. pneumoniae*. Overview of synthesis of PG precursors in the cytoplasm, translocation of the PG precursors across the cytoplasmic membrane and incorporation of new PG material into the existing cell wall outside the cell membrane. Figured modified after (Laddomada et al., 2019) in Biorender.com

The lipid II must be flipped across the membrane for cell wall synthesis, which is done by the flippase MurJ (Sham et al., 2014). On the extracellular side of the membrane, Lipid II is directly linked to the transglycosylation activity leading to the formation of glycan chains which are crosslinked via transpeptidase reactions. The core of this complex is made up of a PBP and a Shape, Elongation, Division, and Sporulation (SEDS) protein (see section 1.2.3). PBPs can perform both transglycosylation and transpeptidation, or only transpeptidation, depending on the type of PBP (see section 1.2.3), while SEDS work in conjunction with some PBPs to catalyze transglycosylation reactions. (Teo and Roper, 2015).

1.2.3 Penicillin Binding Proteins in *S. pneumoniae*

There are six PBPs in *S. pneumoniae*. Depending on the structure and the catalytic activity of their N-terminal domain, five of them are divided into either class A or B PBPs; three class A PBPs (PBP1a, PBP1b, PBP2a) and two class B PBPs (PBP2b, PBP2x). The class A PBPs perform both transpeptidase and transglycosylase reactions, while the monofunctional class B PBPs only have transpeptidase activity. The N-terminal domain of class B PBPs is believed to

play a central role in cell morphogenesis when interacting with other proteins involved in the cell cycle. The transglycosylation activity of the class A PBPs is utilized to extend the glycan strands, while the transpeptidase activity is important for creating peptide cross-links between two adjacent glycan chains (Sauvage et al., 2008, Zapun et al., 2008). In addition, *S. pneumoniae* has one PBP with D, D-carboxylase activity called PBP3. PBP3 regulates the extent of cross-linking in peptidoglycan by cleaving off the D-Ala residue at position five from the pentapeptide side chains, reducing the availability of donor stem peptides for the transpeptidase activity (Morlot et al., 2005).

Both PBP2b and PBP2x are essential and are involved in synthesizing the primary PG in the pneumococcus, while the genes encoding class A PBPs can be deleted individually, demonstrating that none of them are essential for growth. It is also possible to isolate *pbp1b/pbp2a* and *pbp1a/pbp1b* double mutants, whereas the double deletion of *pbp1a/pbp2a* is lethal (Paik et al., 1999). A study by Straume et al., 2020 showed that class A PBPs have an autonomous function that is important for maturation and/or strengthening of the primary cell wall in *S. pneumoniae*. Recently, it was shown by atomic force microscopy that the mature Gram-positive cell wall consists of two layers: A dense inner peptidoglycan surface with spaced glycan strands (less than 7nm) and a low density outer peptidoglycan area (Pasquina-Lemonche et al., 2020). A model is proposed where the three class A PBPs in *S. pneumoniae* work together to synthesize this inner PG layer and/or repair gaps and imperfections in the primary PG synthesized by PBP2x/FtsW and is likely to contribute to the strength of the cell wall by e.g. cross-links (Straume et al., 2020).

It has been discovered that the monofunctional class B PBP2x and PBP2b operate in conjunction with the dedicated transglycosylases FtsW and RodA, which belong to the SEDS family. PBP2x forms a complex with FtsW and PBP2b forms a complex with RodA. PBP2b/RodA and PBP2x/FtsW make up the core functional units of the elongasome and the divisome, respectively (described in section 1.3) which synthesise the primary PG (Meeske et al., 2016, Emami et al., 2017)

1.3 Cell division in *S. pneumoniae*

The ovoid shape of *S. pneumoniae* results from a combination of lateral and septal PG synthesis performed by two machineries called the elongasome and divisome, respectively. PBP2x is part of the so-called divisome, while PBP2b is a part of the elongasome. Studies show that depletion of PBP2b results in cells growing in long chains, compressed in the longitudinal axis, giving a lentil-like shape, while depletion of PBP2x results in elongated lemon-shaped cells (Figure 4)(Berg et al., 2013).

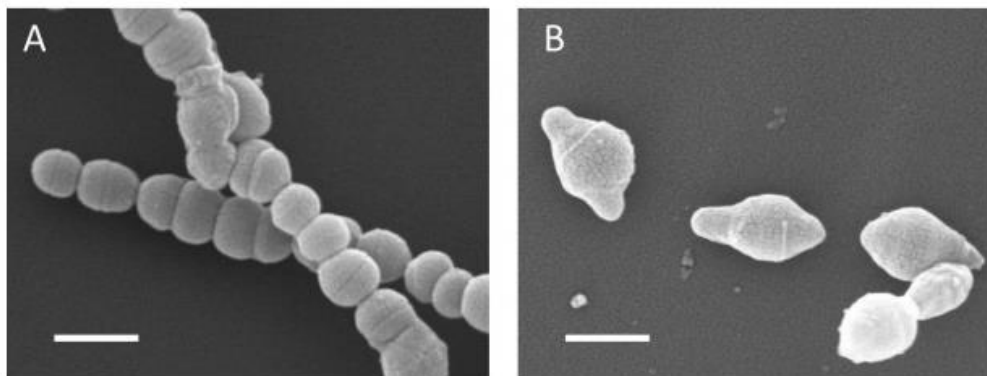


Figure 4 Scanning electron micrographs from Berg et al., 2013 illustrating pneumococcal cells depleted of A) PBP2b and B) PBP2x. The PBP2b depleted cells becomes compressed along the longitudinal axis, while most of the PBP2x cells have a lemon-like appearance. Scale bars are 1 μm . (Berg et al., 2013).

PBP2x along with other divisome proteins are guided by FtsZ to incorporate new PG in a circular motion while the cytoplasmic membrane constricts inwards, creating a septal PG disc separating the two daughter cells. The elongasome stays at the transition between the peripheral and septal PG disc to incorporate PG outward from midcell to elongate cells (Perez et al., 2019). The elongasome has recently been shown to introduce new PG material into the existing layer in patches, which must involve controlled opening of the old cell wall. The enzyme MltG is a possible candidate to open PG (Perez et al., 2020). How this is accomplished without making critical damage to the cell wall is not known. By following the two machineries using high-resolution microscopy it was shown that the divisome and elongasome co-localizes in early-to mid-divisional cells, while the divisome separates from the elongasome and locates at the centre of the septum in mid-to-late divisional cells (Figure 5) (Tsui et al., 2014). A study by Straume et al., 2017 supports this by identifying pneumococcal proteins that are functionally linked to PBP2b. The depletion of the four proteins RodA, MreD, DivIVA and CozE resulted in spherical cells, the same phenotypical trait as cells depleted of PBP2b (members of the elongasome) (Straume et al., 2017). The depletion of the GpsB protein (a part of the divisome) reported to

be essential *S. pneumoniae*, leads to formation of elongated cells. This is similar to the phenotypes caused by selective inhibition of PBP2x, which blocks septal closure (Land et al., 2013). This leads to the conclusion that PBP2b is a part of the peripheral machinery known as the elongasome, while PBP2x is a part of the divisome (Berg et al., 2013).

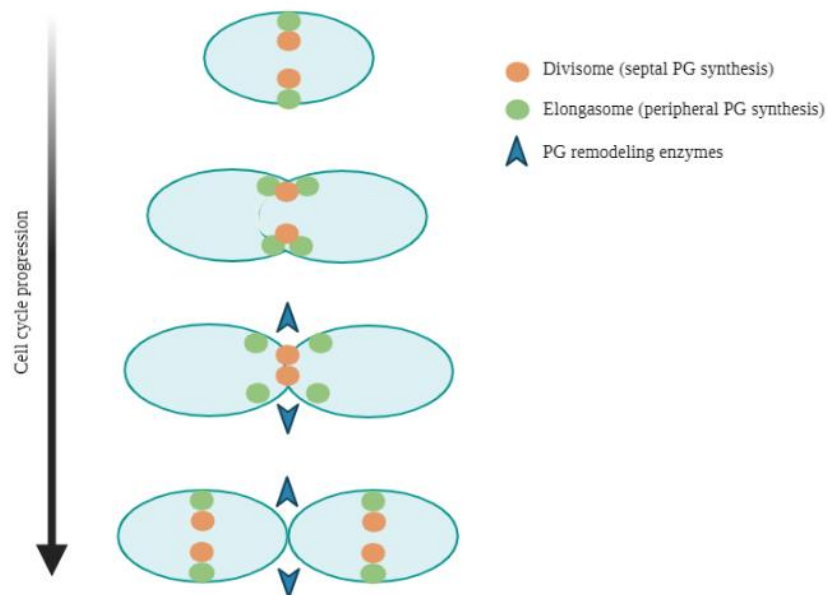


Figure 5 Simplified pneumococcal cell division including the positions of the elongasome, divisome, and PG remodelling enzymes throughout the cell cycle. RodA/PBP2b and FtsW/PBP2x makes up the functional units of the elongasome and divisome. Figure from (Sham et al., 2012), adapted in Biorender.com.

1.3.1 Coordination of lateral and septal PG synthesis in *S. pneumoniae*

There are two proteins in *S. pneumoniae* which are important in controlling cell division; a single Ser/Thr protein kinase known as StkP and a soluble protein phosphatase called PhpP. The membrane protein StkP has an N-terminal intracellular kinase domain, a membrane spanning α -helix, and four extracellular Penicillin-binding protein Associated (PASTA) domains on its C-terminus outside the cell (Novakova et al., 2005). The PASTA domains can bind peptidoglycan and are thought to sense external signals related to cell wall integrity and convey these two to the inside of the cell through autophosphorylation (Jones and Dyson, 2006, Zucchini et al., 2018). StkP phosphorylates several proteins that are important for cell division and cell wall synthesis in *S. pneumoniae*. At the right time during cell cycle, StkP phosphorylates proteins known for participating in PG synthesis and cell division, EloR, MapZ and DivIVA (part of the elongasome), MacP (PBP2a function), FtsA (divisome) and MurC (Fenton et al., 2018, Fleurie et al., 2014, Holečková et al., 2015,

Massidda et al., 2013, Sun et al., 2010, Nováková et al., 2010, Falk and Weisblum, 2013). It is known that PhpP modulates the activity of StkP by dephosphorylation of StkP kinase domain, but what decides the balance between the two (auto/de-phosphorylation) is not known (Beilharz et al., 2012, Osaki et al., 2009).

EloR is a RNA binding protein conserved in many Gram-positive genera including streptococcus, bacillus and clostridium. EloR is involved in cell elongation in *S. pneumoniae* and consists of three domains, an N-terminal jag domain, a KH-II domain and R3H domain. The two latter ones are both RNA-binding domains (Grishin, 1998, Valverde et al., 2008) while the Jag domain has an unknown function (Figure 6).

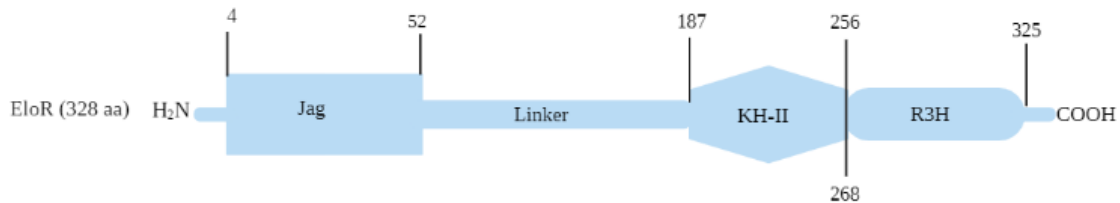


Figure 6 Schematic presentation of EloR, with the predicted domains with corresponding domain borders. EloR consists of a Jag domain, a linker with unknown function, and two RNA binding domains, KH-II and R3H (Winther, 2020), figure adapted in Biorender.com

A study done by Stamsås et al., found that i) StkP plays an important role in regulating the activity of EloR and thus cell elongation through phosphorylation, and (ii) the phosphorylated form of EloR is the elongasome stimulating form. Both phosphorylation sites (Thr89 and Thr 126) are found in the linker region of EloR (Figure 6). EloR is not phosphorylated when the PASTA domain of StkP is removed (Stamsås et al., 2017). This leads to a conclusion that StkP uses the extracellular PASTA domain to sense the status of the cell wall, and how far along the cell cycle has progressed to appropriately time the phosphorylation of EloR. StkP and PhpP are working in unison in *S. pneumoniae* to control different cellular processes, including cell division (Stamsås et al., 2017).

1.4 The EloR-KhpA-MltG complex

In a study performed by Stamsås et al., 2017 they attempted to identify novel genes important for cell elongation in *S. pneumoniae* by obtaining suppressor mutants that allowed survival without the essential PBP2b. Three of the mutants displayed mutations in the *mltG* gene and three other suppressors had mutations in the *spr1851* gene and in *khpA* (*spr0683*), giving rise

to truncated versions of the proteins and shorter cell chains compared to the morphology of the wild type (Zheng et al., 2017). It was also found that pneumococci were no longer dependent upon cell elongation in a $\Delta spr1851$ background, since *pbp2b* and *rodA* were no longer essential. This gave reason to believe that Spr1851 had a regulatory function related to cell elongation and the protein was therefore named elongasome regulating protein, EloR (Stamsås et al., 2017). Another study done by Ulrych et al., 2016 also discovered the same morphology in a $\Delta spr1851$ mutant and over-expression of EloR resulted in elongated cells (Ulrych et al., 2016).

EloR forms a complex with another RNA binding protein called KhpA; where site-specific point mutations and protein cross-linking has shown that KhpA interacts with itself and the KH-II domain of EloR (Figure 8) (Zheng et al., 2017, Winther et al., 2019). Both EloR and KhpA localize to the division zone of streptococci, but KhpA is dependent upon EloR for localization (Winther et al., 2019). Point mutations inactivating the RNA-binding domains of EloR suggest that the phosphorylation of EloR by StkP leads to the release of bound RNA, stimulating cell elongation (Stamsås et al., 2017). KhpA is a cytosolic RNA-binding protein consisting of a single KH-II domain. A study by Zheng et al., 2017 showed that a $\Delta khpA$ mutant phenocopies $\Delta eloR$ mutant so the essential *pbp2b* and *rodA* genes can be deleted, and the cells displays shortened morphology (Zheng et al., 2017). Also, if the EloR/KhpA complex is broken, the cells become shorter leading to the loss of elongasome function and are no longer dependent on the PBP2b/RodA pair. The reduced elongation is most likely due to loss of RNA-binding. Both PBP2b and RodA are essential in wild type cells because without these, other elongasome proteins are not regulated properly and elongation becomes uncontrolled, leading to cell death (Winther et al., 2019). The method behind this is unknown, but it has been speculated that the lytic transglycosylase MltG is involved, and is possibly caused by the uncontrolled actions of MltG that is lethal to the cells (Stamsås et al., 2017).

Biochemical studies of MltG by Yunck et al., 2016 in *E. coli* revealed that MltG is an inner membrane enzyme with inner endolytic transglycosylase activity which is capable of cleaving glycan polymer. This study also showed that MltG and PBP1b interacts in *E. coli* using bacterial two-hybrid analysis. Also, mutants lacking MltG showed longer glycan chains in their PG relative to wild type cells. This proves that MltG is associated with PG synthesis, cleaving polymers and participates in elongation (Yunck et al., 2016). It was proved by Tsui et al., 2016 that *mltG* encodes the structural and functional pneumococcal homologue of the membrane-

bound endo-lytic transglycosylase of *E. coli*. MltG consists of a cytoplasmic domain, a membrane spanning α -helix and an extracellular lytic transglycosylase domain (Figure 7) (Tsui et al., 2016b). Also, multiple suppressor mutations showed that the *mltG* gene relieves the requirement for PBP2b and it has been hypothesized that MltG is the enzyme that releases newly synthesized glycan strands during peripheral PG synthesis (Tsui et al., 2016a).

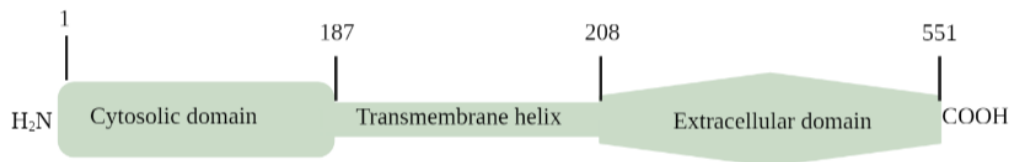


Figure 7 Schematic presentation of MltG, with the predicted domains with corresponding domain borders. MltG consists of a cytosolic domain, a transmembrane domain and an extracellular domain (Winther, 2020). Figure adapted in Biorender.com

Possible hypothesis of different functions of MltG has been suggested although it has not been published definite evidence of the function of the enzyme. It is believed that EloR/KhpA is likely to have a regulatory role in the MltG activity. One possibility is that MltG opens the peripheral PG meshwork to allow new material to be incorporated by RodA/PBP2b. It is important that this process is tightly regulated since the PG layer would quickly be weakened and cell lysis would occur if MltG was allowed to “roam free”. MltG activity seems to be lethal without RodA/PBP2b present and vice versa, maybe because this complex is necessary for filling in the gaps that MltG makes. Based on this, it is believed that MltG opens the PG layer for insertion of new PG by RodA/PBP2b and StkP/EloR/KhpA are involved in tight regulation of this process (Figure 8) (Winther, 2020).

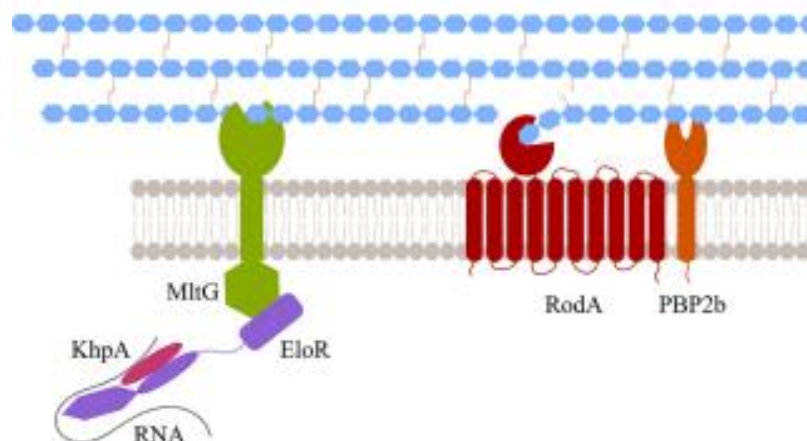


Figure 8 Model of the protein complex MltG/EloR/KhpA. It has been speculated that the EloR/KhpA complex modulates the activity of MltG via the RNA-binding domains. It is suggested that MltG can open the PG layer, allowing PBP2B/RodA to insert new PG into the existing layer leading to elongation of the cell. Figure from (Winther et al., 2021).

A study done by Winther et al., 2019 found EloR in midcell co-localizing with FtsZ during cell division. It is of great interest to find the part of EloR directing it to the division centre and find possible interaction partners like MltG, a protein being a part of the elongasome (Tsui et al., 2016b, Winther et al., 2019).

1.5 Aim of Study

A new regulatory signalling pathway has been identified which controls when the bacteria elongate in the cell cycle. It is speculated that the two RNA binding proteins called EloR and KhpA regulates MltG in the division zone and participates in controlling when the bacteria should extend the cell wall in the longitudinal direction. The mechanism of the EloR-KhpA-MltG complex is not known, and in this project, genetic and molecular methods will be utilized to characterize this protein complex. Questions to be answered involves interactions within the complex and with other cell division proteins. There will also be done further studies on how different manipulations of the protein complex influence the cell division process. One of the main goals of this work is to find whether the bacteria can survive the lack of cell elongation if the interaction between EloR and MltG breaks. EloR, MltG and other essential proteins which is a part of this regulatory pathway is potential drug targets for future antibiotics.

2. Materials

2.1 Bacterial strains and plasmids

Table 2.1 Bacterial strains and plasmids with relevant characteristics.

<i>S. pneumoniae</i> strains	Characteristics	Source of Reference
R704	R6 derivat <i>comA::ermA</i> ; Ery ^r	JP. Claverys*
RH425	R704, but streptomycin resistant: Ery ^r , Sm ^r	(Johnsborg and Håvarstein, 2009a)
Aw407	$\Delta comA$, $P_{comX}::eloR$ - <i>mKate2</i> ; Ery ^r Sm ^r	(Winther et al., 2021)
Aw408	$\Delta comA$, $P_{comX}::jag$ - <i>mKate2</i> ; Ery ^r Sm ^r	(Winther et al., 2021)
Aw409	$\Delta comA$, $P_{comX}::jag$ - <i>linker-mKate2</i> ; Ery ^r Sm ^r	(Winther et al., 2021)
Aw410	$\Delta comA$, $P_{comX}::linker$ - <i>mKate2</i> ; Ery ^r Sm ^r	(Winther et al., 2021)
Aw420	$\Delta comA$, $P_{comX}::eloR^{K36A}$ - <i>mKate2</i> ; Ery ^r Sm ^r	(Winther et al., 2021)
Aw424	$\Delta comA$, $P_{comX}::eloR^{K37A}$ - <i>mKate2</i> ; Ery ^r Sm ^r	(Winther et al., 2021)
Aw425	$\Delta comA$, $P_{comX}::eloR^{F39A}$ - <i>mKate2</i> ; Ery ^r Sm ^r	(Winther et al., 2021)
Aw426	$\Delta comA$, $P_{comX}::eloR^{L40M}$ - <i>mKate2</i> ; Ery ^r Sm ^r	(Winther et al., 2021)
Aw453	$\Delta comA$, $P_{comX}::eloR$ - <i>mKate2</i> $\Delta stkP::janus$; Ery ^r Km ^r	(Winther et al., 2021)
Aw415	$\Delta comA$, $P_{comX}::eloR$ - <i>mKate2</i> $\Delta yidC2::janus$; Ery ^r Km ^r	(Winther et al., 2021)
Aw417	$\Delta comA$, $P_{comX}::eloR$ - <i>mKate2</i> $\Delta rodZ::janus$; Ery ^r Km ^r	(Winther et al., 2021)
MH43	$\Delta comA$ <i>m(sf)gfp-mltG</i> ; $\Delta yidC2::janus$; Ery ^r Km ^r	This work and published in (Winther et al., 2021)
MH16	$\Delta comA$, <i>mltG^{ADUF}</i> , P_{comX} - <i>mltG</i> ; Ery ^r Sm ^r	This work
MH17	$\Delta comA$, $\Delta mltG::janus$, P_{comX} - <i>mltG^{ADUF}</i> Ery ^r Km ^r	This work
MH19	$\Delta comA$, <i>mltG^{ADUF}</i>	This work
MH28	$\Delta comA$, $\Delta janus::P_{comX}$ - <i>mltG^{ADUF}</i> ; Ery ^r Km ^r	This work
MH31	$\Delta comA$, $\Delta mltG::janus$, P_{comX} - <i>mltG^{ADUF}</i> ; Ery ^r Sm ^r	This work
MH44	$\Delta comA$, $\Delta mltG::janus$, P_{comX} - <i>mltG^{ADUF}</i> , <i>eloR</i> - <i>mKate2</i> - <i>aad9</i> ; Ery ^r Sm ^r , Spc ^r	This work
MH50	$\Delta comA$, <i>gfp-mltG</i> , $\Delta janus::flag$ - <i>jag</i> ; Ery ^r Km ^r	This work
<i>E. coli</i> strains		
XL1 blue	Host strain	Agilent Technologies
BTH101	BACTH expression strain <i>cyo</i>	Euromedex
Plasmids		
Genhogs (ds972)	pRSET-His-MltGcyt	This work
BL21 (ds974)	pRSET-MltGcyt 6xHis N-term v.2.0 DUF1346	This work
pUT18C	Plasmid used in BACTH analysis	Euromedex
pKNT25	Plasmid used in BACTH analysis	Euromedex
pKT25	Plasmid used in BACTH analysis	Euromedex
pKT25- <i>zip</i>	T25 fused to a leucine zipper domain	Euromedex
pUT18C- <i>zip</i>	T18 fused to a leucine zipper domain	Euromedex
pKNT25- <i>eloR</i>	T25 domain fused to the C terminus of EloR	(Stamsås et al., 2017)
pKT25- <i>jag</i>	T25 domain fused to the N terminus of the Jag domain of EloR	(Winther et al., 2021)
pKNT25- <i>jag</i>	T25 domain fused to the C terminus of the Jag domain of EloR	This work
pUT18C- <i>mltG</i>	T18 domain fused to the N terminus of MltG	(Stamsås et al., 2017)
pUT18C- <i>mltGcyt</i>	T18 domain fused to the N terminus of the cytoplasmic domain of MltG	This work and published in (Winther et al., 2021)
pUT18C- <i>mltGcyt</i> Δ DUF	T18 domain fused to the N terminus of the cytoplasmic domain of MltG without DUF	This work and published in (Winther et al., 2021)
pUT18C- <i>pBP2b</i>	T18 domain fused to the N terminus of PBP2b	(Straume et al., 2017)
pUT18C- <i>rodA</i>	T18 domain fused to the N terminus of RodA	(Straume et al., 2017)
pUT18C- <i>rodZ</i>	T18 domain fused to the N terminus of RodZ	(Straume et al., 2017)

pUT18C- mreC	T18 domain fused to the N terminus of MreC	(Straume et al., 2017)
pUT18C- mreD	T18 domain fused to the N terminus of MreD	(Winther et al., 2021)
pUT18- cozE	T18 domain fused to the C terminus of CozE	(Straume et al., 2017)
pUT18- yidC2	T18 domain fused to the C terminus of YidC2	(Winther et al., 2021)
pKT25- jag ^{B6}	T25 domain fused to the N terminus of B6 Jag	This work
pKT25- jag ^{M25A}	T25 domain fused to the N terminus of Jag ^{M25A}	This work
pKT25- jag ^{K37A}	T25 domain fused to the N terminus of Jag ^{K37A}	This work
pKT25- jag ^{M25A, K37A}	T25 domain fused to the N terminus of Jag ^{M25A, K37A}	This work
pUT18C-mltGcyt from <i>S. thermophilus</i>	T18 domain fused to the C terminus of <i>S. thermophilus</i>	This work
pUT18C- mltGcyt from <i>S. sanguinis</i>	T18 domain fused to the C terminus of <i>S. sanguinis</i>	This work
pUT18C- mltGcyt from <i>S. mitis</i>	T18 domain fused to the C terminus of <i>S. mitis</i>	This work
pUT18C- mltGcyt from <i>S. infantis</i>	T18 domain fused to the C terminus of <i>S. infantis</i>	This work

*Gift from Professor Jean-Pierre Claverys, CNRS, Toulouse, France

2.2 Primers

Table 2.2 List of primers used in this work.

Name	Sequence (5'-3')	Reference
Primers used to create the mltGcyt^{ADUF} amplicon and introducing it into BACTH plasmid pUT18C		
Mlh1	GCTATGATGAAGTTCTGAAAGAAGAAACACCTACGCCTGC TAC	This work and (Winther et al., 2021)
Mlh2	TCTTTCAGAACTTCATCATAGC	This work and (Winther et al., 2021)
aw268	GATCTCTAGAGTTGAGTGAAAAGTCAAGA GAAGAA	(Winther et al., 2021)
aw269	GATCGAATTCTTAGAATGAAATCACAAAAGCTTTCAC	(Winther et al., 2021)
KHB430	TGGCACGACAGGTTTCCCG	Dr. Kari Helene Berg
KHB434	GAAAACCTCTGACACATGCAG	Dr. Kari Helene Berg
Primers used to create the mltG^{ADUF} amplicon		
Mlh1	GCTATGATGAAGTTCTGAAAGAAGAAACACCTACGCCTGC TAC	This work
Mlh2	TCTTTCAGAACTTCATCATAGC	This work
ds361	AAACTAGCCGCAGGTTGCTC	(Straume et al., 2017)
ds362	AATTAAGATCATTTCAGGCAAGC	(Straume et al., 2017)
Primers used to create sph131 amplicon (Janus)		
KHB31	ATAACAAATCCAGTAGCTTTGG	(Berg et al., 2011)
KHB34	CATCGGAACCTATACTCTTTTAG	(Berg et al., 2011)
Primers used to create MltGcyt amplicon in different Streptococcal species, for BACTH analysis		
Mlh3	GATCTCTAGAGATGTTAGGGATTATGATGAAGGAG	This work
Mlh4	GATCGAATTCTTACGTTGTCATAATCCTGCGGG	This work
Mlh5	GATCTCTAGAGTTGAGTGAAAAGCCAAGAGAAG	This work
Mlh6	GATCGAATTCTTATAGAGAAATGAAGAAAGCTT TCAAAT	This work
Mlh7	GATCTCTAGAGTTGACTGAAAATTCACAAGATAAT GAT	This work
Mlh8	GATCGAATTCTTACGTCCAGACAATTCTTTTGGCG	This work
Mlh9	GATCTCTAGAGTTGAGCGAAAATTCTCGAGAAG	This work

Mlh10	GATCGAATTCTTATACTGTTACGAAAAATCCTTTC AAG	This work
Mlh11	GATCTCTAGAGTTGACGGACAAGCATAATGAA TAC	This work
Mlh12	GATCGAATTCTTAGTTTCTTGCAACTCGTCCTG	This work
Mlh13	GATCTCTAGAGTTGGTGGACAAAGAAACAACCTGAA	This work
Mlh14	GATCGAATTCTTAAATCACAGCAATGATTTTTCTGC	This work
Mlh15	GATCTCTAGAGATGCTTTTGGACTGAAAAATCAAGAG	This work
Mlh16	GATCGAATTCTTAAACTGTTACTAGGCAACCTTTAG	This work
Primers used to create MltG^{ADUF} amplicon, place it behind P_{comX}		
KHB31	ATAACAAATCCAGTAGCTTTGG	(Berg et al., 2011)
KHB34	CATCGGAACCTATACTCTTTTAG	(Berg et al., 2011)
Mlh1	GCTATGATGAAGTTCTGAAAGAAGAAACACCTACGCCTGCTAC	This work
Mlh2	TCTTTCAGAACTTCATCATAGC	This work
Primers used to create the ΔMltG::Janus amplicon		
ds361	AAACTAGCCGCAGGTTGCTC	(Straume et al., 2017)
ds362	AATTAAGATCATTGAGGCAAGC	(Straume et al., 2017)
Primers used to create the ΔYidC2 amplicon		
ds403	ATATTGATCCAGCTATCATTCC	(Winther et al., 2021)
ds406	GCTCATCACCTTCAGAGTAAC	(Winther et al., 2021)
Primers used to create the eloR-mKate2-aad9 amplicon		
ds374	CGAAACCTTGGGATACGCAG	(Stamsås et al., 2017)
ds377	CAGCACCCACGTTAAGCAAC	(Stamsås et al., 2017)
aw318	CTAGTAAATTGGGACACCGTTAATTAATGTGCTATAATA CTAGAAAATACTTGTGTGAGGAGGATATATTTGAATACAT ACGAACAAATTAATAAAG	Dr. Anja Ruud Winther
Primers used to create Flag- jag amplicon		
Mlh22	ATTTATATTTATTATTGGAGGTTCAatgGATTATAAAGATC ATGATGGTGATTA	This work
Mlh23	ATTGGGAAGAGTTACATATTAGAAA TTATTTGACAACAG TCGTTTCACT	This work
KHB31	ATAACAAATCCAGTAGCTTTGG	(Berg et al., 2011)
KHB36	TGAACCTCCAATAATAAATATAAAT	(Berg et al., 2011)
KHB33	TTTCTAATATGTAACCTTTCCCAAT	(Berg et al., 2011)
KHB34	CATCGGAACCTATACTCTTTTAG	(Berg et al., 2011)
Primers used to create Jag^{M25A}, Jag^{K37A}, Jag^{M25A,K37A} and B6 Jag for BACTH analysis.		
Aw271	GATCTCTAGAGGTAGTATTTACAGGTTCAACTGTT	(Winther et al., 2021)
Aw260	gca GGCTTTCTTGGTCTATTTGGTA	(Straume et al., 2017)
Aw261	TACCAAATAGACCAAGAAAGCC tgc TTTCTCCCTAGAAATGAC TTTGAT	(Winther et al., 2021)
ds336	CACGACAGGTTTCCCGACTG	This work
KHB430	TGGCACGACAGGTTTCCCG	This work
Mlh17	gatcGAATTCTtaTTTAATGACCGTTGTTTCACTAATAG	This work
Mlh20	GATTGAAAGAATTAGATATTTCCAAGAGCAAAGGCTCATATCA AAGTCATTTCTA	This work
Mlh21	TGC TC TTG GAA TAT CTA ATT CTT TCA ATC	This work
Primers used to create 6x-His- TEV-		
Aw257	gatc CATATG CATCATCATCATCATGAGAAC	Dr. Anja Ruud Winther
Mlh24	gatcGAATTCTtaTTTGACAACAGTCGTTTCACTAATC	This work
Primers used to create N-terminal 6x-His- MltGcvt amplicon		
ds731	gatcCATATGCATCATCATCATCATGAGGACTGAAAGAAGAT GAGGCAGTAG	This work
ds732	gatcGAATTCTTATGTTTCTGGACCTGCTTGTTTC	This work

Primer used to create His-tag, TEV, Jag-linker

Aw256	gatc AAGCTT TTATTGTTCAATATCAAAGTTCGTTTC	Dr. Anja Ruud Winther
Aw257	gatc CATATG CATCATCATCATCATGAGAAC	Dr. Anja Ruud Winther
Sequencing primers		
KHB439	ACCGTGCATACGGCGTGG	This work
KHB458	GAGACGGTCACAGCTTGTC	This work
ds393	CGAAGGCCAGTCCCAGTC	This work
ds394	GACGAACCAATTTCAATTCTTC	This work
css26	TAAAGTCGGTTTCACCTCTTC	master student
css29	CAACAATCAAGTGGTATACAG	master student
aw234	TCCGGATCTGGTGGAGAAG	(Winther et al., 2021)
ds380	CTATACTGGACAGTGTCTAATG	This work
ds381	TTCGGGCCTCTTGTCCTTG	This work
KHB436	CAATGCCGCCGGTATTCC	This work
KHB457	CATTCAGGCTGCGCAACTG	This work
KHB430	TGGCACGACAGGTTTCCCG	This work
KHB434	GAAAACCTCTGACACATGCAG	This work
ds336	CACGACAGGTTTCCCGACTG	This work
KHB431	GCAAAAAGCACCGCCGGAC	This work

2.3 Kits

Table 2.3 Kits used in this work and a description of area of use.

Name	Area of Use	Supplier
E.Z.N.A Plasma DNA mini Kit I	Extraction and cleaning of plasmid- DNA from <i>E.coli</i>	Omega bio-tek
Nucleospin® Gel and PCR Clean- up kit	Purification of PCR-products and DNA from agarose gel	Macherey- Nagel

2.4 Antibiotics

Table 2.4 List of different antibiotics used in this work with corresponding stock solutions and concentrations used

Antibiotic	Stocksolution	Working concentration
Ampicillin	100 mg/ml	100 µg/ml
Kanamycin	100 mg/ml	50 µg/ml
		400 µg/ml
Streptomycin	100 mg/ml	200 µg/ml
Spectinomycin	100 mg/ml	200 µg/ml

2.5 Chemicals

Table 2.5 Overview over the different chemicals used in this work.

Acetic acid, Acrylamide, Agarose, APS, Biotine, bis acrylamide, Bromophenol blue, BSA, CaCl₂, Ca pantheothenate, Casitone, Choline, Coomassie brilliant blue, CSP, CuSO₄·5H₂O, Cysteine HCl, Dimethylformamide, EDTA, Ethanol, FeSO₄·7H₂O, Glacial acetic acid, Glutamine, Glycerol, HCl, Imidazole, IPTG, KCl, KH₂PO₄, K₂HPO₄, L-Tryptophane, Mangan (II)chloride, Methanol, Mg²⁺, MgCl₂, MgCl₂·6H₂O, MgSO₄, MnCl₂·4H₂O, Na acetate, NaCl, Na₂HPO₄, Nicotinic acid, PBS, PeqGREEN, Riboflavin, Sodium dodecyl sulphate (SDS), sucrose, Sodium pyruvate, TBS, TEMED, Thiamine hydrochloride, Todd Hewitt, Tris base, Tris-HCl, Triton X-100, Tryptone, , X-gal, Uridine adenosine, yeast extract.

2.6 Equipment

Table 2.6 List of equipment used in this work and the corresponding model, excluding standard laboratory equipment.

Name	Model
ÄKTA pure	25L
Azure biosystems	c400, AH diagnostics
Fast Prep	FastPrep@24, MP Biomedicals
Gel imager	Gel Doc-1000, Biorad
Microscope	LSM700 Zeiss
PCR	ProFlex PCR systems, Agilent
Spectrophotometer	NanoDrop 2000
Transblot® turbo transfer systems	BioRad

2.7 Growth mediums and buffers

2.7.1 Solutions for C-medium

Adams I

150 µl 0.5 mg/ml Biotine

75 mg Nicotinic acid

87.5 mg Pyrodoxine hydrochloride (4°C)

300 mg Ca pantheothenate

80 mg Thiamine hydrochloride

35 mg Riboflavin

Add dH₂O to a final volume of 500 ml, adjust pH to 7.0. Finally, sterile filter (0.2 µm) and store at 4°C.

Adams II-10x

500 mg Iron (II)sulphate heptahydrate ($\text{FeSO}_4 \cdot 7\text{H}_2\text{O}$)

500 mg Copper sulphate pentahydrate ($\text{CuSO}_4 \cdot 5\text{H}_2\text{O}$)

500 mg Zinc sulphate heptahydrate ($\text{ZnSO}_4 \cdot 7\text{H}_2\text{O}$)

200 mg Mangan(II)chloride tetrahydrate ($\text{MnCl}_2 \cdot 4\text{H}_2\text{O}$)

10 ml HCl concentrate

Add dH₂O to a final volume of 100 ml. Finally, sterile filter and store at 4°C.

Adams III

128 ml Adams I

3.2 ml Adams II-10x

1.6 g L-Asparagine.H₂O

160 mg choline

0.4 g CaCl₂ anhydride

16 g Magnesium chlorine hexahydrate ($\text{MgCl}_2 \cdot 6\text{H}_2\text{O}$)

Add dH₂O to a final volume of 800ml, adjust pH to 7.6. Finally, sterile filter and store at 4°C.

Yeast extract

40 g yeast extract

360 ml dH₂O

37% HCl to pH=3

16 g active coal

Mix solution for 2-5 hours at 4°C. After incubation, filter solution through a column with glass wool and celite overnight. Adjust pH to 7.8 and add dH₂O to a final volume of 400 ml.

Finally, sterile filter the solution and store in 4 ml aliquots at -80°C.

Pre C-medium

22.5 g Cysteine HCl

4 g Na acetate

10 g Casitone

12 g L-Tryptophane

17 g Di-calcium phosphate (K_2HPO_4)

Add dH₂O to a final volume of 2 L. Finally, autoclave and store in 150 ml aliquots at room temperature.

C-medium

Added to 150 ml pre C-medium:

150 µl 0.4 mM Mangan (II)chloride

1.5 ml 20% Glucose

3.75 ml ADAMS III

110 µl 3% (w/v) Glutamine

2.5 ml 2% (w/v) Soidut pyruvate

95 µl 1.5 M Sucrose

1.5 ml 2 mg/ml Uridine adenosine

1.5 ml 8% (w/v) BSA

3.75 ml Yeast extract

The solution was sterile filtered before use to prevent contamination. The C-medium was made the same day of use and stored at 4°C.

2.7.2 Buffers and solutions for agarose gel electrophoresis

1% agarose gel

0.5 g agar

50 ml TAE buffer

Heat up solution until agar is dissolved and add 1 µl PeqGREEN.

6x loading dye

60 mM Tris-HCl pH 8.0

6 mM EDTA

40% (w/v) sucrose

0.025% (w/v) Bromophenol blue

1kb DNA ladder

50 µl 1kb ladder (10 µg)

200 µl 10x loading buffer

750 µl dH₂O

50x Tris-acetate-EDTA (TAE buffer)

Tris acetate protects the DNA from hydrolysis, while EDTA, a chelator of cations such as magnesium, protects nucleic acids against enzymatic degradation.

242 g Tris base

57.1 ml Acetic Acid

100 ml 0.5 M EDTA, pH 8.0

Adjust volume to 1L with dH₂O.

2.7.3 Buffers and solutions for SDS-PAGE

10 ml 4x SDS sample buffer

2.5 ml 1M Tris-HCl pH6.8
0.5 ml dH₂O
1 g SDS
0.8 ml 0.1% bromophenol blue
14.3 M β-mercaptoethanol
Adjust to 10 ml with dH₂O

10x SDS running buffer

144 g Glycine
30.2 g Tris base
10 g SDS
The solution was adjusted to 1L with dH₂O

12% Separation gel (makes 2): 40% acrylamide+ bis-acrylamide

4.3 ml ddH₂O
2.5 ml 1.5M Tris-HCl, pH 8.8
0.1 ml 10% SDS
3.0 ml 40% acrylamide+0.8% bis acrylamide
0.1 ml 10% APS
0.005 ml TEMED
APS was made fresh. Mixing all reactants together except from APS and TEMED which is added last, right before casting the gel.

15% Separation gel (makes 2) 40% acrylamide + bis-acrylamide

3.55 ml ddH₂O
2.5 ml 1.5M Tris-HCl, pH 8.8
0.1 ml 10% SDS
3.75 ml 40% acrylamide + 0.8% bis acrylamide
0.1 ml 10% APS
0.005 ml TEMED
APS was made fresh. Add APS and TEMED last, then cast the gels immediately

4% Stacking gel (makes 2)

3.15 ml ddH₂O
1.25 ml 0.5M Tris-HCl, pH 6.8
0.05 ml 10% SDS
0.5 ml 40% acrylamide +0.8% bis-acrylamide
50 μl Bromophenol blue
0.05 ml 10% APS
0.0005 ml TEMED
APS was made the day of use. All reagents, except APS and TEMED were mixed. Just before casting the gels, APS and TEMED were added to start the polymerization reaction. The separation gels were made first and allowed to polymerize before stacking gels were cast on top.

2.7.4 Buffers and solutions for Western blot and co- immunoprecipitation

TBS-T (1L)

20 ml 1M Tris pH 7.4

30 ml 5M NaCl

0.5 ml Tween

Add everything to a flask and adjust the volume to 1L with dH₂O.

1xTBS (500 ml)

10 ml 1M Tris HCl, pH 7.4

15 ml 5M NaCl

Add dH₂O up to 500 ml

Lysis buffer for co-immunoprecipitation (10 ml)

50 mM Tris-HCl, pH 7.4 (500 µl)

150 mM NaCl, (750 µl)

1 mM EDTA (20 µl)

1% Triton X-100 (1 ml)

Adjust volume to 10 ml

Western transfer/ Towbin buffer/(1L)

3.0 g Tris Base

14.4 g glycine

200 ml methanol

Coomassie staining (100ml)

0.2 g Coomassie brilliant blue

40 ml ethanol,

Dissolve and then add:

7.5 ml Glacial acetic acid

52.5 ml H₂O

Filter before use

Coomassie de-staining buffer (100ml)

40 ml ethanol

7.5 ml glacial acetic acid

52.5 ml H₂O

2.7.5 Buffers for IMAC and Gel filtration

Buffer A (binding buffer)

20 mM Tris HCl

500 mM NaCl

20 mM Imidazole

Add everything to a flask and adjust the volume to 250 ml dH₂O

Buffer B (elution buffer)

20 mM Tris HCl

500 mM NaCl

500 mM imidazole

Add everything to a flask and adjust the volume to 250 ml dH₂O

TBS, pH 7.4

150 mM NaCl

20 mM Tris HCl, pH 7.4

2.7.6 Other buffers and solutions

1M Tris HCl buffers

121.14 g Tris base

Dissolve in 800 ml dH₂O, adjust to desired pH with HCl, add dH₂O to a final volume of 1000 ml.

LB growth medium:

10 g Tryptone

5 g yeast extract

10 g NaCl

Add dH₂O to a final volume of 1L and autoclave.

LB agar:

LB growth medium

7.5 g agar in 500mL

After autoclaving, add appropriate antibiotics and inducers at approximately 55 °C before pouring plates.

PBS (1%)

8 g NaCl

0.2 g KCl

1.44 g Na₂HPO₄

0.24 g KH₂PO₄

800 ml dH₂O

Adjust pH to 7.4 fill up to 1000 ml with dH₂O.

CaCl₂ (0.1 M in 0.25 L)

CaCl₂ = 147.02 g/mol

3.67 g CaCl₂

250 ml dH₂O

Sterile filter and store at 4°C

SOC medium

0.5 g yeast extract

2.0 g tryptone

0.0584 g NaCl

0.0186 g KCl

0.24 g MgSO₄

Fill up the flask with 98 ml dH₂O.

Add 2 ml filtered sterilized 20% glucose and store at -20°C.

Todd Hewitt agar plates:

15 g TH

7.5 g agar

Add dH₂O to 500 ml

To prepare the selective medium, cool the medium to 55°C after autoclaving and add appropriate antibiotics. Pour the medium into petri dishes and let them solidify.

3. Methods

3.1 Growth and storage of bacteria

3.1.1 *Streptococcus pneumoniae*

S. pneumoniae was grown under anaerobic conditions at 37°C. When grown in liquid medium, airtight tubes and C-medium were used. When grown on solid medium, Todd Hewitt (TH) agar was used and incubated in an-airtight container with an Oxoid™ AnaeroGen™ sachet. The AnaeroGen sachet absorbs atmospheric oxygen reducing it to 1% within 30 minutes, simultaneously producing CO₂ (ThermoFisher). When necessary, the appropriate antibiotic was added as indicated in Table 2.4.

For long time storage of *S. pneumoniae*, cells were grown in C-medium with appropriate antibiotics (kanamycin=400 µg/ml and streptomycin=200 µg/ml) and ComS inducer when needed, until exponential phase OD₅₅₀ ≈ 0.3. Glycerol stocks were made by adding glycerol to a final concentration of 16% (v/v) and stored at -80°C.

3.1.2 *Escherichia coli*

Bacterial strains of *E. coli* are listed in Table 2.1. Strains of *E. coli* were grown in LB medium with shaking or on LB agar plates under optimal aerobic conditions at 37°C. When appropriate, the following concentration of antibiotics were added in the growth medium: ampicillin = 100 µg/ml and kanamycin = 50 µg/ml.

For long time storage of *E. coli*, cells were grown until exponential phase OD₆₀₀ ≈ 0.6-1.0 before glycerol stocks were made by adding glycerol to a final concentration of 16%. Frozen stocks were stored at -80°C.

3.2 Plasmid isolation

Many bacteria have small independent replicating circular DNA molecules known as plasmids. Plasmids is not essential for bacterial growth but often carry genes that confer desirable traits to bacteria, such as antibiotic resistance.

Plasmids were isolated using E.Z.N.A.® Plasmid Mini Kit I by following the manufacturer protocol. This protocol was used for plasmid isolation from *E. coli*. Cells were harvested from 5 ml overnight (o/n) culture by centrifugation. The cell pellet was resuspended in 250 µl Solution I, containing RNase A, to degrade RNA. Cells were lysed by adding 250 µl Solution II. After inverting the tube to obtaining a clear lysate, 350 µl of the neutralization buffer, Solution III was added. This resulted in precipitation of chromosomal DNA and cellular debris, while plasmid DNA remained in the solution. The precipitate was pelleted by centrifugation at max speed (13,000 x g) for 10 min, and the cleared supernatant was transferred to a pre-equilibrated E.Z.N.A HiBind® DNA mini column (50 µl equilibration buffer was added to the column and centrifuged at 13,000 x g for 1 min). The flowthrough was discarded and 500 µl HBC buffer was added to the column to bind plasmid DNA to the silica column. The bound DNA was washed twice using 700 µl of the supplied wash buffer. Finally, the empty column was centrifuged to remove any residual ethanol from the wash buffer and plasmid DNA was eluted using 30-100 µl elution buffer. In this work, 30 µl elution buffer were used when isolating low copy number plasmids, and 50 µl elution buffer when isolating high copy number plasmids. Isolated plasmids were stored at -20°C.

3.3 The Polymerase Chain Reaction

Polymerase chain reaction (PCR) is an effective and versatile method used for amplifying DNA from a specific region on a template DNA molecule. The main components in a PCR reaction are DNA serving as the template, primer oligos complementary to specific regions on the template DNA, a thermostable DNA polymerase such as Taq or Phusion, and the four deoxynucleotide triphosphates (dNTPS) dATP, dCTP, dGTP and dTTP. The primer is a short nucleotide sequence that provides a 3`end from which synthesis begins and marks the left and the right boundaries of the DNA to be amplified. At the start of each cycle, the two strands of the double stranded DNA template are separated by heating, and the primers anneal to the DNA when lowering the temperature. DNA polymerase then replicates each strand independently and all the newly synthesised DNA molecules produced by the polymerase serves as template for the next round of replication (Bruce Alberts, 2015, Saiki et al., 1985).

The PCR reaction can be divided into three steps, a series of heating and cooling cycles repeated 25-30 times. The first step is to heat the double stranded DNA briefly to separate the two strands, before the DNA is exposed to a large excess of a pair of specific primers designed to

anneal to the region of DNA that is to be amplified. In the last step, the temperature is set to 72°C to let the DNA polymerase extend the primers by incorporating dNTPs (Figure 9). Billions of copies of a DNA region can be generated in matters of hours and the amplified genetic information is then available for further analysis (Saiki et al., 1985, Bruce Alberts, 2015).

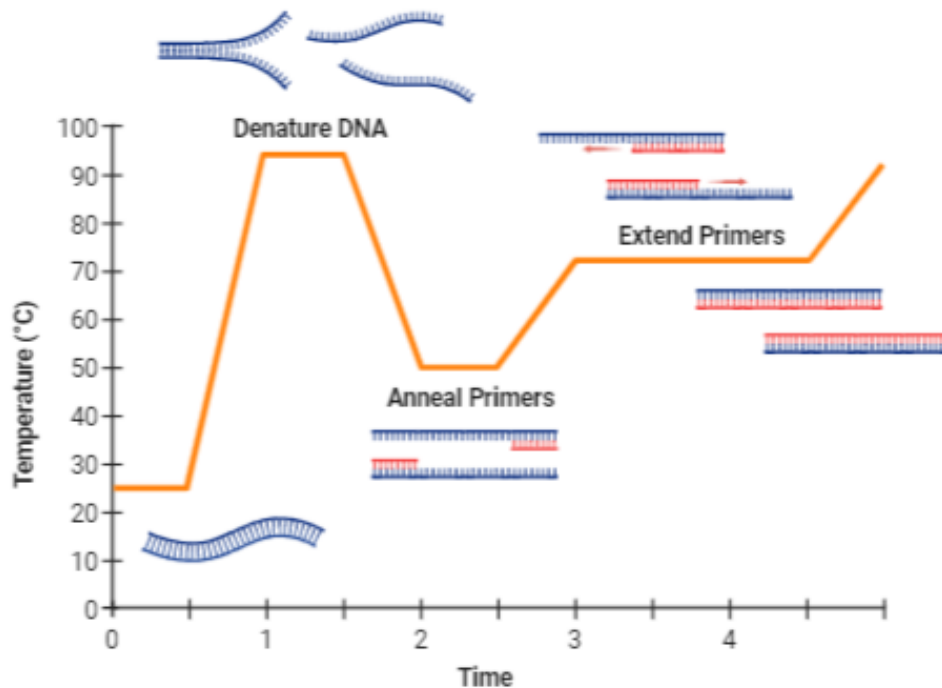


Figure 9: Illustration of the PCR cycle with temperature over time and the different stages of denaturing of DNA, annealing of primers and extending primers. The PCR temperature cycle: (1) the temperature is raised to about 95°C to separate the double helical DNA, (2) the temperature is lowered to let primers anneal to the template with a temperature between 58-60°C. (3) the temperature is set to 72°C to let the polymerase extend the primers by incorporating the dNTPs (Bryksin and Matsumura, 2010). Figure adapted from Biorender.com

3.3.1 Primer design and preparation

The main goal of primer design is to obtain specificity (low mispriming occurrence) and ensuring a PCR product of sufficient quality. In addition, the primers can be designed to introduce restriction sites, point mutations, and tags encoding sequences in the PCR product. When designing primers; their melting temperature (T_m) and possible homology among primers are the primary factors affecting the reaction (Dieffenbach et al., 1993). When designing primers, there is some general properties that should be followed: The length of the primer should be between 18 and 24 bases (when possible), the primer should have a GC content of 40-60% and a 3' end with 1-2 G/C pairs. The primer pairs should have the same T_m and not be complementary to each other.

S. pneumoniae is a low GC containing bacteria which gives a distribution of G and C bases lower than 40-60% (Tettelin et al., 2001). When possible, primers were designed with a G or C at the 3' prime end, providing strong binding where the DNA polymerase starts to polymerize new DNA, while long stretches of A and T were avoided. The melting point for the primers was designed to be between 58-60°C, using the salt adjusted T_m. For this work, a software such as "OligoCalc: Oligonucleotide properties calculator" was used to find the salt adjusted T_m. For primer design (and plasmid design) the software "ApE- A plasmid editor" was used.

All primers were ordered from Invitrogen by Thermo Fisher. Before using the primers for any PCR reaction, the dry primers were diluted to a 100 µM stock solution, then 10 µM working solution. Stock and working solutions were stored at -20°C.

3.3.2 PCR using Phusion high fidelity DNA polymerase

Phusion ® High Fidelity (HF) polymerase (from New England Biolabs, NEB) has high proof-reading capacity and was used when the PCR end-product was to be used in further experiments such as transformation, subcloning or sequencing. The recommended extension time when using Phusion is generally 30 sec per 1 kb, but can increase or decrease depending on the template (BioLabs, 2021).

The following protocol was used for Phusion ®HF DNA polymerase: a reaction mixture containing primers, dNTPs, 5x Phusion ® buffer, template and polymerase was prepared on ice, adding the polymerase last. All reagents with corresponding volumes and concentrations are listed in Table 3.1. For some of the overlap extension PCR reactions (see section 3.3.4) Mg²⁺ was added to achieve optimal activity with Phusion DNA polymerase. It is important to note that excessive use of Mg²⁺ can cause inefficient denaturation of DNA as well as non-specific binding of primers reducing the product yield (BioLabs, 2021).

Table 3.1 PCR reaction using Phusion high fidelity DNA polymerase

Reagent	50 µl reaction	final concentration
10 µM Forward primer	2.5 µl	0.5 µM
10 µM Reverse primer	2.5 µl	0.5 µM
10 mM dNTPs	1.0 µl	200 µM
5x Phusion buffer	10.0 µl	1x
Template	1.0 µl	10-100 ng (template dependent)
Phusion polymerase (HF)	0.5 µl	1 units/50 µl PCR
dH ₂ O	32.5 µl	

The thermocycler PCR program for amplifying DNA-fragments was adjusted based on the T_m of primers and the length and quality of the DNA template. The standard Phusion® PCR program used in this work is listed in Table 3.2

Table 3.2 PCR program for amplification of DNA- fragments using Phusion High-fidelity DNA polymerase.

Step	Temperature	Time	Cycles
Initial denaturation	98°C	5 min	1
Denaturation	98°C	30 sec	
Annealing	58°C	30 sec	25-35
Elongation	72°C	20-30sec/1kb	
Final extension	72°C	5 min	1
Hold	4°C	∞	

3.3.3 Screening of transformants using Red Taq® Ready Mix™

The PCR RedTaq was used in this work for screening transformant. Colonies from plates with transformants were picked with a sterile toothpick and transferred to PCR tubes, serving as template in PCR reactions. Primers targeting specific DNA sequences, only present in the transformant were used to verify if the transformation was successful.

The Red Taq® Ready mix™ consists of a mixture of *Taq* polymerase, the deoxynucleotides (dNTPs) dATP, dGTP, dCTP, dTTP, reaction buffer and an inert red dye functioning as a loading dye. The ready mix is beneficial for reducing contamination and provides consistent performance (SigmaAldrich, 2021). The reaction solution was prepared on ice by mixing the reagents listed in Table 3.3 before the samples were applied to the thermocycler.

Table 3.3 Reaction mix per PCR reaction with RedTaq® ReadyMix™ PCR reaction mix.

Reagent	Final concentration
5 µl Red Taq ® ReadyMix™PCR reaction mix, 2X	1X
1 µl 10 µM forward primer	0.1-1.0 µM
1 µl 10 µM reverse primer	0.1-1.0 µM
3 µl dH ₂ O	
1 colony DNA template	200 pg/µL

Final volume per PCR reaction: 10 µl

The standard program for the thermocycler in this work is listed in Table 3.4. Compared to the Phusion ® HF DNA polymerase, the RedTaq PCR program have lower denaturation temperature of 95°C when using colony DNA as template and a longer elongation step 1min/1kb compared to 30 sec/1kb for Phusion® polymerase.

Table 3.4 RedTaq program for screening of transformants.

Step	Temperature	Time	Cycles
Pre- denaturation	95°C	5 min	1
Denaturation	95°C	30 sec	35
Annealing	58°C	30 sec	
Elongation	72°C	1 min/1kb	
Final extension	72°C	5 min	1
Hold	4°C	∞	

3.3.4 Overlap extension PCR

Overlap extension PCR is a versatile technique that allows fusion of DNA fragments, insertion and deletions of point mutations as well as longer stretches of DNA. When performing an overlap extension PCR, two or sometimes three PCR products serve as template in one PCR reaction. The oligo primers used to generate the first PCR products contain overlapping ends. When mixed in an overlap PCR, the complementary ends of these PCR products anneal, allowing the 3' overlap of each strand to serve as primers for the 3' extension of the complementary strand. In total, this will generate a full-length product by flanking primers. Specific alterations in the nucleotide sequence can be introduced by incorporating nucleotide changes into the overlapping oligo primers (Ho et al., 1989, Heckman and Pease, 2007).

In this work overlap extension PCR was performed to introduce point mutations and various constructs for deleting genes, for gene replacements via the Janus cassette (described in section 3.12) and for inserting genes behind the P_{comX} promoter. The hybrid genes produced by overlap extension PCR can be cloned into a standard plasmid or be used to genetically alter *S. pneumoniae* through natural transformation. By using Phusion High-fidelity DNA polymerase, the number of unwanted mutations in the final product will be limited and the 3' to 5' exonuclease activity breaks the DNA-strand made by the flanking primers in the first rounds of overlap extension PCR.

For example, overlap extension PCR was used to make a construct for deleting the sequence encoding the DUF domain (domain of unknown function) of MltG. When deleting a longer stretch in a gene, the PCR fragments that are to be combined is amplified by using primers introducing complimentary overhang as illustrated in Figure 10. The forward primer located in the cytosolic domain of *mltG*, mlh1, harbored a 5' overhang complementary to the reverse primer of the other end of cytosolic *mltG*, mlh2. These two primers make it possible to delete the DUF domain of MltG. The first step involves using the flanking primers upstream from the MltG_{cyt} domain, ds362 in a PCR reaction with mlh2. A parallel reaction is set up for the downstream fragment of *mltG_{cyt}* by using the mlh1 primer and the flanking primer ds361 (Figure 10A). The second step is to combine these two PCR products via their overlapping region to delete DUF from MltG_{cyt}. The polymerase uses the overlapping sequences introduced by the primers mlh1 and mlh2 as a starting point for 3' DNA extension. In combination with the elongation from the flanking primers, this generates the spliced DNA-fragments (Figure 10B).

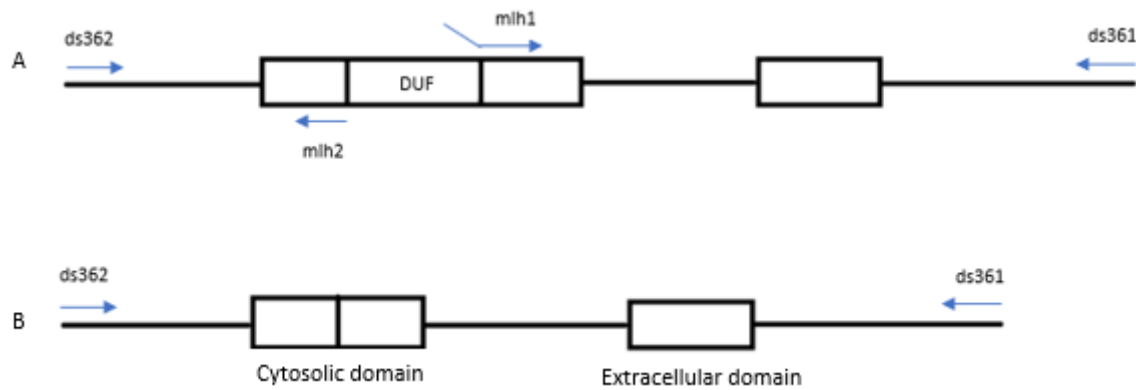


Figure 10: Illustration of overlap extension PCR making the *mltG* Δ DUF amplicon using the overlapping primers mlh1 and mlh2 with the upstream and downstream primers ds362 and ds361. The boxes illustrate the different domains of MltG and the arrows (pointing in a 5'-3' direction) indicate the primers used. A) the first step includes the amplification of the up- and downstream fragments of the DUF domain of *mltG*. In the case of *mltG* Δ DUF, this includes the ~1000bp upstream and downstream of the MltG operon. The mlh1 primer has a 5' overhang which is complementary to the mlh2 primer, introducing the overlapping sequence that enable the splicing of the fragments in a second PCR reaction. B) The second step is to fuse the two individual PCR products from A: splicing the upstream and downstream fragment of DUF. In this step, the flanking primers ds362 and ds361 are used.

3.4 Gel electrophoresis

Gel electrophoresis is a method to separate macromolecules such as DNA, RNA or proteins based on size and/or charge. If the charge per molecular size is constant, e.g., like DNA molecules, they are separated according to size when subjected to an electrical field through a porous gel matrix. DNA is negatively charged and will move towards the positive charged part of the gel. Larger molecules have more difficulty moving through the pores in the gel and will therefore move through the gel slower than the smaller molecules. The same principle applies for proteins after they have been linearized and coated with negatively charged detergent called sodium-dodecyl-sulphate (SDS). Each band on the gel represents molecules of different size and by comparing the band to a ladder with a known set of size standards, the size of the molecule in the band can be determined (Barril and Nates, 2012, Bruce Alberts, 2015). In this work, agarose gel electrophoresis was used to separate DNA-fragments, and SDS-PAGE was used to separate proteins (section 3.7).

3.4.1 Agarose gel electrophoresis

Agarose (a polysaccharide isolate from seaweed) forms a gel matrix by hydrogen-bonding when heated in a buffer and allowed to cool. The agarose gel does not have as great resolution power compared to polyacrylamide, which is ideal for both DNA and RNA, but the agarose gel

is faster to make and it is easier to extract DNA from the agarose gel. The low resolving power can lead to fuzzy and spread-apart bands because of pore size. Normally, the agarose gel has a concentration in the range of 0.2-3% (w/v). The lower the concentration of agarose gel, the faster DNA fragments migrate. This means when running smaller DNA fragments, a higher concentrated agarose gel might be necessary (Barril and Nates, 2012, James D, 2014). The agarose gel electrophoresis setup consists of an agarose gel with a fluorescent dye, placed in an electrophoresis chamber connected to a power supply. The gel is covered with a buffer, and the samples are loaded into small wells at the top of the gel. A ladder is also loaded into one of the wells and is used to identify the approximate size of a molecule. When the electrical field is applied, the negatively charged DNA molecules will travel towards the positively charged anode. For visualization of the DNA, a fluorescent dye such as peqGREEN, fluoresces under UV light upon binding DNA (Lee et al., 2012).

The following protocol for separating PCR fragments was used: a 1% agarose gel was made as standard for all fragments by mixing 0.5 g agarose with 50 ml 1xTAE buffer. The solution was heated until the agarose was completely dissolved. When the solution had a temperature of approximately 60°C, 1 µl peqGREEN was added and the gel solution was poured into a leakproof cast with a comb to create the wells into which the samples were loaded. The gel was transferred to an electrophoresis chamber covered with 1xTAE buffer, when set. Before loading the samples in the wells, a loading buffer containing glycerol or sucrose was mixed with the samples, giving them higher density than the electrophoresis buffer making them easier to apply to the wells. For samples made with RedTaq®, there was no need to add loading buffer as the loading buffer is already present in the reaction mix. A 1 kb ladder (NEB) and a 100 bp ladder (NEB) for fragments with size <100 bp, was used as size reference. As mentioned above, a ladder consists of a set of known standards (DNA fragments of known sizes), making it possible to estimate the sizes of the sample fragments. The electrophoresis was run on 90 V for approximately 20 min to allow DNA-fragments to separate. The fragments were visualized in UV light using a Gel Doc-1000 (BioRad).

3.4.2 PCR product clean up and extraction of DNA from agarose gels

After separation on an agarose gel, the PCR products were cleaned for excess buffers, dNTPs and primers. If the whole PCR product was loaded onto the gel, the band with the correct size was cut from the gel using a clean scalpel for each band and further dissolved in 500 µl NTI

buffer at 55°C for 5-10 min. The Nucleospin® Gel and PCR-Clean up kit (Macherey-Nagel) was used following the manufacturer protocol. A NucleoSpin® Gel and PCR Clean-Up Column was placed into a collection tube and the dissolved gel or PCR product was added to the column followed by centrifugation for 30 s at 11,000 x g. The buffer NTI contains chaotropic salts, and in the presence of chaotropic salts, the DNA is bound to the silica membrane of a NucleoSpin® Gel and PCR Clean-Up Column. The silica membrane was then washed with 700 µl Buffer NT3 for removing contaminations. After washing, the empty column was centrifuged to dry of any residual ethanol from buffer NT3. Finally, the pure DNA is eluted in a clean Eppendorf tube under low salt conditions using 15-30 µl of the slightly alkaline Elution Buffer NE (5 mM Tris/HCl, pH8.5). The column with the elution buffer was incubated at room temperature for 1 min and centrifuged for 1 min at 11,000 x g. The eluted DNA was stored at -20°C (Macherey-nagel, 2017).

3.5 DNA restriction cutting and ligation

Restriction cutting takes advantages of naturally occurring enzymes that cleave dsDNA at specific sequences, either leaving blunt or sticky ends. For example, a widely used restriction enzyme is EcoRI which recognizes the sequence 5'-GAATTC-3', and cuts once every 4 kb on average. EcoRI cleaves covalent (phosphodiester) bonds between G and A at staggered points on each strand to give 5' overhang ends which are complementary to each other. These are called “sticky” since they readily anneal through base pairing to each other or to molecules cut with the same enzyme (Figure 11)(James D, 2014) . The restriction cutting reaction is presented in Table 3.5.

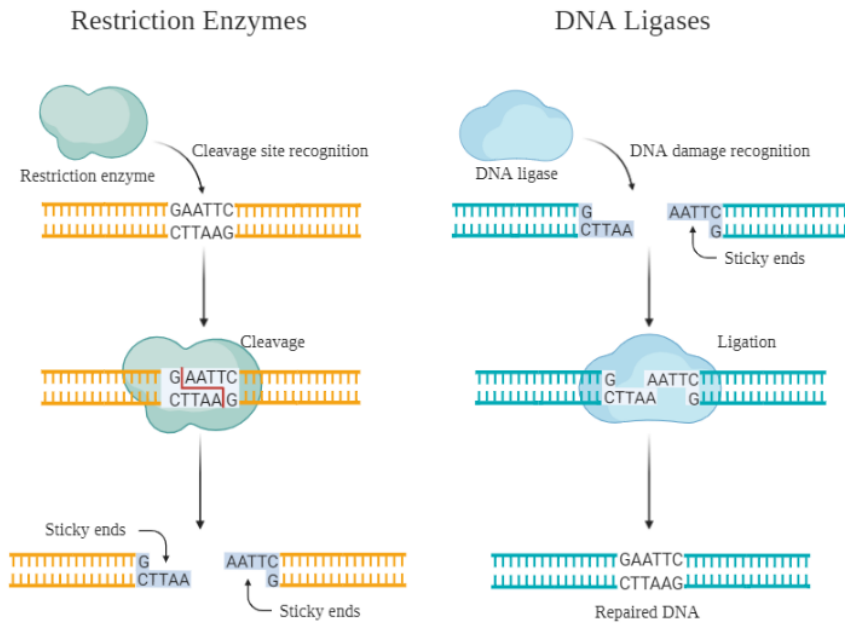


Figure 11 Illustration of restriction cutting and ligation. Restriction enzymes recognizes specific DNA sequence and cleaves, creating sticky ends or blunt ends. DNA ligases recognizes DNA damage and ligates to repair DNA. Figure adapted from Biorender.com

In this work constructs used to produce BACTH plasmids were amplified from *S. pneumoniae* genomic DNA, cleaved with restriction enzymes (XbaI and EcoRI from NEB), and ligated into the preferred plasmid using Quick ligase (NEB). The plasmids used in this work is listed in Table 2.1.

Table 3.5 Overview over the components for one restriction cutting reaction

Component	Volume
10 x reaction buffer	3 μ l
Enzyme 1	1 μ l
Enzyme 2	1 μ l
dH ₂ O	3 μ l
DNA	22 μ l

A master mix of the components listed in Table 3.5 was made, adding DNA last in an Eppendorf tube. The samples were incubated for 2 h in a water bath at 37°C. For samples where plasmids were cleaved, 1 μ l CIP (Alkaline phosphatase, Calf Intestinal) was added after 1h of incubation. CIP removes the phosphate group to avoid self-ligation of the plasmid. The restriction cutting of either insert or plasmid, was followed by a clean-up using agarose gel (section 3.4.2) or directly from the restriction reaction using 60 μ l buffer NTI per 30 μ l reaction (2:1). Finally,

cleaved plasmid and insert was ligated as shown in Table 3.6. All components were added in an Eppendorf tube and ligated in room temperature for 5 min. The ligated product can be stored at -20°C or transformed using 10 µl of the ligation mix.

Table 3.6 overview over the components for one ligation reaction

Component	Volume
Plasmid	3 µl
Insert	6 µl
2x buffer	10 µl
Quick ligase	1 µl

3.6 DNA sequencing

DNA sequencing is used to determine the order of bases in DNA. Sanger sequencing was used in this work and is the basis for many sequencing methods (Sanger et al., 1977). The sequencing in this project was performed by Eurofins. The sequencing reaction contains dNTPs (dATP, dTTP, dCTP and dGTP), a DNA polymerase, one primer and template DNA. In addition, a sequencing reaction requires dideoxy nucleotides (ddATP, ddTTP, ddCTP, ddGTP). These are identical to the dNTPs, except for the reactive hydroxyl group (-OH), which on ddNTPs is replaced with a hydrogen atom. When incorporated into a growing DNA strand, further elongation of the strand is blocked. The position where a ddNTP is incorporated is random, and each chain will end with a nucleotide which is labelled with a particular colour dye depending on the base it carries. The goal is to let a dideoxy-nucleotide be incorporated into every single position of the target DNA. After approximately 30 cycles of denaturing, primer annealing, elongation, the reaction contains fragments of different lengths that end at each of the nucleotide position in the original DNA. The fragments are read in a process called capillary gel electrophoresis which let the fragments migrate and separate by size through a long thin tube containing a polyacrylamide gel. One by one, the color of dyes is registered by a laser detector as a series of peaks in fluorescent intensity, shown in a chromatogram. The one limitation of Sanger, is the short reading length (Sanger et al., 1977, Bruce Alberts, 2015), but because the method is used for sequencing of bacterial genes that are relatively short, the method is applicable for this work.

3.7 SDS-PAGE

SDS-PAGE (sodium dodecyl sulphate- polyacrylamide gel electrophoresis) is a method for separation of proteins by size. The SDS-PAGE gel consists of highly cross-linked polyacrylamide as the inert matrix through which proteins migrate. The gel is prepared by polymerisation of acrylamide monomers and the proteins are dissolved in a solution that includes a powerful negative charged detergent, such as SDS. As a result of SDS binding to the proteins, conformational changes occur, causing them to unfold into extended polypeptide chains, making them freely soluble in the detergent solution. In addition, the reducing agent β -mercaptoethanol is usually added to break S-S linkages in the proteins, so the proteins are completely linearized and can be analyzed separately. Proteins bind negatively charged SDS molecules, (1 SDS molecule for every 2 amino acids) causing them to move towards the positive electrode when voltage is applied. The net charge of the proteins becomes the same and proteins therefore move through the gel depending on their size and therefore provides information about molecular weight (Bruce Alberts, 2015, Deyl, 2011). The proteins of different sizes are fractionated into a series of protein bands where the major proteins are readily detected by staining the gel with a dye such as Coomassie blue (Bruce Alberts, 2015, Walker, 2002). In this work, SDS-PAGE was used to separate proteins after co-immunoprecipitation (see section 3.9), using the discontinuous gel system that included a stacking gel and a separation gel. The separation gel has higher pH and lies under the stacking gel. The stacking gel allows the proteins applied to enter the separation gel at the same time so that the separation according to size will not be disrupted.

The following protocol was used: The samples were prepared by mixing immunoprecipitated proteins and control with a 4xSDS loading buffer to a total volume of 60 μ l. The proteins were denatured by incubating the samples for 10 min at 95°C. Next, the stacking and separation gel was made. A 12% or 15% separation gel were made by mixing the reagents listed under section 2.7.3. The acrylamide, bis-acrylamide, Tris HCl buffer pH 8.8 and dH₂O was added first, then newly made 10% APS and TEMED were added last because they initiate the polymerization of the gel. A volume of 3.2 ml of gel solution was quickly added into the cast and further topped with dH₂O. The dH₂O is added to “press down” the gel, making an equal level of the gel surface. After the separation gel had set, the overlaying dH₂O was removed and the 4% stacking gel was made by mixing the reagent listed in section 2.7.3, together with 50 μ l bromomethyl blue dye (0.05% w/v), following the same steps as the separation gel. The bromophenol blue was added

to the stacking gel to allow easy detection of the wells for loading of samples. A volume of approximately 1 ml of the gel solution was added on top of the separation gel, filling the cast completely. A 10-well comb was inserted into the stacking gel before it polymerized. After polymerization, the casting chamber was inserted into the gel electrophoresis chamber and filled with running buffer. The proteins were separated through the stacking gel using 100 V, and then 200 V when the proteins entered the separation gel. The electrophoresis was stopped when the bromophenol blue dye had reached the bottom of the separation gel. Proteins separated in the SDS-PAGE gel was either transferred (Western blot) to a PVDF (polyvinylidene fluoride) membrane for immunodetection or stained with Coomassie brilliant blue solution.

3.8 Co-immunoprecipitation (pulldown)

Co-immunoprecipitation is a method used for studying protein-protein interactions and protein complexes. Usually a protein is used as “bait” and by employing antibodies specific for this protein it can be “pulled out” from the solution. If the bait protein has interaction partners and this complex is stable in the experimental conditions used, they will follow the bait protein and can be detected. In this work a Flag-tag was fused to the protein(s) of interest facilitating pull-down by using agarose beads conjugated with anti-flag antibodies.

The following protocol was used in the co-IP experiment: cells were grown in 50 ml C-medium to an OD₅₅₀ of \approx 0.3 and collected by centrifugation before resuspended in 1 ml pulldown lysis buffer. The cells were then lysed with 5 μ g/ml LytA at 37°C for 5 min. The lysate can be stored at -80°C. The agarose beads (ANTI-FLAG® M2 Affinity Gel, Sigma) were prepared by transferring 40 μ l to an Eppendorf tube (one per sample), pelleted at 8000 x g for 30 sec, and the glycerol was removed. They were then washed twice in 0.5 ml 1xTBS. The lysate was added, and the samples rotated gently on 4 °C o/n. After o/n incubation the beads were centrifuged at 8000 x g for 30 seconds, supernatant removed, and the beads were washed 3 times with 0.5 ml 1xTBS. To release the proteins from the beads, 60 μ l 1x SDS loading buffer were added and incubated at 95° for 10 min. The incubated samples can be kept at -20 °C or loaded directly on an SDS gel, see section 3.7. Finally, Immunoblotting was performed.

3.9 Immunoblot analysis

After protein have been fractionated using SDS-PAGE, a specific one can be identified by using antibodies that target the protein of interest using a technique called immunoblotting. The proteins are transferred from the gel to a membrane (Western blotting), with strong electrical current transferring the negatively charged (because of SDS coating) proteins onto the PVDF membrane. The membrane nonspecifically binds proteins via hydrophobic interactions, and the remaining binding sites are blocked by incubating with a solution such as skim milk, containing proteins unrelated to those being studied. Then, the membrane is incubated with a primary antibody that specifically recognizes the protein of interest. After washing away excess primary antibodies, a secondary antibody is added to the membrane. This antibody binds to the primary antibody and is usually labeled with for example Horse Radish Peroxidase (HRP) to visualize the protein of interest (James D, 2014).

This method was carried out in order to analyse the precipitated proteins after co-IP and SDS-PAGE. After sample preparation as described in section 3.8. SDS sample buffer was added to the lysate and separated on a 12% and 15% SDS PAGE gel, as described in section 3.7. The proteins in the SDS gel were transferred to a polyvinylidene fluoride (PVDF) membrane. The membrane was first activated by soaking it in methanol for 30 sec and then in Towbin buffer for 1 min. Thereafter, 4 filter papers and the gel were soaked in transfer buffer for 1 min. The stack was made in the following order: 2 filter papers, membrane, gel, and 2 filter papers. The membrane and gel were placed so that the membrane faced the anode allowing the negatively charged proteins to migrate from the gel and onto the membrane. All air bubbles were removed from the stack before the separated proteins were electroblotted onto the PVDF-membrane using a Transblot turbo transfer system (BioRad) with a standard protocol for 7 min. All the following steps were performed with gentle agitation. After transferring the proteins onto the membrane, the membrane was blocked for 1 hour with 5% (w/v) skim milk powder in 1xTBST (see section 2.7.4). The primary antibodies α -flag (in a ratio 1:5000) or α -GFP (in a ration 1:3000) were added in 1xTBST before incubation in room temperature for 1h followed by washing with 1xTBST 3x10 min. The secondary antibodies anti-rabbit was added in 1xTBST (in a ratio 1:5000) before incubation in room temperature for 1h followed by washing with TBST 4x10 min. The blot was developed by adding HRP substrate for 1min. The proteins were visualized in an Azure Imager c400 (Azure Biosystems).

3.10 Chemically competent *E. coli* cells

Prior to CaCl₂ treatment, the cells are negatively charged with natural repulsion between the cell membrane and the plasmid DNA. After CaCl₂ treatment, the calcium from CaCl₂, interacts with the negative charges, which leads to an electrostatically neutral environment.

A 5 ml culture of the strain of interest were grown o/n in 100 ml LB at 37°C. The o/n culture was diluted to an OD₆₀₀ ≈ 0.05, and grown to early log phase OD₆₀₀ ≈ 0.02-0.4 (approximately 90-180 min depending on the strain) and then cooled on ice for 30 min. The cells were collected by centrifugation, 5000x g for 5 min at 4°C. The cells were then kept on ice in all further steps. After centrifugation, the cells were resuspended in ½ culture volume (here: 100 ml culture-resuspend in 50 ml) of ice-cold 0.1 M CaCl₂. The cells were kept on ice for 2 h. Cells were collected as before and gently resuspended in 1/10 culture (10 ml) 0.1 M CaCl₂. The competent cells can be stored by mixing them with ice-cold sterile glycerol to a final concentration of 15% (v/v), then placed on ice for 30 min before storing the cells at -80°C.

3.10.1 Transformation of chemically competent *E. coli*

The competent *E. coli* cells were thawed on ice and mixed with 10 µl ligation mix or 1 µl purified plasmid (see section 3.5 and 3.2). The cells were then incubated on ice for 1 h before performing heat shock at 42°C for 45 seconds. After cooling the cells on ice for 2 min, 500 µl SOC medium was added to the cells, and they recovered for 1.5 h at 37°C with shaking. Finally, the cells were transformed with a ligation reaction and collected with centrifugation, the pellet resuspended in approximately 30 µl SOC and spread on LB agar with the appropriate antibiotics. For the cells transformed with purified plasmid, 50 µl of the transformed cells were plated on LB agar containing antibiotic(s). The plates were incubated o/n at 37°C.

3.11 Transformation of *S. pneumoniae*

As described in section 1.1.2, pneumococci have the ability to become naturally competent for genetic transformation, meaning they can take up and incorporate exogenous DNA from closely related species, through homologous recombination (Straume et al., 2015). This “quorum-sensing” like mechanism is known for a number of bacterial species, belonging to the phylogenetic mitis group. The competent state in pneumococci can be reached by simply

growing the cells in exponential phase, at rather low cell density (Håvarstein et al., 1995). The competent state is controlled by the extracellular concentration of a competence stimulating peptide CSP (CSP-1 for *S. pneumoniae*) (Steinmoen et al., 2002). To ensure that the *S. pneumoniae* strains used in the laboratory do not auto-induce into the competent state, the native CSP transporter *comA* is deleted in strains used in this work (Johnsborg and Håvarstein, 2009b).

Volumes of 1 ml exponential growing pneumococci, reaching an $OD_{550}=0.05-0.1$ was transformed by adding CSP-1 to a final concentration of 250 ng/ml together with 100-200 ng of the transforming DNA. For every transformation experiment, a negative control lacking DNA was induced. Cultures were then grown for 2 h to allow DNA uptake and homologous recombination to occur. A volume of 30 μ l culture was plated on Todd Hewitt agar plates with appropriate antibiotics (and ComS when necessary) and then incubated anaerobically o/n at 37°C. Potential transformants were verified using PCR-screening described in section 3.3.3 and/or sequencing (section 3.6).

3.12 The Janus cassette

The Janus cassette is designed to be counter selectable and can be used in a two-step transformation procedure, allowing construction of silent mutations and deletions or other gene replacements (Sung et al., 2001). The Janus cassette comprises a *rpsL*⁺ DNA cassette that have both resistance to kanamycin (Kan^r) and dominant sensitivity for streptomycin (Sm^s). When introduced in a *Sm*-resistant background, the Janus can subsequently be removed by selection on streptomycin containing grown media. Replacement of the Janus cassette restores streptomycin resistance and kanamycin sensitivity. The Janus cassette is based on a recessive mutation of the *rpsL* gene in *S. pneumoniae*, giving streptomycin resistance (Sung et al., 2001).

In this work, the Janus cassette was used to introduce different mutations in genes of interest (listed in Table 2.1). Gene replacement is a two-step process, where the first step is the replacement of the target gene with the Janus cassette (Kan^r , Sm^s), and the second step is the replacement of the Janus cassette with the altered gene. After the second step, the streptomycin resistance and the kanamycin sensitivity are restored (Kan^r is lost). To identify transformants where the Janus cassette is successfully introduced, the transformed cells were plated on TH agar containing kanamycin (400 μ g/ml). When removing the Janus cassette, the transformants were plated on TH agar containing streptomycin (200 μ g/ml). The Janus cassette and the

replacement gene were made with ~1000 bp regions flanking upstream and downstream the target gene for replacing the Janus cassette with homologous recombination.

3.13 Ectopic overexpression of genes using the ComRS system

All bacteria have essential genes, a gene where the protein product is essential to the cell. Because the genes are of vital importance for the cell, gaining insight into their function is of great interest. Functional studies of essential genes are challenging as gene knockouts or introduction of mutations have a lethal outcome. The ComRS system (Berg et al., 2011) is a gene expression system developed for studying the function of essential genes in pneumococcal cells. The system, originating from *S. thermophilus* (Fontaine et al., 2010), consists of three component; an inducer peptide (ComS*), a transcriptional activator (ComR), and a ComS*-inducible promoter (P_{comX}) with a binding site for ComR. The signal peptide ComS* is transported into the cytoplasm by *S. pneumoniae*'s endogenous oligopeptide system Ami. Inside the cell, ComR becomes activated upon binding the ComS* peptide, which again activates the expression from the *comX* promoter P_{comX} (Berg et al., 2011)(Figure 12).

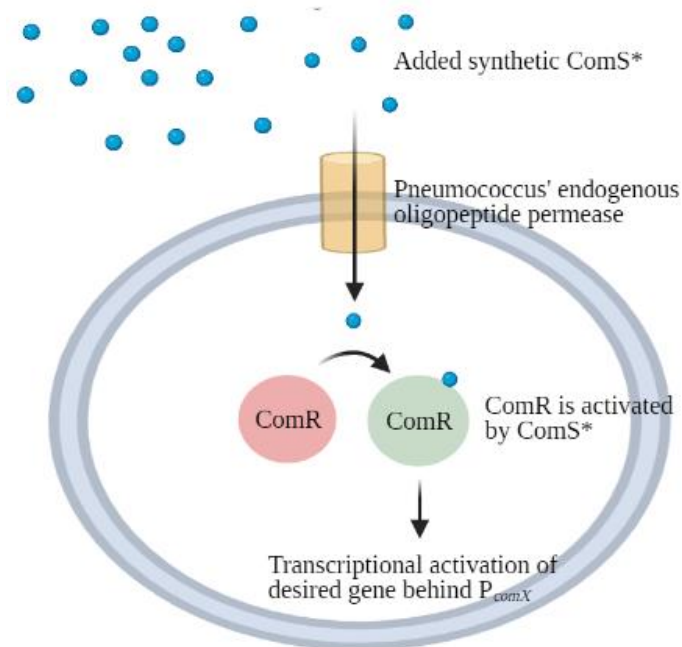


Figure 12 The mechanism of the ComRS system in *S. pneumoniae*. Synthetic ComS* is added to the growth medium and transported into the cell by the endogenous oligopeptide permease. When inside, ComS* activates ComR upon binding. The activated ComR works as a transcriptional activator, binding to an inverted repeat sequence in the P_{comX} promoter. This initiates ectopic expression of genes inserted behind P_{comX} (Berg et al., 2011). Figure adapted in Biorender.com

The ComRS system is exploited as a tool to study essential genes in *S. pneumoniae*, by expressing the genes in question ectopically under the control of P_{comX} . The level of expression of genes inserted behind P_{comX} can be fine-tuned by different concentrations of ComS* in the growth medium. By changing the concentration of the synthetic inducer peptide ComS*, the expression of the ectopic gene can either be depleted or overexpressed. This makes it possible to delete the native gene without it being lethal, study its function by varying its ectopic expression and examining the effects on for example morphology. Since there are no close homologues of the ComRS proteins encoded in the pneumococcal genome, it is unlikely to interfere with the normal cellular functions (Berg et al., 2011).

In this work, the ComRS system was utilized to ectopically express variants of the essential gene-*mltG* in the *S. pneumoniae* genome. A final concentration of 0.1 μM of the inducer peptide ComS* was added in liquid culture, and on plates when necessary. Furthermore, the ComRS system was also used for ectopic expression of variations of the *eloR* gene for microscopy experiments. Here, a final concentration of 2 μM was added to the culture.

3.14 BACTH: Bacterial Adenylate cyclase Two- Hybrid System

BACTH is a system used to investigate protein-protein interactions *in vivo*. The system is based on the complementation of the T18 and T25 domain of a adenylate cyclase activity derived from *Bordetella pertussis* (Karimova et al., 1998). The antibiotic resistance genes for ampicillin and kanamycin are on the plasmids expressing T18 and T25, respectively. The two proteins of interest are fused to either a T18 or T25 fragment to test protein-protein interaction. When T25 and T18 are separate they are inactive, but when they are brought together, the adenylate cyclase activity is restored. This leads to the synthesis of cAMP which induces the expression of β -galactosidase (Figure 13). β -galactosidase cleaves X-gal added to the LB plates producing a blue dye. The system is used in adenylate cyclase negative *E. coli* strains. An interaction between the two proteins tested against each other will therefore result in blue bacterial spots on the agar plate, while a lack of interaction results in white bacterial spots.

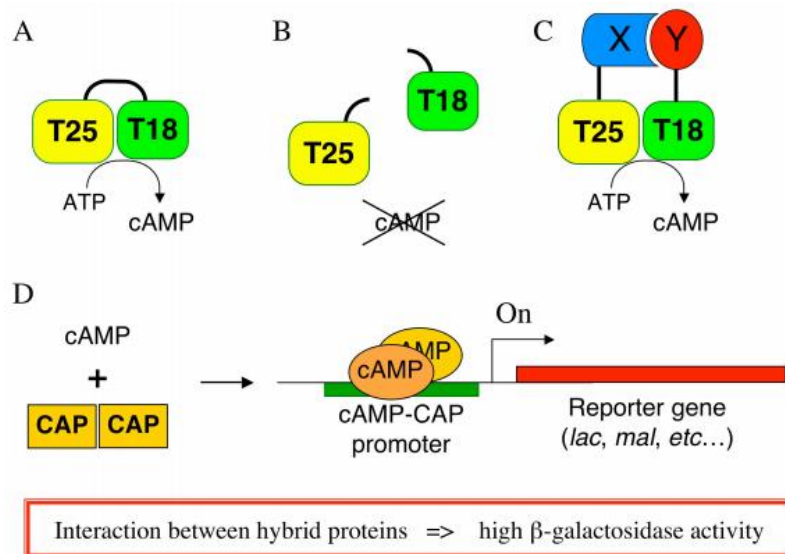


Figure 13: Principle of the bacterial two-hybrid system in *E. coli* ΔcyA (Euromedex). BACTH analysis is based on blue (positive) and white (negative) colour selection, where the blue colour comes from the cleavage of X-gal in the medium by β -galactosidase. Briefly, the two proteins tested for interaction are fused to either the T18 or T25 domain. If an interaction between the two proteins occurs, T18 and T25 reconstitute an adenylate cyclase producing cAMP, which induces the expression of β -galactosidase.

The BACTH assays were performed accordingly by the manufacturer (Euromedex). For the BACTH experiments performed in this work, the negative control had two plasmids expressing T18 and T25 alone (pUT18C and pKT25), meaning there had not been cloned any pneumococcal gene in-frame with the two domains (T18 and T25). The positive control consists of an *E. coli* having the pKT25-zip and pUT18-zip plasmids (provided by the manufacturer). These two plasmids have a leucine zipper fused to either T18 and T25. The leucine zippers will interact and give rise to blue bacterial spots on X-gal containing agar plates. All plasmids used in the BACTH analysis is listed in table 2.1

The following protocol was used for all BACTH experiments: PCR was used to amplify the gene of interest. The primers were designed with restriction sites for the restriction enzymes EcoRI and XbaI ensuring in-frame ligation of the T18/T25 encoding sequence with the desired gene sequence. The ligations were transformed into *E. coli* XL1-blue cells. After confirming the DNA sequence of the T18/T25-fusions, one plasmid encoding a T25 fusion and another plasmid encoding a T18 fusion were co-transformed into *E. coli* BTH101 cells. Successful co-transformants were selected using LB plates with kanamycin and ampicillin. To get a conclusive result, five random colonies were picked and grown to exponential growth. After

incubation, 3 μ l of the culture was spotted onto LB plates containing ampicillin, kanamycin, IPTG and X-gal and incubated at 30°C o/n. Bacterial spots that appeared blue were considered as a positive protein-protein interaction between the protein of interest. Five out of five white or blue bacterial spots gives a conclusive result.

3.15 Microscopy analysis and construction of fluorescent fusion proteins

Cells were prepared for microscopic imaging by thawing start cultures in 37°C water bath. The cells were collected by centrifugation at 4000 x g for 5 min. The cell pellet was resuspended in 2 ml fresh C-medium and diluted to an $OD_{550} \approx 0.05$. All strains of *S. pneumoniae* that were used in microscopy experiments were grown with 2 μ M ComS to induce the expression of fusion proteins from the P_{comX} promoter and incubated at 37°C. Microscopy analysis was performed after 2 hours of incubation when the cells were in exponential growth phase. Cells were spotted directly onto a multisport microscope slide with a thin layer of 1.2% agarose in PBS. All strains used in microscopy analysis are listed in Table 2.1.

Proteins fused with fluorescent mKate2 were visualized using a Zeiss AxioObserver with Zen Blue software, an ORCA-Flash 4.0 digital complementary metal-oxide semiconductor (CMOS) camera (Hamamatsu Photonics) and a 100x phase contrast objective. An HXP 120 Illuminator (Zeiss) was used as a fluorescence light source. Images were prepared and analysed using the Image-J software with the Microbe-J plugin. For subcellular localisation analysis, the Maxima function in Microbe J was used to define fluorescence maxima within the cells and these subcellular localizations of these maxima were plotted using the XYCellDensity plot (focus density plots) in Microbe J (Ducret et al., 2016).

3.16 Gel filtration

3.16.1 Overexpression and protein purification

pRSET A is a vector designed for high-level expression of recombinant proteins in *E. coli*. Over expression of a gene is made possible by placing it behind the *T7/lac* promoter in the pRSET A vector. This promoter derives from the T7 bacteriophage and require the T7 RNA polymerase for transformation. By using the genetically modified BL21 strain, which has the T7 RNA polymerase encoding gene in its genome, as host for the pRSET A, the gene behind *T7/lac* can be overexpressed. The *T7/lac* promoter also contains a binding site for repressor LacI, which

functions as a transcriptional roadblock. However, LacI can bind allolactose, upon which it is released from DNA allowing transcription to occur. IPTG have a structural similarity to allolactose, which can bind to a pocket in *LacI*. IPTG is required to maximally induce the expression of the T7 RNA polymerase and is always present since it don't metabolise. This results in a conformational change in *LacI* and it will no longer block the transcription of the promotor it was bound to (Sciences, 2000).

In this work we wanted to purify the Jag domain and MltGcyt and perform a gel filtration experiment to further examine interaction between the two proteins. First, a gene encoding 6x-His-MltGcyt was made using PCR and cloned into pRSET A. This plasmid was then transformed into *E. coli* genhogs cells which are more suitable for difficult transformations. Then, the plasmids that screened correctly were isolated from genhogs and further transformed in BL21 and sequenced. The same was done for and 6x-His-TEV-jag-linker. Because of pandemic lock-down (Covid-19), cloning and transformation of 6x-His-MltGcyt and 6x-His-TEV-jag-linker, were performed by laboratory staff. Overexpression was done by growing pre-cultivated strains of aw440 (6x-His-TEV-jag-linker) and ds974 (6x- His-MltGcyt) in 500 ml LB medium with 100 µg/ml ampicillin, starting at OD₆₀₀=0.1. When reaching OD₆₀₀=0.4-0.5, IPTG was added to a final concentration of 100 mM to induce the expression of 6x-His-MltGcyt and 6x-His-TEV-jag-linker. The cells were induced for 4 h at 25°C and cells were harvested by centrifugation. The cells were then lysed to release the over expressed protein and the cell pellet were dissolved in 5 ml buffer A (see section 2.7.5). Acid-washed glass beads were distributed in tubes with the sample and lysed by using FastPrep 24 ® for 3x20 sec at 6.5 m/s. The lysate was then centrifuged at 13000 g x for 5 min at room temperature, and the supernatant with the free proteins were transferred to a new tube.

The proteins were purified directly from bacterial lysates using immobilized metal affinity chromatography (IMAC) columns for His-tag recombinant protein purification. HisTrap HP columns are packed with pre-charged Ni²⁺ that selectively retains proteins with exposed histidine group (Biosciences, 2003). His-tagged proteins was retained in the column by the Ni²⁺-ions, while the remaining substances will run through the column. In this experiment, the ÄKTA pure were equilibrated with 10 ml binding buffer (Buffer A) before injecting the sample. Elution buffer (Buffer B, see section 2.7.5) containing 500 mM imidazole eluted the his-tagged protein by a 0-30 ml (0-100%) linear gradient. The His-tagged proteins are eluted from the column and can be detected using UV light. The fractions were collected in 1 ml aliquots during

the gradient of imidazole, by using a fraction collector (Figure 14). The purification is checked by analysing an aliquot of the collected samples on SDS- PAGE (see section 3.7).

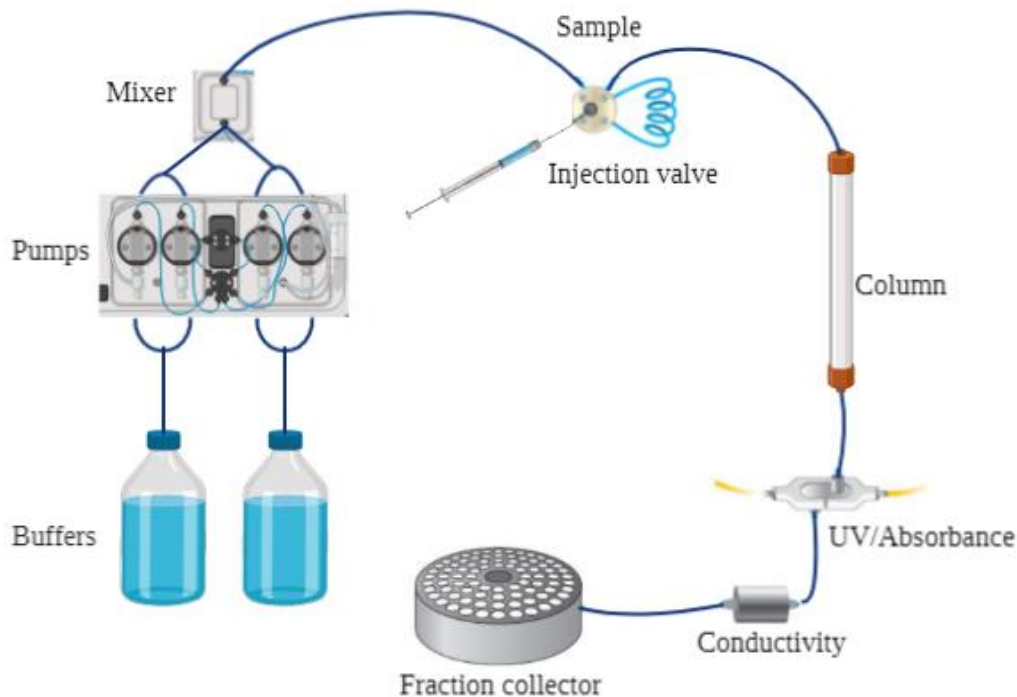


Figure 14 Overview over the ÄKTA pure system. Proteins are separated in the column. Buffers and other liquids are delivered via the system pump, and samples were applied using a syringe to fill a sample loop. Detectors such as UV, absorbance, conductivity, and pH are placed after the column to monitor the separation process. Eluted proteins are collected in the fraction collector. Figure adapted in biorender.com

To remove imidazole and excess salts, the protein was dialysed in 10 mM Tris HCl with a pH 7.4. The purified protein was combined in a slide analyzer ® 2k dialysis cassette G2, with 3 kDa cut off, and incubated for 1 h in Tris-HCl with a pH 7.4 with gentle stirring. The cassettes use a cellulose membrane, designed to retain proteins and other macromolecules that are larger than 3 kDa, while buffers and small contaminants diffuse from high to low concentration across the membrane and into the dialysis buffer.

3.16.2 Gel filtration on purified proteins

Size exclusion chromatography (SEC), also called gel filtration (GF), separates molecules by differences in size and shape as they pass through a resin packed column. This is a versatile separation technique, suited for biomolecules sensitive to changes in pH, concentration of metal ions or cofactors. SEC resin consists of a porous matrix which is equilibrated with buffer that

fills the pores of the matrix and the space between the particles. The buffer solution does not directly affect resolution (the degree of separation between the peaks), as the molecules does not bind to the column. Sample components are eluted isocratically; the buffer composition remains consistent through the separation and its only necessary to use one buffer. If the molecules are larger than the largest pores in the matrix, they cannot enter the matrix and are eluted together in the void volume (V_0), passing directly through the column. Molecules having partial access to the pores are separated and elute from the column according to size, largest first. Salt molecules and other small molecules are not separated moving down the column and usually elute at the total liquid volume of the column (V_t), before the 1 CV (column volume) of buffer has passed through the column (Sciences, 2000).

The purified proteins (section 3.16.1) are concentrated using an Amicon ® ultra-15 centrifugal filter and centrifuged at 4000 x g at room temperature until desired concentrate. Then, 200 µl of each sample is combined in an Eppendorf tube and incubated at 37°C for 20 min. Precipitation that might have formed is removed by centrifugation at 20 000 g for 5 min, held on room temperature. This is done to prevent any clogging in the Superdex™ 75 10/300 GL column. Before running the samples through the column, its equilibrated with TBS buffer. Fractions are collected in 1 ml aliquots by the fraction collector (Figure 14).

4. Results

4.1 Microscopy analysis suggesting the Jag domain exclusively directs EloR to the division zone

Previous studies has shown that KhpA and EloR form a complex when EloR localizes to mid-cell (Winther et al., 2019, Zheng et al., 2017) . Even though it is known that KhpA depends on its interaction with EloR to localize to the division zone, little is known how EloR find the localization to midcell. We have hypothesized that EloR depends on interaction(s) with other elongasome proteins to localize accurately (now published in (Winther et al., 2021)). Figure 15A illustrates a schematic presentation of the domain organization of EloR. EloR consists of three domains, an N-terminal Jag domain with unknown function, a KH-II domain and an R3H domain both of which are ssRNA binding. Since the Jag domain is connected to the KH-II domain via a linker domain and both KH-II and R3H binds RNA, it's reasonable to believe that the Jag-linker part of the protein could be important for subcellular localization of EloR.

This was tested by fusing the fluorescent protein mKate2 to full length EloR, the Jag domain, the linker domain, and Jag-linker domain producing the strains; AW407, AW408, AW410 and AW409, respectively (see Table 2.1). These fusions were expressed ectopically from an inducible promotor using the ComRS system (see section 3.13). The inducer ComS was supplied to the growth medium, while the native *eloR* gene was kept unchanged in the genome. Image-J with the microbe-J plugin was used to analyse the micrographs (Figure 15B). The localization of EloR-mKate2 was found to concentrate at midcell for 77% of the cells investigated (Figure 15B and C). Similarly, Jag-mKate2 and Jag-linker-mKate2 fusion displayed midcell localization for 75% and 55% of the cells investigated, respectively. The exception in this analysis was the linker-mKate2 fusion; the fluorescent signal from mKate2 was distributed in the entire cell, with no midcell localization (Figure 15B and C). Only 2% of the cells investigated displayed a midcell fluorescence signal. From these results, it was concluded that the Jag domain is exclusively responsible for localizing EloR to midcell, independently of the linker domain.

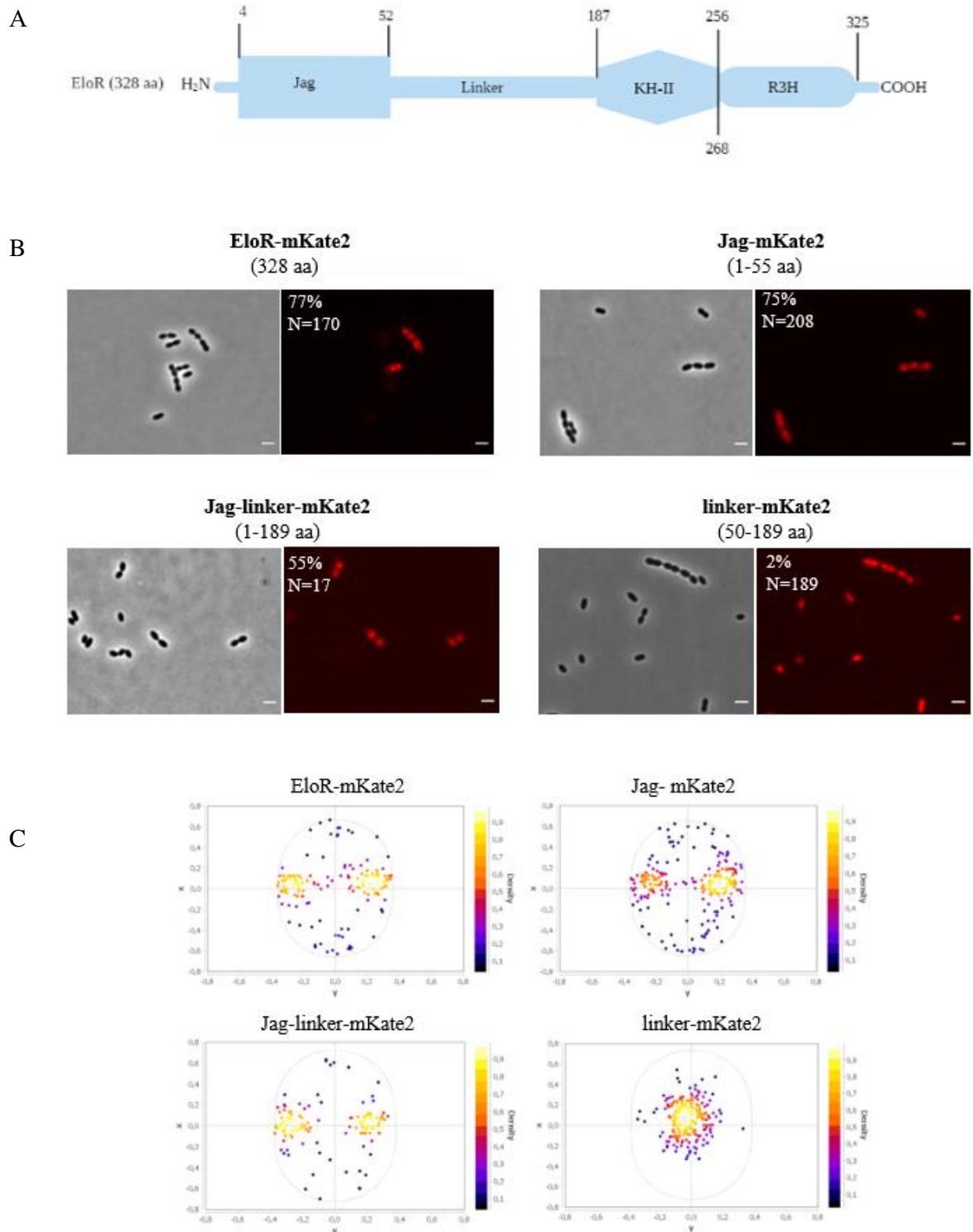


Figure 15 The Jag domain directs EloR to midcell. A) schematic presentation of EloR, with the predicted domains with corresponding domain borders. B) Phase-contrast and fluorescent micrographs of EloR-mKate2 (AW407), Jag-mKate2 (AW408), Jag-linker2 (AW409), and linker-mKate2 (AW410), showing the subcellular localization. The percentages of the cells that displayed midcell localization of the mKate2 fusion are indicated, as are the numbers of cells included in the analysis. Numbers of amino acids (aa) of EloR in the different construct are localized above the micrographs. Scale bars are 2 μ m. The images were analysed using Image J with the Microbe J plugin. C) Analysis of subcellular localization of the above-mentioned constructs. Fluorescence maxima were detected and plotted in focus density plots using MicrobeJ (linker-mKate2 had no midcell localization). The axes of the cell density plots denote the relative length and width of the axes (from -0.8 to 0.8).

4.2 Exploring possible interaction partners of EloR

It was of great interest to explore what other protein interactions EloR forms in addition to the one with KhpA. Different elongasome proteins were tested against EloR with the T25 fusion to explore if the proteins were important for EloR localization to midcell and to understand its regulatory function in cell elongation. EloR was probed against a range of known cell division proteins; PBP2b, RodA, RodZ, MreC, MreD, CozE, and MltG for possible interaction partners (Figure 16). A gene called *yidC2*, which codes for an insertase assisting in insertion of membrane proteins into the lipid bilayer, shares an operon with *eloR* suggesting a possible functional link between the two proteins. YidC2 was therefore also probed against EloR in BACTH. The Jag domain of EloR was also tested against MltGcyt and MltGcyt^{ΔDUF} to test interaction between the proteins. Of all the proteins tested using the BACTH assay, the results indicating interaction with EloR (blue spots) were RodZ, YidC2, MltG and MltGcyt.

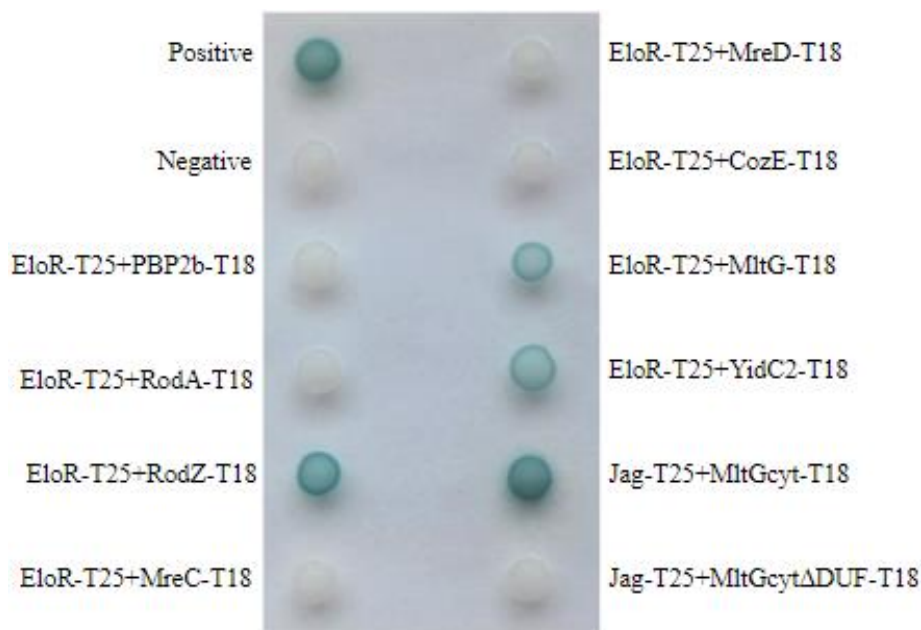


Figure 16: The Jag domain of EloR-T25 was probed against different proteins central for pneumococcal cell elongation, where RodZ, MltG and YidC2 have a positive interaction with EloR. The other positive interaction in the BACTH assay is MltGcyt probed against Jag, proving that the Jag domain of EloR interacts with the cytosolic domain of MltG. The interaction was lost (white spot) when the DUF domain was deleted.

4.3 StkP is not critical for EloR localization

The Jag domain alone clearly displayed midcell localization, showing that the linker domain is not crucial for subcellular localization of EloR (section 4.1). Anyhow, since the threonine 89, which is phosphorylated by the midcell localized kinase StkP, we wanted to examine if the

absence of phosphorylation and interaction with StkP would have any effect on EloR localization in the cells. EloR-mKate2 was therefore expressed in a genetic background lacking *stkP* (aw453). From Figure 17A where *stkP* is deleted, EloR-mKate2 was still concentrated at midcell, demonstrating that the absence of StkP, and thus lack of EloR phosphorylation, did not significantly affect the localization of EloR.

The BACTH results from section 4.2, indicates that RodZ and the insertase YidC2 interacts with EloR. Similarly to EloR, RodZ is considered to be a part of the elongasome and studies in *E. coli* indicates that RodZ is important for the elongated shape (Shiomi et al., 2008). Therefore, it was tested to see if EloR midcell localization would change in cells lacking *rodZ* or *yidC2*. Mutants expressing EloR-mKate2 in a $\Delta rodZ$ (aw417) and $\Delta yid2$ (aw415) genetic background were designed. From the result presented in Figure 17B, cells in the genetic background lacking *rodZ*, did not abrogate midcell localization of EloR-mKate2, while it was detected accumulation of EloR-mKate2 at the cellular poles of the cells in the genetic background lacking *yidC2*, as well as at midcell (Figure 17C).

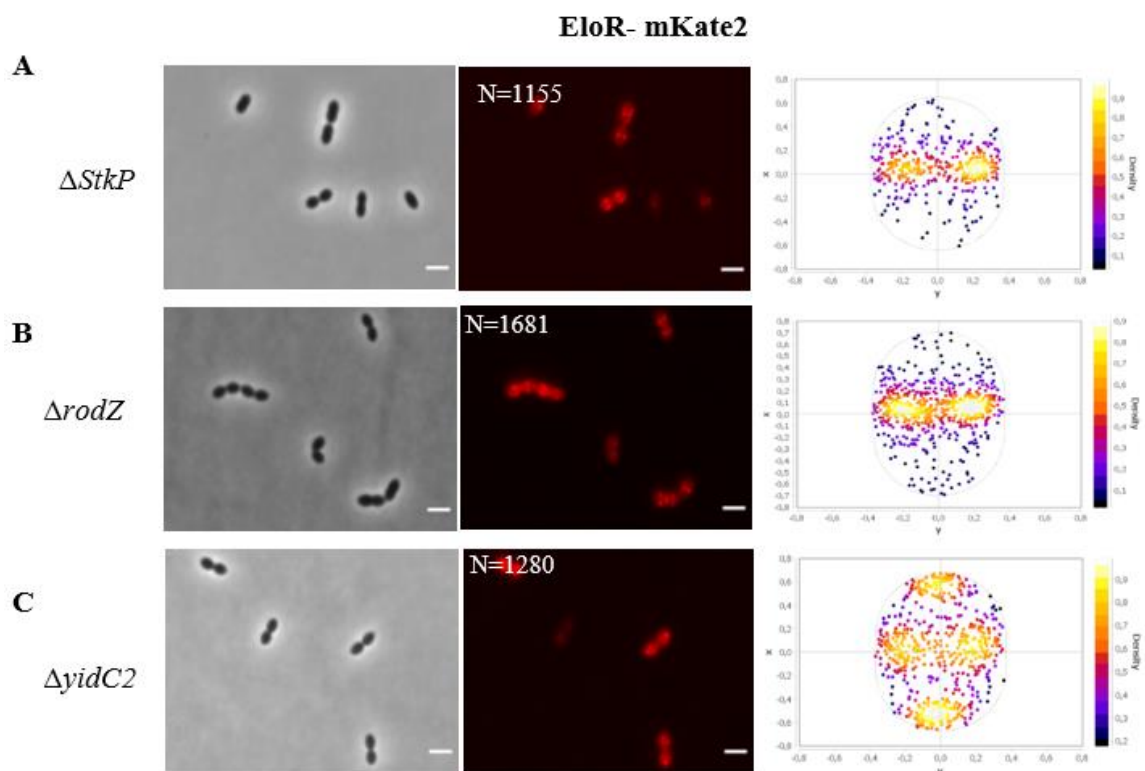


Figure 17 Microscopy analysis of EloR-mKate2 expressed in different genetic backgrounds. Showing the subcellular localization of EloR-mKate2 in (A) $\Delta stkP$, (B) $\Delta rodZ$ and (C) $\Delta yidC2$ mutants by micrographs and corresponding fluorescence maxima were detected and plotted in focus density plots using Microbe J. The x and y in the cell density plots denote relative length and width. Scale bars are 2 μ m.

4.4 The Jag domain of EloR interacts with the DUF domain of MltG

Neither $\Delta stkP$, $\Delta rodZ$ or $\Delta yidC2$ affected the localization of EloR (Figure 17). MltG is essential in wild-type cells and cannot be deleted, and we tried to make another mutant like MltG ^{Δ DUF} to study if this could affect localization of EloR. Studies has shown that the Jag domain of EloR is important for localization and since Jag interacts with DUF, it is likely that MltG is the protein recruiting EloR to septum.

One transmembrane segment embeds MltG into the cytoplasmic membrane with its transglycosylase domain on the outside and a domain of unknown function (DUF) facing the cytoplasm. Since EloR is a cytoplasmic protein, we hypothesized that it had to interact with the DUF domain of MltG. We confirmed this in BACTH assays, which showed that when the Jag domain was tested against MltG ^{Δ DUF}, the interaction between the two domains were lost (Figure 16). Since MltG is essential in wild-type cells it is impossible to track EloR-mKate2 in a $\Delta mltG$ mutant. However, results published by Tsui and co-workers showed that *S. pneumoniae* could survive with an MltG version in which the DUF domain had been deleted (Tsui et al., 2016a). Based on this we wanted to examine how EloR localized in a mutant expressing MltG without its DUF domain (MltG ^{Δ DUF}). Tsui et al., 2016a managed to create a *mltG* ^{Δ DUF} mutant in *S. pneumoniae* D39, and we reasoned that the same would be possible in the *S. pneumoniae* R6 strain, which is an unencapsulated D39 derivate. The goal was to create a mutant expressing EloR-mKate2 in an *mltG* ^{Δ DUF} genetic background. Since *mltG* is an essential gene, an ectopic copy of the gene was expressed in addition to the altered gene. The mutant we intended to make, would express MltG ^{Δ DUF} from the native promotor, and wild type MltG ectopically behind the P_{comX} promoter in R6 *S. pneumoniae* (MH16). Sequencing of the transformants with *mltG* ^{Δ DUF} in the native *mltG*-locus showed that the *mltG* ^{Δ DUF} gene contained additional mutations. For example, one transformant had a point mutation A943T (alanine to a threonine) located in the extracellular part of the protein (result not shown). Alanine only has a small side chain, while threonine has a hydroxy group, which is polar and might be playing a role in folding of the protein. Since it was difficult to predict the consequences of this mutation, it was decided to not continue with this mutant.

Another option was to replace the native *mltG* gene with a Janus cassette, while expressing *mltG* ^{Δ DUF} from the promotor P_{comX} , induced with ComS (MH17). When looking at the cells in the microscope, the cells appeared to be rounder and shorter compared to wild type

pneumococci. This mutant proved again that MltG needs its DUF domain to function properly and that the MltG^{ΔDUF} in *S. pneumoniae* R6 is lethal. It is hard to tell why this happens in the R6 strain, when it is possible in the D39 strain. In theory, Jag could interact with an unknown protein in septum in addition to MltG, and the unknown protein is recruiting EloR to midcell. This is not likely but cannot be excluded completely since we did not manage to deplete MltG or make MltG^{ΔDUF} in *S. pneumoniae*.

4.5 Does MltG follow the same localization pattern as EloR in a $\Delta yidC2$ genetic background?

MltG and EloR are a part of the same complex. Based on this protein-protein interaction-and EloR localization results, it seems most likely that MltG recruits EloR to the division zone. Interestingly, EloR had an altered localization in the $\Delta yidC2$ genetic background, i.e., also found in the cell poles (section 4.3). We therefore hypothesised that this polar localization of EloR could be a result from MltG also being enriched at the poles in a $\Delta yidC2$ mutant. To examine this, *yidC2* was deleted in a strain expressing MltG fused to super folder green fluorescent protein (sfGFP-MltG). The microscopy images and cell density plots in Figure 18 show that sfGFP-MltG was found at midcell in the $\Delta yidC2$ mutant, similar to wild type cells. This leads to the conclusion that the deletion of *yidC2* did not affect the localization of MltG, like it did with EloR (Figure 17B). Since MltG localizes to midcell in a $\Delta yidC2$ mutant, this might suggest that EloR have additional interaction partners or the RNA molecules binding to EloR are concentrated at the poles in the $\Delta yidC2$ mutant.

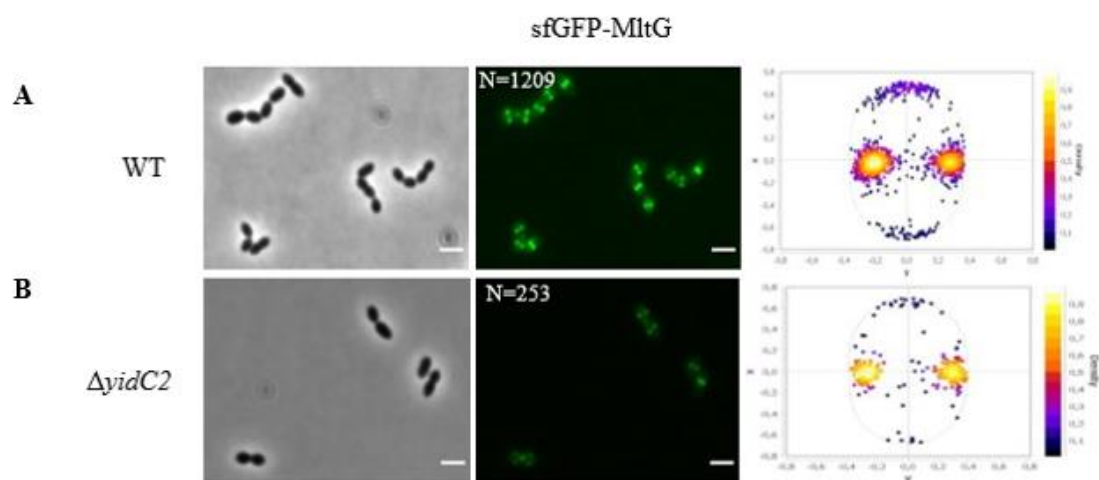


Figure 18 Localization of sfGFP-MltG with the associated cell density plots. sfGFP-MltG localization in A) wild type background, B) $\Delta yidC2$ mutant. N indicates the number of cells analyzed for each strain. X and Y in the focus density plots denote the relative length-and width-axis, respectively. sfGFP-MltG was found localized at midcell in all genetic backgrounds investigated. Scale bars are 2 μ m.

4.6 Amino acids in the conserved motif KKGFLG in Jag could be involved in protein-protein interactions

The three-dimensional (3D) structure EloR, including the Jag domain, has previously been solved for the EloR homologue in *Clostridium symbiosum* (PDB 3GKU). The Jag domain has a β - α - β - β fold with the α -helix laying on top of the three-stranded β -sheet where the conserved motif KKGFLG (Appendix 1.1) is found in the loop connecting the β 2-and β 3-strands. The predicted structure of the Jag domain of EloR from *S. pneumoniae* seems to be similar (Appendix 1.2). The Jag domain is responsible for localization of EloR to midcell. It is therefore reasonable to believe that the conserved motif in Jag could be involved in a protein-protein interaction important for EloR's interaction with MltG and hence its localization to midcell. Substitutions of residues in this motif (K36A, K37A, F39A, L40M) has previously been done by Winther et al., 2021, showing that no dramatic changes in localization occurred. However, since these were images of a limited number of cells, it was necessary to do more comprehensive study analysing a bigger number of cells to obtain more conclusive data as to whether these mutations could affect EloR localization (Winther et al., 2021). Microscopy analysis performed on these strains in this study show a midcell localization of EloR despite the introduced point mutations. This is clearly illustrated by the cell density plots in Figure 19. The substitutions of the different residues did not abrogate midcell localization of EloR.

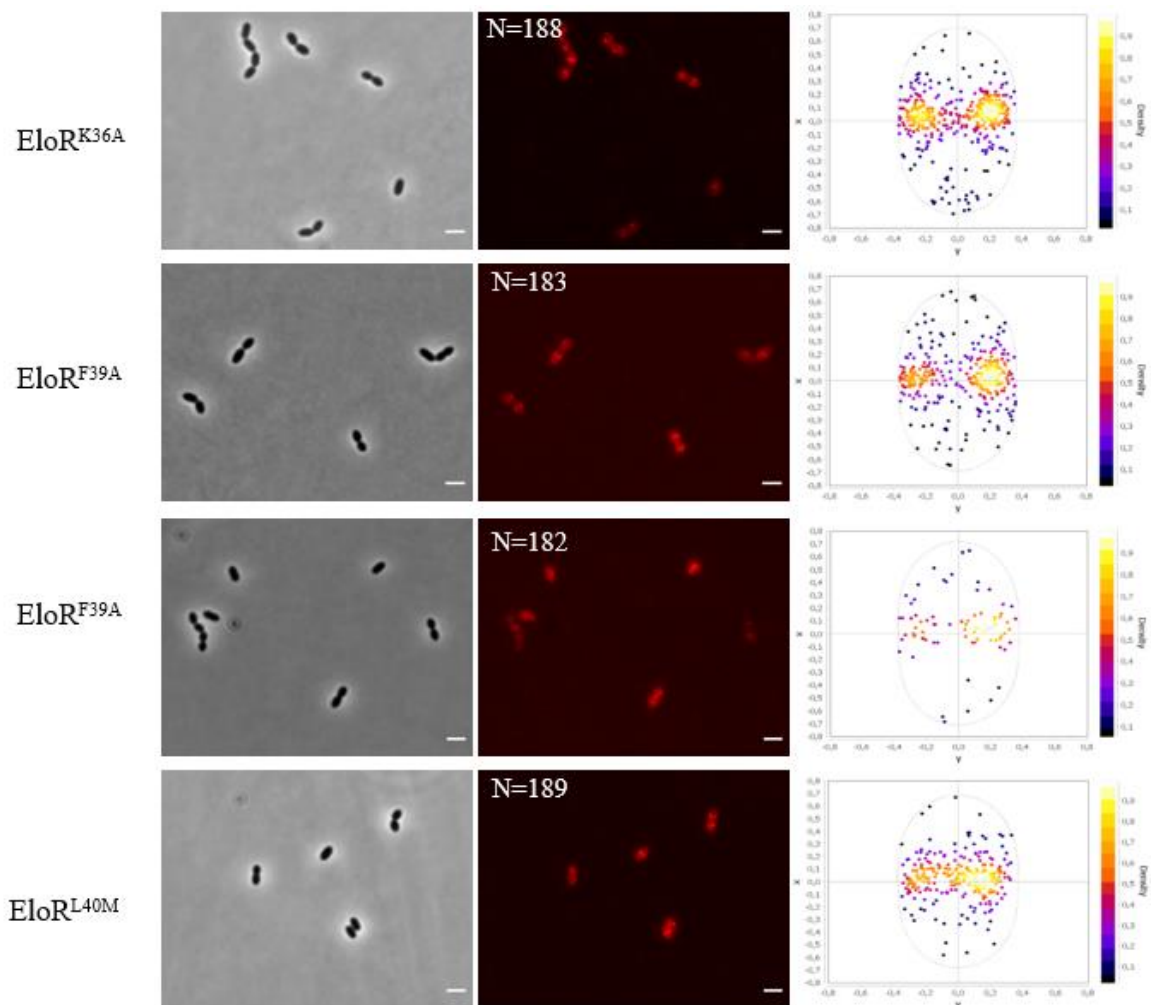


Figure 19 Localization of EloR-mKate2 with the amino acid substitutions K36A, K37A, F39A and L40M. Phase contrast and fluorescence microscopy images are shown with the corresponding focus density plots of the detected foci. EloR-mKate2 is found concentrated at midcell with all the introduced mutations. N indicates the number of cells analysed. Scale bars are 2 μ m.

4.6.1 Testing the interaction between EloR and MltGcyt from other streptococci

It is difficult to pinpoint the amino acids that could be important for interaction between EloR and MltG. We did not succeed in identifying residues in the Jag domain critical for its MltG interaction. It was therefore attempted to look for amino acids in the cytosolic domain of MltG that were important for the EloR-MltG interaction. MltG is conserved among Streptococci (Appendix 2) but contains variations across species, particularly in the cytoplasmic domain. We wanted to look for conserved regions and variable regions in the cytoplasmic domain and test these natural variations in BACTH assays to screen for MltG versions with weaker or loss of interaction with the Jag domain. If some variants lost interaction with EloR, we could potentially see which part of the cytoplasmic domain of MltG that differs from the variants

producing positive interactions. The cytosolic domain of MltG from *S. thermophilus*, *S. sanguinis*, *S. mitis*, *S. infantis* and *S. oralis* (listed in Table 2.1) were tested against EloR in the BACTH system (Figure 20). This makes it possible to see if any of the MltGcyt versions from closely related species could interact with EloR. If there was an interaction, the differences between the domains with no interaction versus the ones with interaction could give a pointer of the interaction surface between MltG and EloR.

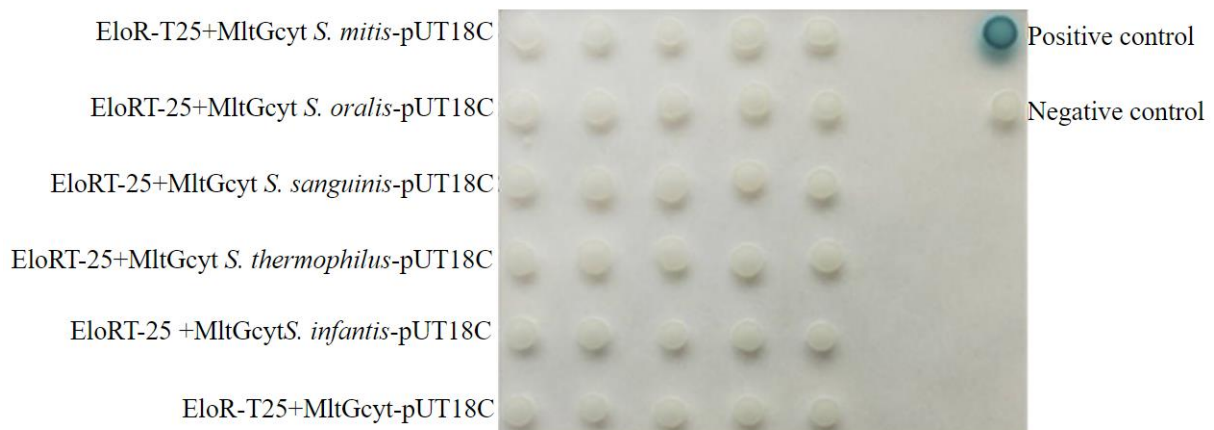


Figure 20 The cytosolic domain of MltG from closely related bacteria to *S. pneumoniae* are probed against EloR. The white spots give a conclusive result on no interaction between the MltGcyt and EloR. Even though the species are closely related, the MltGcyt domains are not similar enough to give a positive interaction.

This experiment was repeated 3 times and the result presented here were the only one giving a conclusive result with five identical bacterial spots for each protein; interaction between MltGcyt from the different Streptococcal species and EloR was negative. This might be due to MltGcyt from *S. mitis*, *S. oralis*, *S. sanguinis*, *S. thermophilus* and *S. infantis* is not similar enough to MltGcyt in *S. pneumoniae* to interact. Also, from this BACTH experiment the interaction between EloR and MltGcyt is negative in *S. pneumoniae*, indicating a potential technical error since these two proteins has shown to interact in previous BACTH experiments. MltGcyt from the different Streptococcal species was also probed against the Jag domain, but this gave inconclusive results; some bacterial spots were blue but the majority was white (result not shown). From BACTH experiments, it was only *S. mitis* that consistently had white spots, with both Jag and EloR.

4.6.2 Will point mutations in Jag reveal the amino acid important for interaction between Jag and MltG?

Since *S. mitis* is closely related to *S. pneumoniae* and the cytosolic domain of MltG from *S. pneumoniae* did not interact with EloR from *S. pneumoniae* (section 4.6.1), we aligned the Jag domains of EloR from the two species (Appendix 3) The only difference between EloR from *S. pneumoniae* R6 and *S. mitis* B6 is two amino acids, M25 and K37. In a final attempt to pinpoint interaction between Jag and MltG, the two amino acids were mutated to alanine and introduced into Jag in *S. pneumoniae*. A double mutation of both methionine and lysine to alanine was also introduced (M35A, K37A) (Figure 21).

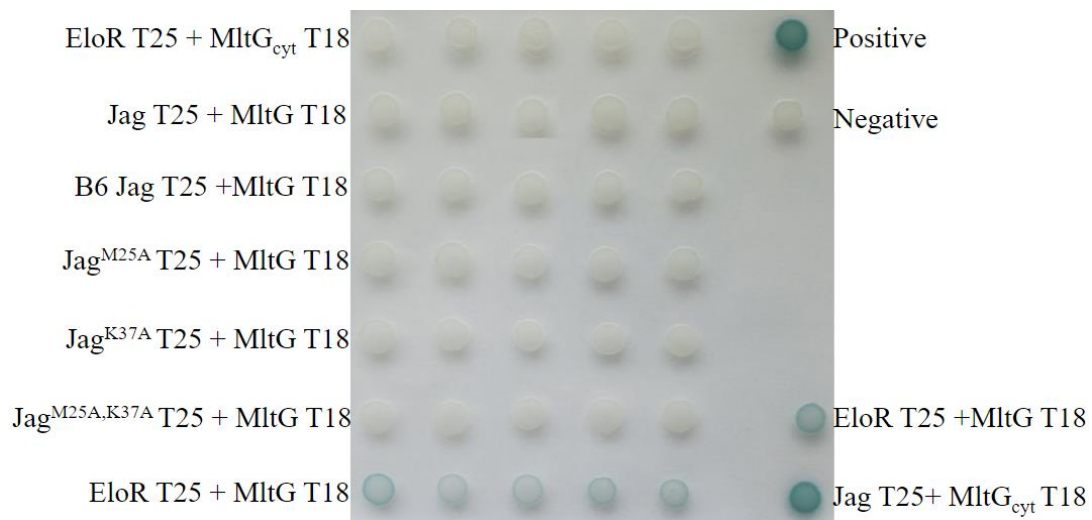


Figure 21: Introducing point mutations in R6 Jag. EloR and MltG is being consistent with blue bacterial spots in BACTH analysis, indicating interaction. MltG_{cyt} and Jag is on the other had not showing blue spots, despite for doing so in section 4.3. Regardless, when testing Jag against MltG_{cyt} the bacterial spots are blue, indicating interaction. When introducing the point mutations into Jag, they all gave white spots indicating, that interaction is lost.

When testing the interaction between the point mutated version of Jag and MltG in BACTH, all bacterial spots were white, indicating lack of interaction. This experiment was also performed by probing the point mutations in Jag against MltG_{cyt}, but these spots were also negative (results not shown). Probing Jag-T25 against MltG_{cyt}-T18 has previously given blue bacterial spots, indicating interaction. However, another batch of *E. coli* was used in this experiment and probing Jag against MltG_{cyt}, resulted in white bacterial spots. Since the interaction is lost when probing Jag with point mutations against MltG_{cyt}, we cannot be certain if the point mutated amino acids are central for interaction between Jag and MltG_{cyt}. Another alternative is to point mutate the methionine and lysine to a different amino acid than alanine to see if this could have another outcome.

4.7 Co-immunoprecipitation of EloR and MltG

Since the BACTH assays analysis showed that the Jag domain of EloR interacts with MltG and is a part of the same complex, it was attempted to use EloR as bait to co-precipitate MltG to confirm the interaction *in vivo* in *S. pneumoniae*. Strains expressing Flag-tagged EloR and sfGFP-tagged MltG (aw447) was already created in the laboratory. In addition, to test if MltG could be pulled down using the Jag domain as bait alone, a mutant expressing sfGFP-MltG and Flag-Jag (MH50) was created in this work. Additional strains were included in the experiment as controls (RH425, ds515, aw98 and aw459) which were created by other members in the lab.

By using resin beads tethered with α -Flag antibodies, the Flag-tagged proteins were pulled out from the cell lysates of the strains. The immunoprecipitated proteins were analysed using α -Flag and α -GFP antibodies. The immunoblot in Figure 22 show that when pulling out Flag-EloR, sfGFP-MltG followed in the same fraction (fifth lane). This indicates that EloR and MltG are part of the same complex in *S. pneumoniae*. Also, when pulling out Flag-Jag, sfGFP-MltG followed in the same fraction. In this experiment, the strain ds515 expressing sfGFP-MltG was used as negative control for a possible GFP/anti-flag interaction. We unfortunately got a band in the lane where this precipitate was probed with α -GFP antibodies. This indicates the presence of GFP-MltG in the precipitate where there is no Flag-tagged protein present. This is not consistent with previous results published by the group on this project (Winther et al., 2021). Another control (aw459: Flag-EloR, HlpA-GFP) was used to exclude possible GFP/Flag-EloR unspecific interaction. Here, no HlpA-GFP was pulled down with Flag-EloR. The immunoblot probed with α -GFP, had weaker signal compared to the α -Flag immunoblot which gave a stronger band for Flag-EloR, GFP-MltG. Also, when looking at the immunoblot probed with α -Flag, there is some background noise. The experiment was repeated twice, but the unspecific binding and background was persistent.

This experiment was performed to see if it was possible to verify the interaction between Jag and MltG. Since sfGFP-MltG was pulled down together with both Flag-EloR and Flag-Jag, the results cannot be trusted due to the negative control sfGFP-MltG.

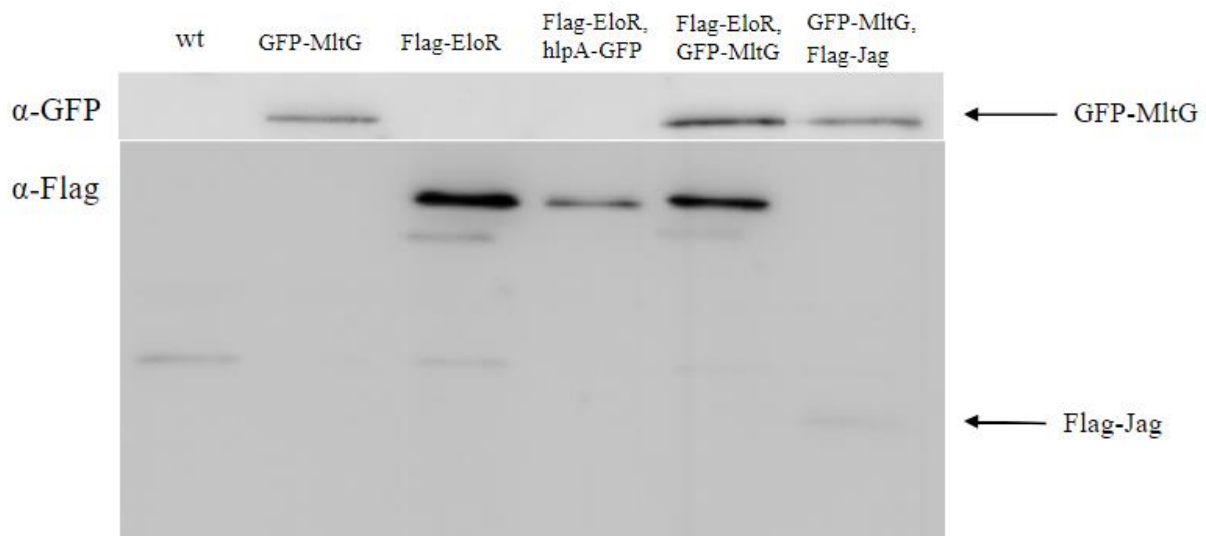


Figure 22 Co-immunoprecipitation analysis of ELoR/Jag-MltG interaction. The lysates were from the strains RH425 (wildtype (wt)), ds515 (*sfgfp-mltG*), aw98 (*flag-eloR*), aw459(*flag-eloR, hlpA-gfp*), aw447 (*flag-eloR, sfgfp-mltG*) and MH50 (*sfgfp-mltG, flag-jag*) and incubated with resin beads to pull down Flag-EloR and Flag-Jag

4.8 Over expression and purification of Jag-linker and MltGcyt

Based on the results presented in previous sections, MltGcyt and Jag/EloR forms a complex important for cell elongation in *S. pneumoniae*. Experiments such as BACTH only gives an indication that two proteins interact and the results in section 4.7 could not give conclusive results since the negative control, sfGFP-MltG was non-specifically pulled down without the presence of Flag-EloR. To verify the complex formation, the proteins in question were purified, concentrated, and combined before performing a gel filtration experiment where proteins in the same complex, elutes together. Gel filtration is a simple chromatographic method that can be used to separate molecules based on size. By using UV light, the absorbance from amino acids with aromatic side groups can be detected at a wavelength of 280nm (described in section 3.16). For this experiment the goal is to verify that Jag-linker and/or EloR is forming a complex with MltGDUF. Before performing the gel filtration, His-tagged versions of both MltGDUF and Jag-linker were overexpressed and purified.

Figure 23A show the purification of Jag-linker. The blue absorbance graph in blue illustrates where the Jag-linker protein is fractionated (approximately after 28 ml), but the peak is almost absent due to lack of aromatic amino acids in the Jag-linker protein. The fraction was collected and examined on SDS PAGE. Figure 23B clearly show that the collected fractions contain other

proteins in addition to Jag-linker. Since it is desirable to be left with only the protein of interest, fractions 8, 9 and 10 was combined to dialyze the protein before performing gel filtration with MltGDUF.

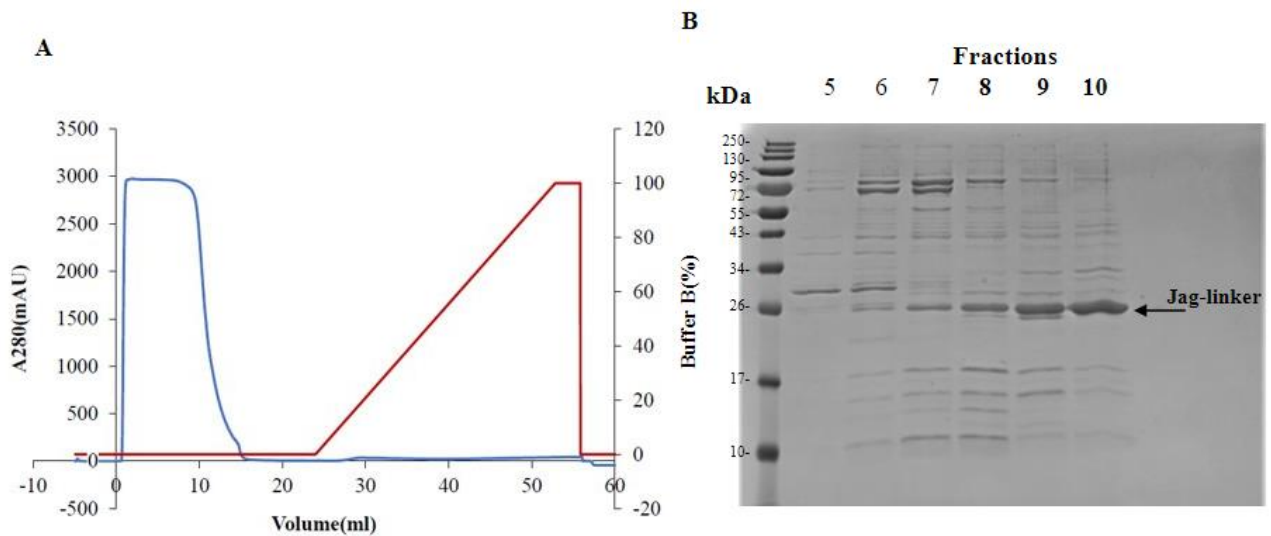


Figure 23 Protein purification of Jag-linker. A) The sample of *E. coli* lysate containing His-tagged Jag-linker was applied on a HisTrap HP column. Bound material was eluted by a linear gradient from 0 to 100 % Buffer B containing 20mM TrisHCl, 500 mM NaCl, and 500 mM imidazole. B) Coomassie stained SDS PAGE gel of fractions 5-10.

Figure 24A show a somewhat larger peak of MltGDUF compared to Jag-linker in Figure 23A. This might be due to DUF having few aromatic amino acids. The concentration of MltGDUF is low and optimally we should have had a higher protein concentration. Fractions 5 to 10 (27-32 ml) was collected as illustrated in Figure 24B. Even though the fractions were not completely purified as there is other bands in the same fraction, we combined fraction 8,9 and 10 for gel filtration with EloR.

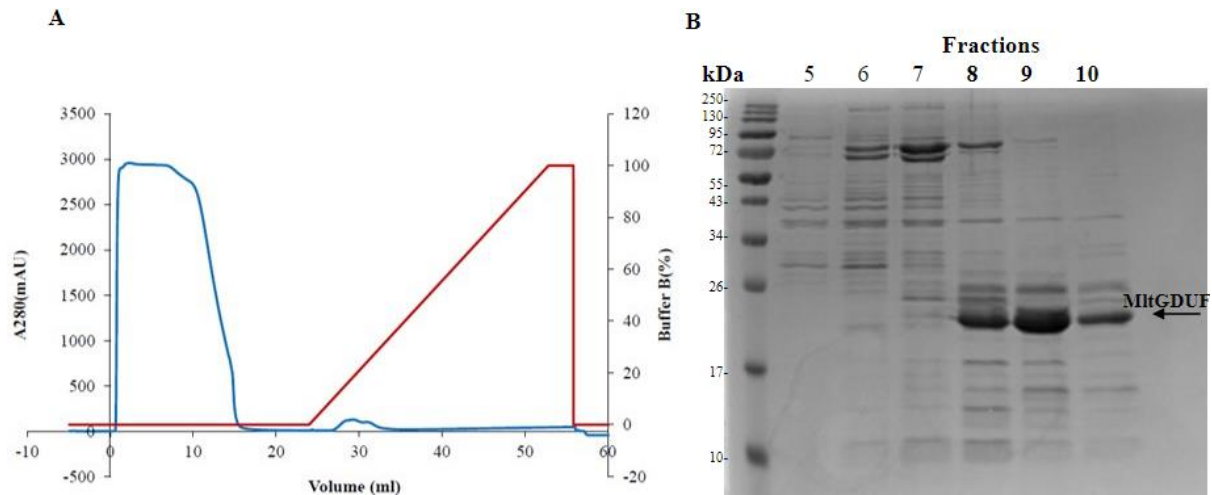


Figure 24 Protein purification of MltGDUF. A) The 5mL sample of E. coli lysate containing MltGDUF-His was applied on a HisTrap HP column. Bound material was eluted by a linear gradient up to 100 % Buffer B containing 20 mM TrisHCl, 500 mM NaCl, and 500 mM imidazole. Fractions eluted after approximately 27 ml, with an increasing imidazole/Buffer B gradient. B) SDS PAGE gel fractions 5-10, where 8,9 and 10 have MltGDUF.

Purified Jag-linker and MltGDUF were concentrated before running the gel filtering experiment. When doing gel filtration, the sample components are eluted isocratically, meaning that the buffer remains consistent through the separation and its only necessary to use one buffer and the molecules are separated from the column according to size, largest first as described in section 3.16. Due to mis-programming of the Äkta pure instrument (programmed to collect fractions only for A280 values higher than 5 mAU), only two fractions was collected during the gel filtration of Jag-linker and MltGDUF. Fraction 2 and 3 which eluted after approximately 10ml (highest peak in Figure 25A). Comparing the size of the bands from the protein purification in Figure 23B and 24B) with Figure 25B, it seems like Jag-linker and MltGDUF has been fractionated together. Because of the unoptimal purification and low concentration of the proteins, it is difficult to verify if a protein complex has been formed between MltGDUF and Jag-linker. Mass spectrometry or immunoblotting would confirm if the upper band indeed was Jag-linker. However, due to Covid-19 situation, there was no time left to perform these analyses.

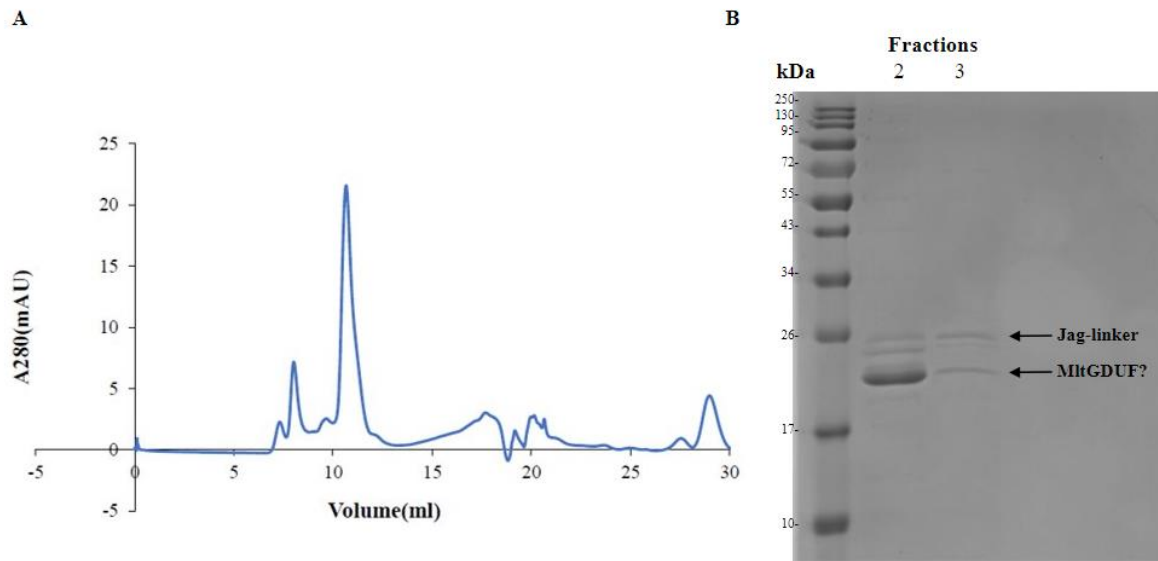


Figure 25 Gel filtration of Jag-Linker and MltGDUF. Fractions 2 and 3 was collected after approximately 10 ml. Comparing the bands we got from the gel filtration with the protein purification, it seems like Jag-linker is eluted first and thereafter together with MltGDUF, forming a complex. But this is har to confirm due to un-optimal MltGDUF purification and is eluted too early.

Since other laboratory members already had purified full-length EloR in the laboratory, we wanted to test if this full-length EloR could form complex with the MltGDUF domain and similarly as above; detect the complex using gel filtration. Purified EloR and MltGDUF are used as controls in the SDS-PAGE. Fractions 2-13 was collected (eluated from 9-21 ml) but only fractions 2 and 3 gave visible protein bands in the SDS PAGE gel after Coomassie staining (Figure 26B). It seems like both fractions have MltGDUF but have not been fractionated together with EloR, making it difficult to prove that they form a complex. Another issue is the two peaks eluting before the fractions were collected, after 6-8 ml. Since the fractions were not collected due to the settings in the program running the gel filtering, it is impossible to interpret this information (Figure 26A). Initially, it would have been an advantage to have a higher concentration of EloR and if there had been more time, this experiment would have been repeated.

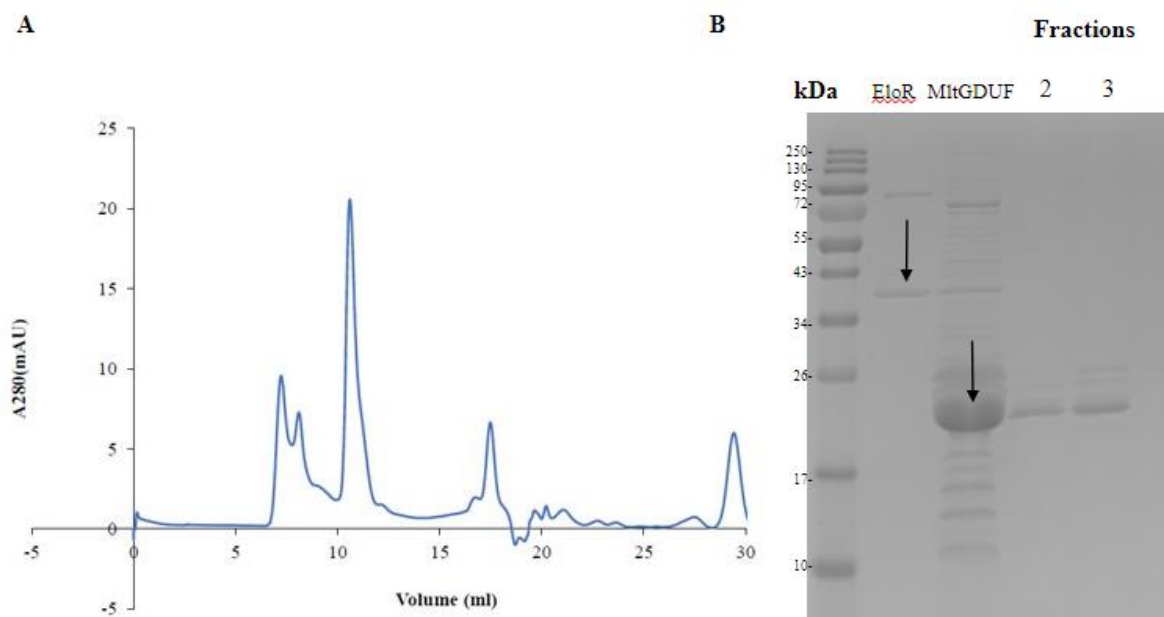


Figure 26 Gel filtration of EloR and MltGDUF. Purified EloR and MltGDUF are used as controls in SDS-PAGE. Fractionated but are not fractionated together in either 2 or 3, making it difficult to prove that they form a complex. The band representing MltGDUF is very thick, which can suggest there is more protein underneath and MltGDUF was not purified optimally.

5. Discussion

In this work, fluorescence microscopy and protein-protein interaction studies were employed to explore how EloR regulates cell elongation in *S. pneumoniae*. Since EloR has several domains, pinpointing which part of the protein that is critical for midcell localization has been important. EloR has been shown to interact with the elongasome protein MltG via the Jag domain. It has therefore been of great interest to study both Jag/EloR and MltG to understand how they interact and influence each other. A possible role of MltG is to position EloR at midcell, and that EloR through phosphorylation by StkP regulates the transglycolytic activity of MltG.

Most studies of RNA binding proteins (RBPs) in bacteria come from analysis of Gram-negative model organisms and the knowledge about RBPs are lagging in Gram-positive species. *E. coli* has approximately 180 annotated RBPs (Holmqvist et al., 2018). A lower number of RBPs are known in other Gram-positive bacterial species including human pathogens of high medical interest such as *S. pneumoniae* and *Staphylococcus aureus*. A study by Lamm-Schmidt et al., 2021 used Grad-Seq analysis to identify RNA-protein and protein-protein complexes in the Gram-positive *Clostridioides difficile*. This led to the identification of the conserved KhpB, originally identified in *S. pneumoniae* as EloR (Ulrych et al., 2016, Stamsås et al., 2017, Zheng et al., 2017). Lamm-Schmidt hypothesised that if EloR facilitates RNA-binding with other complexes, the high but unspecific EloR-binding activity changes through interaction with other protein partners like KhpA. It seems like EloR in both *C. difficile* and *S. pneumoniae* are involved in the regulation of virulence, but understanding the underlying mechanism is still at the starting point (Lamm-Schmidt et al., 2021). A study by Tsui et al., found EloR to bind 5' UTR on transcripts of *ftsA* coding for an important cell dividing protein. They believe that this is how EloR could affect the expression of FtsA. Also, they found that overexpression of FtsA in *S. pneumoniae* D39 is compensated so PBP2b can be deleted in the same way as in a Δ *eloR* mutant.

From previous studies, it is known that EloR interacts with the RNA-binding protein KhpA. Breaking the EloR/KhpA interaction will lead to shorter cells and the function of the elongasome are compromised so that deletion of the essential PBP2b/RodA is no longer lethal for the cells (Stamsås et al., 2017, Zheng et al., 2017). It is suggested that EloR and KhpA have a conserved role in regulating cell elongation since EloR and KhpA is found in several Gram-positive bacteria. Also supporting this is the study by Myrbråten et al., 2019 where the proteins in *Lactobacillus plantarum* led to shortening of the cells (Myrbråten et al., 2019). Even though EloR and KhpA, localizes to the division zone of *S. pneumoniae* where EloR directs KhpA to midcell, it is not known what directs EloR to midcell (Winther et al., 2019, Zheng et al., 2017). A possible hypothesis is that EloR must form interaction with other elongasome proteins for localization to midcell, which is explored in this work.

The first BACTH experiment in this work was performed to identify elongasome proteins that interact with EloR. The BACTH results (Figure 16) suggested that EloR have several interaction partners in the elongasome. These data help us understand how EloR localizes to midcell and the regulatory functions it has in cell elongation. The positive hits were RodZ, YidC2, MltG and MltGcyt. RodZ is considered to be a part of the elongasome, similar to EloR where studies of RodZ in *E. coli* has indicated that RodZ is important for the elongated cell shape (Shiomi et al., 2008).

5.1 Microscopy imaging revealing midcell localization

Analysis of the localization of different domains of EloR fused to mKate2 (see section 4.1), forms the foundation of the other experiments in this work. We unravelled that the Jag domain of EloR is important for midcell localization, independently of the linker domain. The focus of the rest of the thesis has therefore been to improve our knowledge of how Jag interacts with MltG.

One of the microscopy analyses examined whether EloR's midcell localization could be affected by phosphorylation on its threonine 89 in the linker region. The conserved threonine 89 is phosphorylated by StkP to modulate EloR activity. It is therefore reason to believe that the linker could be involved in conformational rearrangements of the EloR protein between active and inactive forms (Stamsås et al., 2017). It turned out that the localization of EloR-mKate2 in a genetic background lacking StkP was not affected, demonstrating neither

phosphorylation of Thr89 nor the presence of StkP is the reason why EloR-mKate2 concentrates at midcell (Figure 17). It has been shown previously using BACTH assays that StkP and EloR interacts (probably in connection with transfer of the phosphoryl group from StkP to EloR), but the results presented here demonstrated that this interaction is not the reason why EloR can be found in the division zone. This result suggests that EloR locates to midcell by interacting with proteins other than StkP. One can imagine that EloR is part of a complex that include StkP, and that at the appropriate time during cell cycle, StkP phosphorylates EloR to regulate other proteins in this complex.

It was also tested if EloR-mKate2 localization was affected in a $\Delta yidC2$ or $\Delta rodZ$ mutant. Here, the localization of EloR-mKate2 was not affected in the genetic background lacking RodZ, but in the cells lacking YidC2, EloR-mKate2 was concentrated at the cellular poles in addition to midcell. Further investigations of the polar localization of EloR-mKate2 revealed that the polar foci were found in old cellular poles (Appendix 4) (Winther et al., 2021). This suggests that EloR could have additional interaction partners that is displaced when YidC2 is absent or that the RNA molecules that EloR binds are concentrated at the poles in a $\Delta yidC2$ mutant. Since YidC2 is an insertase that assist with insertion of membrane proteins during translation, it is possible that EloR and YidC2 are functionally linked to this process by e.g., affecting expression of other membrane bound elongosome proteins. Also, YidC homologues play a central role in the insertion and/or folding of membrane proteins in bacterial membranes (Hennon et al., 2015). Lamm-Schmidt et al., 2021 observed that EloR binds to *yidC2* transcripts, as well as other transcripts encoding (putative) membrane proteins, transporters, two-component sensor histidine kinases and ATPases. From the BACTH experiment in this work, we know that EloR interact with the conserved insertase YidC2 (see section 4.2) which is co-expressed with EloR in both *S. pneumoniae* and *C. difficile* (Lamm-Schmidt et al., 2021). Based on this, YidC2 could have a functional role in the EloR/KhpA regulatory pathway but little is known about this and further experiments need to be performed to unravel this.

Interestingly, EloR changed localization pattern in a $\Delta yidC2$ mutant, i.e., also concentrating at the cell poles. Based on the fact that MltG interacted with the Jag domain, which is essential for EloR midcell localization, we wondered whether EloR was found at the poles in the $\Delta yidC2$ mutant because MltG also could be found there. YidC2 was deleted in a strain expressing sfGFP-MltG from the native locus and the result displayed sfGFP-MltG at midcell in the $\Delta yidC2$ mutant and no polar foci were observed (Figure 18). In future work it would be

interesting to test if the localization to the poles would be dependent of Jag by testing if Jag-mKate2 localized in the poles in a *ΔyidC2* mutant.

In another attempt to discover what part of the Jag domain that is important for protein-protein interaction, we investigated the predicted 3 dimensional structure with the conserved motif (KKGFLG) (Winther et al., 2021). From the results in section 4.6, the substitutions of K36A, K37A, F39A, L40M in this motif did not affect the midcell localisation of EloR. This can indicate that the conserved motif has another function than localization, or that several of the amino acids are important for the localization. If this is the case it might be necessary to mutate several of the amino acids in order to affect the localization, not only the single mutations that we introduced. The probability of the substitutions being significant for localization is low, but at the same time necessary to explore based on the conserved motif and the predicted 3dimensional structure of Jag.

5.2 BACTH experiments to identify EloR and MltG interaction

The BACTH results suggested that the EloR interaction with MltG is direct, because in order for T18 and T25 to reconstitute the adenylate cyclase activity to create blue spots, the tags have to be brought into close proximity to each other. Such proximity indicates a direct interaction between the two proteins carrying the tags. To further pinpoint the EloR/MltG interaction, a BACTH assay with point mutation of the Jag domain of EloR probed against MltG (Figure 21) and the cytosolic part of MltG (result not shown) was performed. The Jag domain interacted with the cytosolic part of MltG. When we tested interaction between the cytosolic part of MltG lacking the DUF domain and the Jag domain of EloR, the interaction between the two was lost (Figure 16). Since there is evidence for interaction between EloR and MltG, this strongly suggests the EloR interacts with the DUF domain. MltG is located at the division zone of *S. pneumoniae* and it is therefore plausible that EloR is recruited to midcell through its interaction with MltG.

Knocking out *yidC2*, *rodZ*, or *stkP* did not abrogate the localization of EloR. Another approach to investigate EloR-MltG interaction was to align MltG from different streptococcal species to compare conserved amino acids and analyse the sequences to find which part of MltG that could be important for interaction. Due to challenges during the BACTH experiment it was difficult to draw any conclusions, but it seems like MltG from *S. mitis* was most similar to MltG in *S.*

pneumoniae. Comparing EloR from *S. mitis* and *S. pneumoniae* it was only two amino acid that distinguished them. It is proved that the Jag domain of EloR and MltG interacts, and since the interaction was lost when point mutating the methionine and lysine, this indicates that these amino acids could be important for interaction (Figure 22). To further verify this, it should have been performed another BACTH experiment to point mutate M25 and K37 to other amino acids than alanine to see if the outcome would change or if the interaction would still be lost.

5.3 Challenges with the essential MltG

Since MltG is essential in *S. pneumoniae* it is difficult to study this protein without interfering with the viability of the cells. Although the DUF domain of MltG constitutes most of the cytosolic part of MltG, Tsui et al., managed to create a mutant that could survive with an MltG version lacking the DUF domain. However, when we tried to create the same mutant in the R6 strain for EloR localization studies, we did not succeed. The cells only accepted a copy of *mltG*^{ΔDUF} when full-length *mltG* was ectopically expressed by inducing with ComS. However, expressing an mKate2 fused version of EloR in this mutant proved to be lethal. The cells with deletion or depletion of MltG was studied in microscopy, (result not shown) looking for morphological changes. The cells were noticeably different from wild type; the cells tended to be smaller both longitudinal and in width, they tended to grow slower than normal and in chains. The cells could only survive in the *S. pneumoniae* R6 when grown with ComS to express a wild type version of MltG. The study by Tsui et al., 2016a succeeded in expressing MltG^{ΔDUF} in the *S. pneumoniae* D39 strain. It is difficult to explain why this is possible in the D39 strain and not in the R6 strain but it might be because of suppressor mutations during the construction of the D39 mutant strain, or the fact that they used the D39 lab strain instead of R6. The D39 strain contains some differences in the genome compared to R6, for example mutations in *pbp1a* (T124A and D388E), which have an important role in peptidoglycan synthesis (Tsui et al., 2016a).

When performing BACTH analysis with MltG_{cyt} from different species of *Streptococci* against EloR, most of the results gave inconclusive results with sporadic blue and white bacterial spots. This is again demonstrating the challenges working with modified versions of MltG, such as MltG_{cyt} or MltG^{ΔDUF}. Some of the BACTH experiments had been performed before by (Winther, 2020) but when we tried to replicate the same experiments, we could not get the same results. We troubleshooted the protocol, the transformation, the plates used for spotting the

bacterial cells, the MltG_{cyt} sequence to see if there were any mutations, but we could not find any errors. Hopefully, if there had been more time it would have been possible to troubleshoot further and find potential technical errors. Since BACTH only gives an indication on protein-protein interaction it's important to do further research to verify the interaction and complex formation by e.g., co-immunoprecipitation and gel filtration.

In comparison to MltG in *S. pneumoniae*, MltG in *E. coli* is not essential and cells lacking MltG has no growth defects (Yunck et al., 2016). MltG in *S. pneumoniae* has an additional cytoplasmic domain (DUF) and the loss of MltG results in growth defects and spherical cell shape (Tsui et al., 2016b). A study by Sassine et al., 2021 has done experiments on MltG in *E. coli* where the lytic transglycosylase activity is higher under glycan strand polymerization and glycan strands with a length of 7 disaccharide units was produced. This suggests that MltG can bind a nascent glycan strand from the membrane to cleave it after 7 disaccharide units. More work needs to be done in order to explore if MltG can be used to produce a sufficient amount of glycan strands with a desirable length for biochemical or structural studies (Sassine et al., 2021).

5.4 Co-IP to verify interaction between EloR/Jag and MltG in vivo

The immunoprecipitation experiment was performed to prove that EloR and/or Jag-linker is in complex with MltG *in vivo* in *S. pneumoniae*. From Figure 22, the negative control strain only expressing GFP-MltG, but not Flag-tagged EloR, a band corresponding to GFP-MltG was detected in the pull-down. The intensity of the Flag-Jag band was significantly lower than that of Flag-EloR. The weak band of Flag-Jag might be because it is less stable in the cells, but further analysis needs to be done to confirm this. Apart from the negative control in this work, it would have been possible to confirm the EloR-MltG and Jag-MltG interaction. A similar co-immunoprecipitation experiment was carried out by Winther et al., 2021 where the EloR/MltG interaction was confirmed. Neither wild type nor the negative control GFP-MltG had any band and Flag-EloR and sfGFP-MltG followed in the same fraction. Based on this, it should be possible to repeat the experiment to confirm Jag-MltG interaction in addition to Jag-MltG interaction.

5.5 Using gel filtration to detect EloR/MltG complex formation

Both MltGDUF and Jag-linker was partly purified in this work. However, using gel filtration to detect possible complex between these two proteins after being combined *in vitro* did not give any conclusive result. Furthermore, substitutions of Jag-linker with full-length EloR in a similar experiment did not result in a detectable complex in the gel filtration analysis. Gel filtration of MltGDUF and EloR displayed peaks that eluted after 6-8 ml, which was before sample collection started (before fraction 2 and 3 Figure 26B). These peaks should have been collected, however, the additional 2.5 ml buffer used to empty the sample loop was not taken into account when determining the void volume. Hence, fractionation began 2 ml after void volume (Figure 26A). Even though the gel filtration experiments did not detect any complex formation of MltGDUF and EloR/Jag-linker, it does not mean they do not interact (see section 4.8). This is a difficult experiment to do successfully *in vitro*. It could be due to wrong buffer, pH, temperature or other conditions. If there had been more time, it would be preferably to perform the experiment with higher concentrations of both proteins. At least, when performing a gel filtering, a dilution of the sample is obtained, and it should have been more concentrated. In addition, MltGDUF was not purified optimally, and a second purification step should be done to obtain more than 90% pure proteins (Figure 24B). On one hand, the conditions will affect the results, but the experiments should also be performed with only Jag, and not with Jag-linker since we know that Jag is solely localizing of EloR to midcell, and thus interacting with MltGDUF. The reason Jag-linker was used was because it was easily available in the lab and the time limit due to Covid19 prevented us to create the His-tagged Jag.

Regarding the calibration of the column used for gel filtration experiment, it is similar to the theoretically calibration from the manufacturer. Despite correct calibration, MltGDUF elutes too early, and it is speculated that MltG might have other abilities such as forming a homodimer. EloR is a dimer where the crystal structure is known from *Clostridium* (Nocek et al., 2011) . If MltG is a dimer, MltG and EloR could interact one to one or another possibility is that MltG could lie in the membrane as a dimer or a multimer.

6. Concluding remarks and further research

In this work it is suggested that Jag domain of EloR acts as a protein-protein interaction domain and is crucial for EloR recruitment to the septum by the transglycosylase MltG. It has been revealed that knocking out the essential *pbp2b* gene results in suppressor mutations in *mltG*, *eloR* and *khpA* and the requirement for the elongasome is lost in *S. pneumoniae* (Tsui et al., 2016a, Stamsås et al., 2017). EloR and MltG is a part of the same regulatory pathway where KhpA is known to interact with EloR. From present studies, MltG, EloR and KhpA form a complex at the division zone, regulating the elongasome on command from StkP (Winther et al., 2021). In this work, expressing MltG from an inducible promotor proved to be difficult, and manipulations of EloR which is a part of the same regulatory pathway, are impossible in cells with altered expression levels of MltG or mutated MltG versions. The EloR/KhpA complex seems to be central for regulation of MltG and it is plausible that this complex modulates the activity of MltG via the RNA binding domains. Another possibility is that EloR regulates the MltG activity directly by interacting with other cell division proteins. MltG is known to be a membrane bound lytic transglycosylase, involved in PG synthesis and in cell division. Resent study by Sassine et al., 2021 hypothesise that MltG in *E. coli* can modulate PG synthesis not only through their catalytic activities, but also through interacting with regulating activities of PG synthases, and ultimately determining the structure of the PG (Sassine et al., 2021).

Finding the crystal structure of MltG could make it easier to study the protein in *S. pneumoniae* and to predicate the part of MltG interacting with Jag. It would also be interesting to explore if EloR facilitates RNA-binding with other complexes, changing the EloR-binding activity through the interaction with other protein partners like KhpA. There are still several open questions regarding the mechanism of the gene regulation of EloR and if it interacts with RBPs other than KhpA? And maybe most importantly, which RNA molecules are binding to the EloR/KhpA complex? It might be important to test RNA-binding with the EloR/KhpA complex and not only EloR.

References

- BARRIL, P. & NATES, S. 2012. Introduction to agarose and polyacrylamide gel electrophoresis matrices with respect to their detection sensitivities. *Gel electrophoresis-Principles and basics*, 3-14.
- BEHR, T., FISCHER, W., PETER-KATALINIĆ, J. & EGGE, H. 1992. The structure of pneumococcal lipoteichoic acid: Improved preparation, chemical and mass spectrometric studies. *European journal of biochemistry*, 207, 1063-1075.
- BEILHARZ, K., NOVÁKOVÁ, L., FADDA, D., BRANNY, P., MASSIDDA, O. & VEENING, J.-W. 2012. Control of cell division in *Streptococcus pneumoniae* by the conserved Ser/Thr protein kinase StkP. *Proceedings of the National Academy of Sciences*, 109, E905-E913.
- BERG, K. H., BIØRNSTAD, T. J., STRAUME, D. & HÅVARSTEIN, L. S. 2011. Peptide-regulated gene depletion system developed for use in *Streptococcus pneumoniae*. *Journal of bacteriology*, 193, 5207-5215.
- BERG, K. H., STAMSÅS, G. A., STRAUME, D. & HÅVARSTEIN, L. S. 2013. Effects of low PBP2b levels on cell morphology and peptidoglycan composition in *Streptococcus pneumoniae* R6. *Journal of bacteriology*, 195, 4342-4354.
- BIOLABS, N. E. 2021. *PCR Protocol for Phusion® High-Fidelity DNA Polymerase (M0530)* [Online]. New England BioLabs Available: <https://www.neb.com/protocols/0001/01/01/pcr-protocol-m0530> [Accessed].
- BIOSCIENCES, A. 2003. *HisTrap HP Kit for purification of histidine-tagged proteins* [Online]. Available: file:///C:/Users/marie/Downloads/HisTrap-HP%20manual%20(1).pdf [Accessed 2021].
- BLAIR, J. M., WEBBER, M. A., BAYLAY, A. J., OGBOLU, D. O. & PIDDOCK, L. J. 2015. Molecular mechanisms of antibiotic resistance. *Nature reviews microbiology*, 13, 42-51.
- BRUCE ALBERTS, A. J., JULIAN LEWIS, DAVID MORGAN, MARTIN RAFF, KEITH ROBERTS, PETER WALTER 2015. *Molecular Biology of The Cell* Garland Science.
- BRYKSIN, A. V. & MATSUMURA, I. 2010. Overlap extension PCR cloning: a simple and reliable way to create recombinant plasmids. *Biotechniques*, 48, 463-465.
- BUI, N. K., EBERHARDT, A., VOLLMER, D., KERN, T., BOUGAULT, C., TOMASZ, A., SIMORRE, J.-P. & VOLLMER, W. 2012. Isolation and analysis of cell wall components from *Streptococcus pneumoniae*. *Analytical biochemistry*, 421, 657-666.
- CARTWRIGHT, K. 2002. Pneumococcal disease in western Europe: burden of disease, antibiotic resistance and management. *European journal of pediatrics*, 161, 188-195.
- CHERAZARD, R., EPSTEIN, M., DOAN, T.-L., SALIM, T., BHARTI, S. & SMITH, M. A. 2017. Antimicrobial resistant *Streptococcus pneumoniae*: prevalence, mechanisms, and clinical implications. *American journal of therapeutics*, 24, e361-e369.
- DENAPAITE, D., BRÜCKNER, R., HAKENBECK, R. & VOLLMER, W. 2012. Biosynthesis of teichoic acids in *Streptococcus pneumoniae* and closely related species: lessons from genomes. *Microbial drug resistance*, 18, 344-358.
- DEYL, Z. 2011. *Techniques*, Elsevier.
- DI GUILMI, A. M. & DESSEN, A. 2002. New approaches towards the identification of antibiotic and vaccine targets in *Streptococcus pneumoniae*. *EMBO reports*, 3, 728-734.
- DIEFFENBACH, C., LOWE, T. & DVEKSLER, G. 1993. General concepts for PCR primer design. *PCR methods appl*, 3, S30-S37.
- DUCRET, A., QUARDOKUS, E. M. & BRUN, Y. V. 2016. MicrobeJ, a tool for high throughput bacterial cell detection and quantitative analysis. *Nature microbiology*, 1, 1-7.
- EMAMI, K., GUYET, A., KAWAI, Y., DEVI, J., WU, L. J., ALLENBY, N., DANIEL, R. A. & ERRINGTON, J. 2017. RodA as the missing glycosyltransferase in *Bacillus subtilis* and antibiotic discovery for the peptidoglycan polymerase pathway. *Nature microbiology*, 2, 1-9.

- EPAND, R. M., WALKER, C., EPAND, R. F. & MAGARVEY, N. A. 2016. Molecular mechanisms of membrane targeting antibiotics. *Biochimica et Biophysica Acta (BBA)-Biomembranes*, 1858, 980-987.
- EUROMEDEX BACTH System Kit Bacterial Adenylate Cyclase Two- Hybrid System Kit. Euromedex
- FACKLAM, R. 2002. What happened to the streptococci: overview of taxonomic and nomenclature changes. *Clinical microbiology reviews*, 15, 613-630.
- FALK, S. P. & WEISBLUM, B. 2013. Phosphorylation of the Streptococcus pneumoniae cell wall biosynthesis enzyme MurC by a eukaryotic-like Ser/Thr kinase. *FEMS microbiology letters*, 340, 19-23.
- FENTON, A. K., MANUSE, S., FLORES-KIM, J., GARCIA, P. S., MERCY, C., GRANGEASSE, C., BERNHARDT, T. G. & RUDNER, D. Z. 2018. Phosphorylation-dependent activation of the cell wall synthase PBP2a in Streptococcus pneumoniae by MacP. *Proceedings of the National Academy of Sciences*, 115, 2812-2817.
- FILIFE, S. R., SEVERINA, E. & TOMASZ, A. 2001. The role of murMN operon in penicillin resistance and antibiotic tolerance of Streptococcus pneumoniae. *Microbial Drug Resistance*, 7, 303-316.
- FLEURIE, A., LESTERLIN, C., MANUSE, S., ZHAO, C., CLUZEL, C., LAVERGNE, J.-P., FRANZ-WACHTEL, M., MACEK, B., COMBET, C. & KURU, E. 2014. MapZ marks the division sites and positions FtsZ rings in Streptococcus pneumoniae. *Nature*, 516, 259-262.
- FONTAINE, L., BOUTRY, C., DE FRAHAN, M. H., DELPLACE, B., FREMAUX, C., HORVATH, P., BOYAVAL, P. & HOLS, P. 2010. A novel pheromone quorum-sensing system controls the development of natural competence in Streptococcus thermophilus and Streptococcus salivarius. *Journal of bacteriology*, 192, 1444-1454.
- GRISHIN, N. V. 1998. The R3H motif: a domain that binds single-stranded nucleic acids. *Trends in biochemical sciences*, 23, 329-330.
- HARDIE, J. & WHILEY, R. 1997. Classification and overview of the genera Streptococcus and Enterococcus. *Journal of applied microbiology*, 83, 1S-11S.
- HECKMAN, K. L. & PEASE, L. R. 2007. Gene splicing and mutagenesis by PCR-driven overlap extension. *Nature protocols*, 2, 924.
- HENNON, S. W., SOMAN, R., ZHU, L. & DALBEY, R. E. 2015. YidC/Alb3/Oxa1 family of insertases. *Journal of Biological Chemistry*, 290, 14866-14874.
- HENRIQUES-NORMARK, B. & TUOMANEN, E. I. 2013. The pneumococcus: epidemiology, microbiology, and pathogenesis. *Cold Spring Harbor perspectives in medicine*, 3, a010215.
- HO, S. N., HUNT, H. D., HORTON, R. M., PULLEN, J. K. & PEASE, L. R. 1989. Site-directed mutagenesis by overlap extension using the polymerase chain reaction. *Gene*, 77, 51-59.
- HOLEČKOVÁ, N., DOUBRAVOVÁ, L., MASSIDDA, O., MOLLE, V., BURIÁNKOVÁ, K., BENADA, O., KOFROŇOVÁ, O., ULRYCH, A. & BRANNY, P. 2015. LocZ is a new cell division protein involved in proper septum placement in Streptococcus pneumoniae. *MBio*, 6.
- HOLMQVIST, E., LI, L., BISCHLER, T., BARQUIST, L. & VOGEL, J. 2018. Global maps of ProQ binding in vivo reveal target recognition via RNA structure and stability control at mRNA 3' ends. *Molecular cell*, 70, 971-982. e6.
- HOSKINS, J., ALBORN, W. E., JR., ARNOLD, J., BLASZCZAK, L. C., BURGETT, S., DEHOFF, B. S., ESTREM, S. T., FRITZ, L., FU, D. J., FULLER, W., GERINGER, C., GILMOUR, R., GLASS, J. S., KHOJA, H., KRAFT, A. R., LAGACE, R. E., LEBLANC, D. J., LEE, L. N., LEFKOWITZ, E. J., LU, J., MATSUSHIMA, P., MCAHREN, S. M., MCHENNEY, M., MCLEASTER, K., MUNDY, C. W., NICAS, T. I., NORRIS, F. H., O'GARA, M., PEERY, R. B., ROBERTSON, G. T., ROCKEY, P., SUN, P. M., WINKLER, M. E., YANG, Y., YOUNG-BELLIDO, M., ZHAO, G., ZOOK, C. A., BALTZ, R. H., JASKUNAS, S. R., ROSTECK, P. R., JR., SKATRUD, P. L. & GLASS, J. I. 2001. Genome of the bacterium Streptococcus pneumoniae strain R6. *Journal of bacteriology*, 183, 5709-5717.
- HÖLTJE, J.-V. 1998. Growth of the stress-bearing and shape-maintaining murein sacculus of Escherichia coli. *Microbiology and molecular biology reviews*, 62, 181-203.
- HÅVARSTEIN, L. S., COOMARASWAMY, G. & MORRISON, D. A. 1995. An unmodified heptadecapeptide pheromone induces competence for genetic transformation in

- Streptococcus pneumoniae*. *Proceedings of the National Academy of Sciences*, 92, 11140-11144.
- JAMES D, W., ALEXANDER GANN, TANIA A. NAKER, MICHAEL LEVINE, STEPHEN P. BELL, RICHARD LOSICK 2014. *Molecular Biology of the Gene* Pearson Education, Inc. .
- JOHNSBORG, O. & HÅVARSTEIN, L. S. 2009a. Pneumococcal LytR, a protein from the LytR-CpsA-Psr family, is essential for normal septum formation in *Streptococcus pneumoniae*. *Journal of bacteriology*, 191, 5859-5864.
- JOHNSBORG, O. & HÅVARSTEIN, L. S. 2009b. Regulation of natural genetic transformation and acquisition of transforming DNA in *Streptococcus pneumoniae*. *FEMS Microbiology Reviews*, 33, 627-642.
- JONES, G. & DYSON, P. 2006. Evolution of transmembrane protein kinases implicated in coordinating remodeling of gram-positive peptidoglycan: inside versus outside. *Journal of bacteriology*, 188, 7470-7476.
- KARIMOVA, G., PIDOUX, J., ULLMANN, A. & LADANT, D. 1998. A bacterial two-hybrid system based on a reconstituted signal transduction pathway. *Proceedings of the National Academy of Sciences*, 95, 5752-5756.
- LADDOMADA, F., MIYACHIRO, M. M., JESSOP, M., PATIN, D., JOB, V., MENGIN-LECREULX, D., LE ROY, A., EBEL, C., BREYTON, C. & GUTSCHE, I. 2019. The MurG glycosyltransferase provides an oligomeric scaffold for the cytoplasmic steps of peptidoglycan biosynthesis in the human pathogen *Bordetella pertussis*. *Scientific reports*, 9, 1-17.
- LAMM-SCHMIDT, V., FUCHS, M., SULZER, J., GEROVAC, M., HÖR, J., DERSCH, P., VOGEL, J. & FABER, F. 2021. Grad-seq identifies KhpB as a global RNA-binding protein in *Clostridioides difficile* that regulates toxin production. *microLife*.
- LANCEFIELD, R. C. 1933. A serological differentiation of human and other groups of hemolytic streptococci. *The Journal of experimental medicine*, 57, 571-595.
- LAND, A. D., TSUI, H. C. T., KOCAOGLU, O., VELLA, S. A., SHAW, S. L., KEEN, S. K., SHAM, L. T., CARLSON, E. E. & WINKLER, M. E. 2013. Requirement of essential P bp2x and GpsB for septal ring closure in *S treptococcus pneumoniae* D 39. *Molecular microbiology*, 90, 939-955.
- LEE, P. Y., COSTUMBRADO, J., HSU, C.-Y. & KIM, Y. H. 2012. Agarose gel electrophoresis for the separation of DNA fragments. *JoVE (Journal of Visualized Experiments)*, e3923.
- LINARES, J., ARDANUY, C., PALLARES, R. & FENOLL, A. 2010. Changes in antimicrobial resistance, serotypes and genotypes in *Streptococcus pneumoniae* over a 30-year period. *Clinical Microbiology and infection*, 16, 402-410.
- LLOYD, A. J., GILBEY, A. M., BLEWETT, A. M., DE PASCALE, G., EL ZOEIBY, A., LEVESQUE, R. C., CATHERWOOD, A. C., TOMASZ, A., BUGG, T. D. & ROPER, D. I. 2008. Characterization of tRNA-dependent peptide bond formation by MurM in the synthesis of *Streptococcus pneumoniae* peptidoglycan. *Journal of Biological Chemistry*, 283, 6402-6417.
- LOUNDON, N., ROGER, G., THIEN, H. V., BÉGUÉ, P. & GARABÉDIAN, E. N. 1999. Evolution of the bacteriologic features of persistent acute otitis media compared with acute otitis media: a 15-year study. *Archives of Otolaryngology–Head & Neck Surgery*, 125, 1134-1140.
- LOVERING, A. L., SAFADI, S. S. & STRYNADKA, N. C. 2012. Structural perspective of peptidoglycan biosynthesis and assembly. *Annual review of biochemistry*, 81, 451-478.
- MACHEREY-NAGEL. 2017. *PCR-Clean-up Gel extraction* [Online]. Macherey-nagel. Available: <https://www.mn-net.com/media/pdf/02/1a/74/Instruction-NucleoSpin-Gel-and-PCR-Clean-up.pdf> [Accessed 21.04.21 2021].
- MASSIDDA, O., NOVÁKOVÁ, L. & VOLLMER, W. 2013. From models to pathogens: how much have we learned about *S treptococcus pneumoniae* cell division? *Environmental microbiology*, 15, 3133-3157.
- MEESKE, A. J., RILEY, E. P., ROBINS, W. P., UEHARA, T., MEKALANOS, J. J., KAHNE, D., WALKER, S., KRUSE, A. C., BERNHARDT, T. G. & RUDNER, D. Z. 2016. SEDS proteins are a widespread family of bacterial cell wall polymerases. *Nature*, 537, 634-638.

- MORLOT, C., PERNOT, L., LE GOUELLEC, A., DI GUILMI, A. M., VERNET, T., DIDEBERG, O. & DESSEN, A. 2005. Crystal structure of a peptidoglycan synthesis regulatory factor (PBP3) from *Streptococcus pneumoniae*. *Journal of Biological Chemistry*, 280, 15984-15991.
- MYRBRÅTEN, I. S., WIULL, K., SALEHIAN, Z., HÅVARSTEIN, L. S., STRAUME, D., MATHIESEN, G. & KJOS, M. 2019. CRISPR interference for rapid knockdown of essential cell cycle genes in *Lactobacillus plantarum*. *Msphere*, 4.
- NOCEK, B., STEIN, A., JEDRZEJCZAK, R., CUFF, M., LI, H., VOLKART, L. & JOACHIMIAK, A. 2011. Structural studies of ROK fructokinase YdhR from *Bacillus subtilis*: insights into substrate binding and fructose specificity. *Journal of molecular biology*, 406, 325-342.
- NOVÁKOVÁ, L., BEZOUŠKOVÁ, S., POMPACH, P., ŠPIDLOVÁ, P., SASKOVÁ, L., WEISER, J. & BRANNY, P. 2010. Identification of multiple substrates of the StkP Ser/Thr protein kinase in *Streptococcus pneumoniae*. *Journal of bacteriology*, 192, 3629-3638.
- NOVAKOVA, L., SASKOVA, L., PALLOVA, P., JANEČEK, J., NOVOTNA, J., ULRYCH, A., ECHENIQUE, J., TROMBE, M. C. & BRANNY, P. 2005. Characterization of a eukaryotic type serine/threonine protein kinase and protein phosphatase of *Streptococcus pneumoniae* and identification of kinase substrates. *The FEBS journal*, 272, 1243-1254.
- OSAKI, M., ARCONDÉGUY, T., BASTIDE, A., TOURIOL, C., PRATS, H. & TROMBE, M.-C. 2009. The StkP/PhpP signaling couple in *Streptococcus pneumoniae*: cellular organization and physiological characterization. *Journal of bacteriology*, 191, 4943-4950.
- PAIK, J., KERN, I., LURZ, R. & HAKENBECK, R. 1999. Mutational analysis of the *Streptococcus pneumoniae* bimodular class A penicillin-binding proteins. *Journal of bacteriology*, 181, 3852-3856.
- PASQUINA-LEMONCHE, L., BURNS, J., TURNER, R., KUMAR, S., TANK, R., MULLIN, N., WILSON, J., CHAKRABARTI, B., BULLOUGH, P. & FOSTER, S. 2020. The architecture of the Gram-positive bacterial cell wall. *Nature*, 582, 294-297.
- PEREZ, A. J., BOERSMA, M. J., BRUCE, K. E., LAMANNA, M. M., SHAW, S. L., TSUI, H. C. T., TAGUCHI, A., CARLSON, E. E., VANNIEUWENHZE, M. S. & WINKLER, M. E. 2020. Organization of peptidoglycan synthesis in nodes and separate rings at different stages of cell division of *Streptococcus pneumoniae*. *Molecular Microbiology*.
- PEREZ, A. J., CESBRON, Y., SHAW, S. L., VILLICANA, J. B., TSUI, H.-C. T., BOERSMA, M. J., ZIYUN, A. Y., TOVPEKO, Y., DEKKER, C. & HOLDEN, S. 2019. Movement dynamics of divisome proteins and PBP2x: FtsW in cells of *Streptococcus pneumoniae*. *Proceedings of the National Academy of Sciences*, 116, 3211-3220.
- SAIKI, R. K., SCHARF, S., FALOONA, F., MULLIS, K. B., HORN, G. T., ERLICH, H. A. & ARNHEIM, N. 1985. Enzymatic amplification of beta-globin genomic sequences and restriction site analysis for diagnosis of sickle cell anemia. *Science*, 230, 1350-1354.
- SANGER, F., NICKLEN, S. & COULSON, A. R. 1977. DNA sequencing with chain-terminating inhibitors. *Proceedings of the national academy of sciences*, 74, 5463-5467.
- SASSINE, J., PAZOS, M., BREUKINK, E. & VOLLMER, W. 2021. Lytic transglycosylase MltG cleaves in nascent peptidoglycan and produces short glycan strands. *The Cell Surface*, 100053.
- SAUVAGE, E., KERFF, F., TERRAK, M., AYALA, J. A. & CHARLIER, P. 2008. The penicillin-binding proteins: structure and role in peptidoglycan biosynthesis. *FEMS microbiology reviews*, 32, 234-258.
- SCIENCES, G. H. L. 2000. *Size Exclusion Chromatography Principles and Methods* [Online]. GE healthcare Life Sciences. Available: [http://wolfson.huji.ac.il/purification/PDF/Gel Filtration/GE Size Exclusion Chromatography Handbook.pdf](http://wolfson.huji.ac.il/purification/PDF/Gel%20Filtration/GE%20Size%20Exclusion%20Chromatography%20Handbook.pdf) [Accessed].
- SCOTT, J. A. G., HALL, A. J., DAGAN, R., DIXON, J. M. S., EYKYN, S. J., FENOLL, A., HORTAL, M., JETTÉ, L. P., JORGENSEN, J. H., LAMOTHE, F., LATORRE, C., MACFARLANE, J. T., SHLAES, D. M., SMART, L. E. & TAUNAY, A. 1996. Serogroup-Specific Epidemiology of *Streptococcus pneumoniae*: Associations with Age, Sex, and Geography in 7,000 Episodes of Invasive Disease. *Clinical Infectious Diseases*, 22, 973-981.

- SELTMANN, G. & HOLST, O. 2013. *The bacterial cell wall*, Springer Science & Business Media.
- SHAM, L.-T., BUTLER, E. K., LEBAR, M. D., KAHNE, D., BERNHARDT, T. G. & RUIZ, N. 2014. MurJ is the flippase of lipid-linked precursors for peptidoglycan biogenesis. *Science*, 345, 220-222.
- SHAM, L.-T., TSUI, H.-C. T., LAND, A. D., BARENDT, S. M. & WINKLER, M. E. 2012. Recent advances in pneumococcal peptidoglycan biosynthesis suggest new vaccine and antimicrobial targets. *Current opinion in microbiology*, 15, 194-203.
- SHIOMI, D., SAKAI, M. & NIKI, H. 2008. Determination of bacterial rod shape by a novel cytoskeletal membrane protein. *The EMBO journal*, 27, 3081-3091.
- SIGMAALDRICH. 2021. REDTaq[®] ReadyMix[™] PCR Reaction Mix with MgCl₂ [Online]. Sigma- Aldrich. Available: https://bioresurs.uu.se/wp-content/uploads/2016/09/bilagan2013_3_d1s80tekniskbulletin.pdf [Accessed 03.02.2021 2021].
- SONG, J. Y., NAHM, M. H. & MOSELEY, M. A. 2013. Clinical implications of pneumococcal serotypes: invasive disease potential, clinical presentations, and antibiotic resistance. *Journal of Korean medical science*, 28, 4-15.
- STAMSÅS, G. A., STRAUME, D., RUUD WINTHER, A., KJOS, M., FRANTZEN, C. A. & HÅVARSTEIN, L. S. 2017. Identification of EloR (Spr1851) as a regulator of cell elongation in *Streptococcus pneumoniae*. *Molecular microbiology*, 105, 954-967.
- STEINMOEN, H., KNUTSEN, E. & HÅVARSTEIN, L. S. 2002. Induction of natural competence in *Streptococcus pneumoniae* triggers lysis and DNA release from a subfraction of the cell population. *Proceedings of the National Academy of Sciences*, 99, 7681-7686.
- STRAUME, D., PIECHOWIAK, K. W., OLSEN, S., STAMSÅS, G. A., BERG, K. H., KJOS, M., HEGGENHOUGEN, M. V., ALCORLO, M., HERMOSO, J. A. & HÅVARSTEIN, L. S. 2020. Class A PBPs have a distinct and unique role in the construction of the pneumococcal cell wall. *Proceedings of the National Academy of Sciences*, 117, 6129-6138.
- STRAUME, D., STAMSÅS, G. A., BERG, K. H., SALEHIAN, Z. & HÅVARSTEIN, L. S. 2017. Identification of pneumococcal proteins that are functionally linked to penicillin-binding protein 2b (PBP2b). *Molecular microbiology*, 103, 99-116.
- STRAUME, D., STAMSÅS, G. A. & HÅVARSTEIN, L. S. 2015. Natural transformation and genome evolution in *Streptococcus pneumoniae*. *Infection, Genetics and Evolution*, 33, 371-380.
- SUN, X., GE, F., XIAO, C.-L., YIN, X.-F., GE, R., ZHANG, L.-H. & HE, Q.-Y. 2010. Phosphoproteomic analysis reveals the multiple roles of phosphorylation in pathogenic bacterium *Streptococcus pneumoniae*. *Journal of proteome research*, 9, 275-282.
- SUNG, C., LI, H., CLAVERYS, J. & MORRISON, D. 2001. An rpsL cassette, janus, for gene replacement through negative selection in *Streptococcus pneumoniae*. *Applied and environmental microbiology*, 67, 5190-5196.
- TEO, A. C. & ROPER, D. I. 2015. Core steps of membrane-bound peptidoglycan biosynthesis: recent advances, insight and opportunities. *Antibiotics*, 4, 495-520.
- TETTELIN, H., NELSON, K. E., PAULSEN, I. T., EISEN, J. A., READ, T. D., PETERSON, S., HEIDELBERG, J., DEBOY, R. T., HAFT, D. H. & DODSON, R. J. 2001. Complete genome sequence of a virulent isolate of *Streptococcus pneumoniae*. *Science*, 293, 498-506.
- TSUI, H.-C. T., ZHENG, J. J., MAGALLON, A. N., RYAN, J. D., YUNCK, R., RUED, B. E., BERNHARDT, T. G. & WINKLER, M. E. 2016a. Suppression of a deletion mutation in the gene encoding essential PBP2b reveals a new lytic transglycosylase involved in peripheral peptidoglycan synthesis in *Streptococcus pneumoniae* D39. *Molecular microbiology*, 100, 1039-1065.
- TSUI, H. C. T., BOERSMA, M. J., VELLA, S. A., KOCAOGLU, O., KURU, E., PECENY, J. K., CARLSON, E. E., VANNIEUWENHZE, M. S., BRUN, Y. V. & SHAW, S. L. 2014. Pbp2x localizes separately from Pbp2b and other peptidoglycan synthesis proteins during later stages of cell division of *S. pneumoniae* D 39. *Molecular microbiology*, 94, 21-40.
- TSUI, H. C. T., ZHENG, J. J., MAGALLON, A. N., RYAN, J. D., YUNCK, R., RUED, B. E., BERNHARDT, T. G. & WINKLER, M. E. 2016b. Suppression of a deletion mutation in the gene encoding essential

- PBP2b reveals a new lytic transglycosylase involved in peripheral peptidoglycan synthesis in *Streptococcus pneumoniae* D39. *Molecular microbiology*, 100, 1039-1065.
- TYPAS, A., BANZHAF, M., GROSS, C. A. & VOLLMER, W. 2012. From the regulation of peptidoglycan synthesis to bacterial growth and morphology. *Nature Reviews Microbiology*, 10, 123-136.
- ULRYCH, A., HOLEČKOVÁ, N., GOLDOVÁ, J., DOUBRAVOVÁ, L., BENADA, O., KOFROŇOVÁ, O., HALADA, P. & BRANNY, P. 2016. Characterization of pneumococcal Ser/Thr protein phosphatase phpP mutant and identification of a novel PhpP substrate, putative RNA binding protein Jag. *BMC microbiology*, 16, 1-19.
- VALVERDE, R., EDWARDS, L. & REGAN, L. 2008. Structure and function of KH domains. *The FEBS journal*, 275, 2712-2726.
- VAN DER POLL, T. & OPAL, S. M. 2009. Pathogenesis, treatment, and prevention of pneumococcal pneumonia. *The Lancet*, 374, 1543-1556.
- VOLLMER, W., BLANOT, D. & DE PEDRO, M. A. 2008. Peptidoglycan structure and architecture. *FEMS microbiology reviews*, 32, 149-167.
- WALKER, J. A., ALLEN, R. L., FALMAGNE, P., JOHNSON, M. K. & BOULNOIS, G. 1987. Molecular cloning, characterization, and complete nucleotide sequence of the gene for pneumolysin, the sulfhydryl-activated toxin of *Streptococcus pneumoniae*. *Infection and immunity*, 55, 1184-1189.
- WALKER, J. M. 2002. SDS polyacrylamide gel electrophoresis of proteins. *The protein protocols handbook*. Springer.
- WINTHER, A. R. 2020. Cell-shape regulation in *Streptococcus pneumoniae*: EloR/KhpA, a new regulatory pathway administering cell elongation.
- WINTHER, A. R., KJOS, M., HERIGSTAD, M. L., HÅVARSTEIN, L. S. & STRAUME, D. 2021. EloR interacts with the lytic transglycosylase MltG at midcell in *Streptococcus pneumoniae* R6. *Journal of Bacteriology*.
- WINTHER, A. R., KJOS, M., STAMSÅS, G. A., HÅVARSTEIN, L. S. & STRAUME, D. 2019. Prevention of EloR/KhpA heterodimerization by introduction of site-specific amino acid substitutions renders the essential elongosome protein PBP2b redundant in *Streptococcus pneumoniae*. *Scientific reports*, 9, 1-13.
- YUNCK, R., CHO, H. & BERNHARDT, T. G. 2016. Identification of MltG as a potential terminase for peptidoglycan polymerization in bacteria. *Molecular microbiology*, 99, 700-718.
- ZAPUN, A., CONTRERAS-MARTEL, C. & VERNET, T. 2008. Penicillin-binding proteins and β -lactam resistance. *FEMS Microbiology Reviews*, 32, 361-385.
- ZHENG, J. J., PEREZ, A. J., TSUI, H. C. T., MASSIDDA, O. & WINKLER, M. E. 2017. Absence of the KhpA and KhpB (JAG/EloR) RNA-binding proteins suppresses the requirement for PBP2b by overproduction of FtsA in *Streptococcus pneumoniae* D39. *Molecular microbiology*, 106, 793-814.
- ZUCCHINI, L., MERCY, C., GARCIA, P. S., CLUZEL, C., GUEGUEN-CHAIGNON, V., GALISSON, F., FRETON, C., GUIRAL, S., BROCHIER-ARMANET, C. & GOUET, P. 2018. PASTA repeats of the protein kinase StkP interconnect cell constriction and separation of *Streptococcus pneumoniae*. *Nature microbiology*, 3, 197-209.

Appendix

A1. Conserved motif KKGFLG and predicted structure of the Jag domain of *S. pneumoniae*

A1.1 Alignment of the jag domains from different bacterial species

S. pneumoniae, *B. subtilis*, *C. symbiosium*, *Listeria monocytogenes*, *Enterococcus faecalis*, *Lactobacillus plantarum*, and *Lactococcus lactis*, respectively. The conserved motif (KKGFLG) is outlined in green.

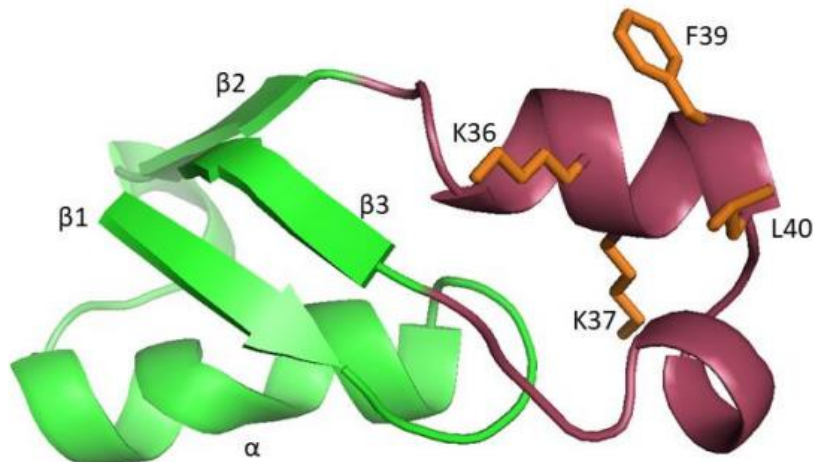
```

      10      20      30      40      50
S  . . . . . M V V F T G S T V E E A I Q K G L K E L D I P R M K A H I K V I S R E K K G F L G L F G K K P A Q V D
B  . . . M R E I T A . T G Q T V E E A V E S A L A Q L N T T K D R T E I T I V E E G K R G L L G L F G A K P A I V K
C  S N A X D X V T V . T A K T V E E A V T K A L I E L Q T T S D K L T Y E I V E K G S A G F L G I . G S K P A I I R
L  . . . . . M P I Y E G N T I E E A T Q K G L Q A L G L T K E D V T I D V L D E G K K G F L G L . G E K L A Q I S
E  . . . . . M V L F T G A T V E E A I E K G L Q E L N I S R L R A H I K V V S R E K K G F L G . F G K K P A K V E
L  . . . . . M T V F E G N T V A A A I A A G L K Q L H R T R D Q V E V E V I A E A K K G F L G L . G K H P A Q V R
L  . . . . . M A I F T G E T V E D A I E R G L N R L N V K R E N V H I H I E Q K E K K G F L O F . G K K R A R V N

```

A1.2 Predicted structure of the Jag domain of EloR in *S. pneumoniae*

The structure is built up by a β - α - β - β fold and the conserved motif KKGFLG is illustrated in orange sticks.



A2 Alignments of the cytosolic domain of MltG from different Streptococcal species

Alignment of *S. pneumoniae*, *S. sanguinis*, *S. mitis* (B6), *S. gordonii*, *S. infantis*, *S. thermophilus*

<i>Pneumo1-501</i>	1LSEKSRREEK..LSFKEQILRDLEKVKGYDEV.....LKE.....DEAVVTRFA.....NEPFAELMADS.....LSTVEEIMRKAPTVPHT.....SQGVFASPADE	83
<i>sanguinis1-499</i>	1	MLGIIMMKVKFLTEKQDKERNLSFKEQILKDLA.....GEHEEQTFS.....TKIADCEVYMAE.....LSAVEKIMENAPRVQ.....SEDFASPAEE	76
<i>B61-564</i>	1MSEKPREDEK..LSFKEQILRDLEKVKQYEGIROEAELDE.....KKSALSVD.....LD.....GFPPSEERNITETN.....KDFBFSENLOKDFSRDTMP.....GKESPVYVSK	81
<i>Streptococcus1-530</i>	1MTENSQNDQQLSFKEQILRDLAN.....ARKEQGSQSH.....LD.....GFPPSEERNITETN.....KDFBFSENLOKDFSRDTMP.....GKESPVYVSK	81
<i>Streptococcus1-586</i>	1MSENBRREEK..LSFKEQILRDLEKLRKREDQIANTKSNDDLFSLNLSNSEAENV.....EFPVDELMAE.....VSLVDELLANAPAVPPRVLODSDVETVASE	95
<i>Streptococcus1-659</i>	1MTDK.....HNEVSEASDOSLSFKNQILRDLEQATRLRSLEEE.....HKKSAVETPLMSADSHAIDSGSANSKYNQNLSSHVASHAIAKMTSETVRDFQVSDLSNSQDASAPDV.....HSNVISSEKQ	126
<i>Pneumo1-551</i>	84	IQRETPGVPSHPSDVPSPFAEESGSRPQP.....VREKRLREYNETP.....TRVAVSYTTAEKKAEOA.....QP..ETPAPTATV.....DIIRDTSR	166
<i>sanguinis1-499</i>	71VDSVY.....KVAENK.....AHPQVYQ	85
<i>B61-564</i>	90	LREEAPIVPSHPSDVPFATBAEASPSRPVPGPD.....VNRPKVYRDLNTPP.....TRVAVSYKTEEPKETOA.....EAPRHEPVVEAEAV.....DVISETPR	176
<i>Streptococcus1-530</i>	82EIRADSDTTTGS.....TOLKRN.....LITR.....VPMELSYGS.....KKEPTNEET.....LARTATVR	136
<i>Streptococcus1-586</i>	99FVYSEFA.....VVEFAVA.....PDLRSTEAPEVVKLEPAQVEKEFMAE.....TRIPKSRFNQAQPSPPRNINIKPOPKPTV.....LAKETPSQEVAPVET.....RTELP	197
<i>Streptococcus1-659</i>	127	VDK.....KNLSIQET.....EIFKR-RFKRV-WETSLSAESEEEYIPADAKELIEAKAKE.....IYTNPKELVSKMTEROKEAFREHHTVSNHSEPVVYVSDLVTDGNEDESIALAAASEKSN	242
<i>Pneumo1-551</i>	167	SRREGAFAK.....PKKESKSHVAFVIFLVLALLS.....AGVFGYQYVLDLFLIDANSKYVTVGIPESNVDEIGTTLKAGLVKHLISFVAKYKYNITDLKASVYNLOKSMSTEDLKE	286
<i>sanguinis1-499</i>	90	RVDEEDKPNELVSRANR.....ANNVKKKRONLARRIMTTVLLIVLLGLVTVSGYTVVSSALKPVDANATEYVTVVEPESSSKIQEILEKKGKLIKNAQVPSLSKIKSFNNYQBGYYNLOKSMOLDITARQ	222
<i>B61-564</i>	177	SRRETVKRV.....KSKKSHLKAFFISLLIFLALIS.....AGVFGYQYVLDLFLIDANSKYVTVGIPESNVDEIGSALHSGVLIKHGVIKAFYAKYKHNHDLKGGYYNLOKSMSTEDLKE	293
<i>Streptococcus1-530</i>	131	RTD-VDK.....GDSLSRSVK.....DGGTKKRONSVAKRIFVITVLLGLL.....VGGFQYRVVVEALQPDVANSKYVTVGIPESNVDEIGSALHSGVLIKHGVIKAFYAKYKHNHDLKGGYYNLOKSMSTEDLKE	263
<i>Streptococcus1-586</i>	198	SRKESVRI.....KSKKSRKLFQFVITVLLGLL.....VGGFQYRVVVEALQPDVANSKYVTVGIPESNVDEIGSALHSGVLIKHGVIKAFYAKYKHNHDLKGGYYNLOKSMSTEDLKE	317
<i>Streptococcus1-659</i>	243	KKRKVKKPKKKSPPKQDGIINEEPIISCSNRNQLNKNRRRAGVARNIIVFLLIISLASLFGYRVVSDAVGAKVYKSTKFTSMEIPEHNGSSYIGQLLESAGVLIKSGVKNYTHYRNISNLKGGYYNLOKSMSTEDLKE	387
<i>Pneumo1-551</i>	287	LOKGGTDPGEPVSLADLTIPEGYTLDLIAQTV.....GQLQGEFKEP.....LTAFAFLAKVQDDEFTISQAVAKYPTLLESFLVYKSBARYRLEGLFPATVYIKESITTEISLIDEMLAAMDKNLSLYSTIKSKNLTVNELLITLASLVE	426
<i>sanguinis1-499</i>	223	LOGBGTDTPGEPVSKVITLPEGYTLDLIAQTV.....GQLQGEFKEP.....LTAFAFLAKVQDDEFTISQAVAKYPTLLESFLVYKSBARYRLEGLFPATVYIKESITTEISLIDEMLAAMDKNLSLYSTIKSKNLTVNELLITLASLVE	367
<i>B61-564</i>	294	LOKGGTPEPEPESLADLTIPEGYTLDLIAQTV.....GQLQGEFKEP.....LTAFAFLAKVQDDEFTISQAVAKYPTLLESFLVYKSBARYRLEGLFPATVYIKESITTEISLIDEMLAAMDKNLSLYSTIKSKNLTVNELLITLASLVE	433
<i>Streptococcus1-530</i>	261	LOKGGTDPGEPVSLADLTIPEGYTLDLIAQTV.....GQLQGEFKEP.....LTAFAFLAKVQDDEFTISQAVAKYPTLLESFLVYKSBARYRLEGLFPATVYIKESITTEISLIDEMLAAMDKNLSLYSTIKSKNLTVNELLITLASLVE	396
<i>Streptococcus1-586</i>	316	LOKGGTDPGEPVSLADLTIPEGYTLDLIAQTV.....GQLQGEFKEP.....LTAFAFLAKVQDDEFTISQAVAKYPTLLESFLVYKSBARYRLEGLFPATVYIKESITTEISLIDEMLAAMDKNLSLYSTIKSKNLTVNELLITLASLVE	455
<i>Streptococcus1-659</i>	388	LOKGBDKGEPVSLADLTIPEGYTLDLIAQTV.....GQLQGEFKEP.....LTAFAFLAKVQDDEFTISQAVAKYPTLLESFLVYKSBARYRLEGLFPATVYIKESITTEISLIDEMLAAMDKNLSLYSTIKSKNLTVNELLITLASLVE	531
<i>Pneumo1-551</i>	427	KEGATDEDRKLIAGVFNRLNRMPLQSNIAILYAQGLKQNIISLADDAADITNIDSPYNDYVHKLMPGPVDSPLDAEASINOTKSDVLYFVANVQDQKVFATTFEEDRNVAEHNKSLTQSSSN	551
<i>sanguinis1-499</i>	368	KEGATDEDRKLIAGVFNRLNRMPLQSNIAILYAQGLKQNIISLADDAADITNIDSPYNDYVHKLMPGPVDSPLDAEASINOTKSDVLYFVANVQDQKVFATTFEEDRNVAEHNKSLTQSSSN	495
<i>B61-564</i>	434	KEGATDEDRKLIAGVFNRLNRMPLQSNIAILYAQGLKQNIISLADDAADITNIDSPYNDYVHKLMPGPVDSPLDAEASINOTKSDVLYFVANVQDQKVFATTFEEDRNVAEHNKSLTQSSSN	554
<i>Streptococcus1-530</i>	400	KEGATDEDRKLIAGVFNRLNRMPLQSNIAILYAQGLKQNIISLADDAADITNIDSPYNDYVHKLMPGPVDSPLDAEASINOTKSDVLYFVANVQDQKVFATTFEEDRNVAEHNKSLTQSSSN	530
<i>Streptococcus1-586</i>	456	KEGATDEDRKLIAGVFNRLNRMPLQSNIAILYAQGLKQNIISLADDAADITNIDSPYNDYVHKLMPGPVDSPLDAEASINOTKSDVLYFVANVQDQKVFATTFEEDRNVAEHNKSLTQSSSN	586
<i>Streptococcus1-659</i>	522	KEGATDDDRKLIAGVFNRLNRMPLQSNIAILYAQGLKQNIISLADDAADITNIDSPYNDYVHKLMPGPVDSPLDAEASINOTKSDVLYFVANVQDQKVFATTFEEDRNVAEHNKSLTQSSSN	656

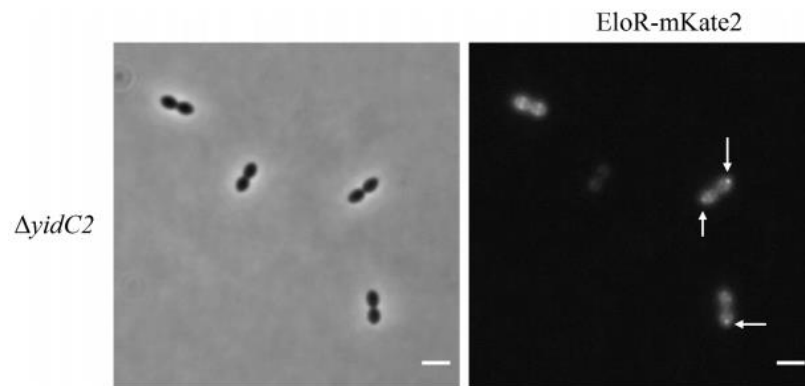
A3 Alignment of EloR in R6 *S. pneumoniae* and B6 *S. mitis*

Alignment of EloR, Jag indicated in blue

R6	1	MVVFTGSTVEEAIQKGLKELDIPRMAKHAHIKVISREKKGFLGLFGKPKPAQVDIEAISETTV	60
B6	1	MVVFTGSTVEEAIQKGLKELDIPRLKAHIKVISREKNGFLGLFGKPKPAQVDIEAISETTV	60
Query	61	VKANQQVVKGVPPKINDLNEPVKTVSEETVDLGHVVDIAIKKIEEEGQGISDEVKAEILKH	120
Sbjct	61	+KANQQVVKGVPPKIN+NEPVKTVSEETVDLGHVVDIAIKKIEEEGQGS+DEVKAEILK+	120
Query	121	ERHASTILEETGHIIEILNELQIEEA-MREEAGADDLETEQDQAESQELEDLGLKVEITNFD	179
Sbjct	121	E+HA+TILEETGHIIEILNELQ+EEA EE +ET+ +Q ESQELEDLGLKVE +FD	180
Query	180	IEQVVATEMAYVQTIIDDMDEATLSNDYNRRSINLQIDTNEPGRIGYHGKVLKALQLL	239
Sbjct	181	IEQVATEVTTYVQTIIDDMDEATISNDYNRRSINLQIDTNEPGRIGYHGKVLKALQLL	240
Query	240	AQNYLYNRYSRFTFYITINVNDYVEHRAEVLQTYAQLATRVLEEGRSHKTDPMNSERKI	299
Sbjct	241	AQNYLYNRYSRFTFYITINVNDYVEHRAEVLQTYAQLATRVLEEGRSHQTDPMNSERKI	300
Query	300	IHRIISRMDGVTYSYSEGDEPNRYVVVDTE	328
Sbjct	301	IHRIISRMDGVTYSYSEGDEPNRYVVVDTE	329

A4 Microscopy imaging of the genetic background lackin *yidC*

The microscopy images display the accumulation of EloR-mKate2 in old cellular poles in addition to midcell localization.



A5 Abbreviations

Abbreviations

APS	Ammonium PeroxiSulfate
BACTH	Bacterial Adenylate Cyclase Two-Hybrid system
dNTPS	deoxynucleotide triphosphates
DUF	Domain of unknown function
EDTA	EthyleneDiamineTetraAcetic Acid
EloR	Elongasome Regulating protein
GlcNAc	<i>N</i> -acetylglucosamine acid
HBC	High Salt Wash
IPTG	Isopropyl β -d-1-thiogalactopyranoside
LB	Lysogeny Broth
LTA	Lipoteichoic acid
MurNAc	<i>N</i> -acetylmuramic acid
OD	Optical density
PAGE	PolyAcrylamide Gel Electrophoresis
PASTA	Penicillin-binding protein And Ser/Thr kinase Associated
PBP	penicillin binding protein
PBS	Phosphate Buffered Saline
PCR	Polymerase Chain Reaction
PG	Peptidoglycan
SDS	Sodium Dodecyl Sulphate
SEDS	Shape, Elongation, Division, and sporulation
SOC	Super Optimal broth with Catabolite repression
TAE	Tris-Acetate EDTA
TBS	Tris Buffered Saline
TBST	Tris Buffered Saline and Tween
TEMED	Tetramethyl ethylenediamine
UDP-MurNAc	UDP- <i>N</i> -acetylmuramyl-pentapeptide
WTA	Wall Teichoic Acid



Norges miljø- og biovitenskapelige universitet
Noregs miljø- og biovitenskapelige universitet
Norwegian University of Life Sciences

Postboks 5003
NO-1432 Ås
Norway